

APPENDIX 3.D: VERTICAL HANDLING OF OVERPACK WITH HEAVIEST MPC

3.D.1 Introduction

There are two vertical lifting scenarios for the HI-STORM 100 during the normal operation procedures at the ISFSI pad. The first scenario considers the vertical lifting of a fully loaded HI-STORM 100 with four synchronized hydraulic jacks, each positioned at each of the four inlet vents located at the bottom end. This operation allows the installation of air pads under the HI-STORM 100 baseplate. The second scenario considers the lifting of a fully loaded HI-STORM 100 vertically through the four lifting lugs located at the top end. The lifting device assemblage is constructed such that the lift forces at each lug are parallel to the longitudinal axis of the HI-STORM 100 during the operation. The stress intensity induced on the cask components as a result of these operations is determined, analyzed, and the structural integrity evaluated. The finite element models for the analyses in this appendix have been color coded to differentiate cask components. The legends for the color codes are listed in Sections 3.D.3 and 3.D.4 below.

3.D.2 Assumptions

- a. Conservatively, the analysis takes no credit for the structural rigidity of the radial concrete shielding between the outer and the inner shells of the HI-STORM 100 and also no credit for the structural rigidity of the MPC pedestal shield. Hence, the weight of the radial concrete shielding, the MPC pedestal shield, and the MPC are respectively applied as surface pressure on the baseplate during the vertical lifting of HI-STORM 100 from the bottom end through the inlet vents and, as lumped mass during the vertical lifting of HI-STORM 100 at the top end through the lifting lugs. Property values used are approximately equal to the final values set in the Tables in Chapter 3. Drawings 1495, 1561 and associated Bills of Materials are used for dimensions.
- b. The acceleration of gravity of 1.15g is considered in order to account for a 15% dynamic load factor due to lifting. The 15% increase, according to Reference 2, is considered in crane standards as appropriate for low speed lifting operations.
- c. e.—The shield shell is not explicitly modeled. The weight of the shield is added to the weight of the inner shell for top end lift and as a lumped mass for the bottom end lift. Added weights are obtained by direct calculation.

- d. *The geometry of the HI-STORM 100 is considered for the analysis of the top lift. This is conservative since the HI-STORM 100S is lighter and the outlet air ducts are moved to the lid in the "S" unit.*

3.D.3 Analysis Methodology - Bottom Lift at the Inlet Vents

A 3-D, 1/4-symmetry, finite element model of the bottom segment of the HI-STORM 100 storage overpack is constructed using the ANSYS 3-D elastic shell element SHELL63. ANSYS is a general purpose finite element program. The Young's modulus, at 300 degree F, the Poisson's ratio, and material density for SA516-70 steel are respectively taken as 29.34E+06 psi, 0.29, and 0.288 pounds per-cubic-inch. The respective thickness of the HI-STORM 100 components are also appropriately considered, i.e., 1.25 inches for the inner shell, 0.75 inches for the outer shell, 2.0 inches for the baseplate, 0.5¹ inches for the radial ribs, 2 inches for the inlet vent horizontal plate, and 0.75 inches for the inlet vent vertical plates. The model is terminated approximately 20 inches above the base of the HI-STORM 100 storage overpack with the weight of the sections of the HI-STORM 100 storage overpack not modeled lumped at the top end of the finite element model. The contact surface between the inlet horizontal plate and hydraulic jack is fixed vertically.

An equivalent pressure load of 31.61 psi from the weights of the heaviest MPC and the pedestal shield is applied on the HI-STORM 100 baseplate over the surface area covered by the pedestal (the applied total load is 116,067 lb. based on a 68.375" outer diameter). The equivalent pressure load of 20.55 psi from the weight of the radial concrete shielding is applied on the baseplate as well as the inlet vent horizontal plates. The applied equivalent pressure loads include the 15% load increase above the dead load to account for inertia effects developed during a lift operation. Figure 3.D.1 shows the plot of the finite element model for the bottom lift scenario. Figure 3.D.1 is color-coded to differentiate cask components as follows:

Figure 3.D.1 Cask Component Color Codes

<u>Component</u>	<u>Color</u>
Baseplate	Blue-Purple-Red
Inner Shell	Green
Outer Shell	Magenta
Rib	Dark Blue

¹ Analysis is conservative since final radial rib thickness is 0.75 inch.

Inlet Vent Vertical Plate	Mustard
Inlet Vent Horizontal Plate	Color Grid

3.D.4 Analysis Methodology - Top End Lift

3.D.4.1 Model at Top near Lift Points

A 3-D, 1/8-symmetry, finite element model of the top segment of the HI-STORM 100 is constructed using ANSYS 3-D elastic shell element SHELL63, 3-D structural solid with rotation SOLID73, and 3-D structural mass element MASS21. The material properties used, i.e., Young's Modulus, the Poisson's ratio, and material density are identical to those listed in Section 3.D.3. The respective thickness of the HI-STORM 100 components (in addition to the inner shell, the outer shell, and the ribs) are also appropriately considered, i.e., 0.75 inches for the top plate, 1.25 inches for the exit vent horizontal plate, 0.5 inches for the exit vent vertical plate, 0.75 inches for the horizontal step plate and the vertical step plate. The model is terminated at about 43 inches from the top end of the HI-STORM 100. The mass of the sections of the HI-STORM 100 not modeled, with the exception of the overpack lid and the shield blocks, are lumped at the lower end of the finite element model. A bounding value for the mass of the overpack lid and the shield blocks are lumped at the top end of the vertical step plates. All lumped masses use the ANSYS MASS21 elements. The lifting lug is explicitly modeled with the ANSYS SOLID73 element. The SOLID73 element is selected for its compatible degrees-of-freedom with the ANSYS SHELL63. The top end of the lifting lug in the finite element model is restricted from vertical translation. Since the lifting lug itself is not part of the HI-STORM 100 system, the model of this component is performed only to a level necessary to properly simulate the location of the lift point. Figures 3.D.2a, 3.D.2b, and 3.D.2c show the detailed plots of the finite element model for the top lift scenario. Figures 3.D.2a, 3.D.2b, and 3.D.2c are color-coded to differentiate cask components as follows:

Figure 3.D.2 Cask Component Color Codes

<u>Component</u>	<u>Color</u>
Inner Shell	Cyan
Outer Shell	Red
Step Horizontal Plate	Purple
Step Vertical Plate	Purple
Exit Vent Horizontal Plate	Green
Exit Vent Vertical Plate	Magenta
Rib	Mustard

Top Plate	Blue
Anchor Block	Cyan
Lug	Cyan

We note that the analysis model used here included small “step” plates. The step plate has been eliminated in the storage overpack in Revision 5 (see drawings in Chapter 1) to simplify fabrication. The removal of the “step” plates also removes a potential area of stress concentration from the configuration. Therefore, the analysis reported here, which retains the step, produces conservative stress results and is bounding for the final configuration in this area of the structure.

3.D.4.2 Model Near Baseplate

The 2-inch thick, HI-STORM 100 baseplate is fabricated from SA-516-Grade 70 carbon steel material. The baseplate is continuously welded to the inner shell, the outer shell, the inlet vents, and the MPC pedestal shell. During a vertical lift using the top end lift lugs, the baseplate supports the MPC, the MPC pedestal, and the radial concrete shielding between the inner shell and the outer shell. The stress intensity and the associated distribution on the HI-STORM 100 baseplate as a result of the vertical lift through the lifting lug is evaluated using the same finite element model as that described in Section 3.D.3 above. For this analysis, the finite element model in Figure 3.D.1 is restrained against vertical translation at the top end of the model away from the baseplate. The weight of the pedestal, the MPC, and the radial concrete shield are applied as pressure loads as described in Section 3.D.1, and no hydraulic jacks are assumed in-place in the inlet vents.

3.D.5 Stress Evaluation

For all analyses, safety evaluation is based on the consideration of all components as Class 3 plate and shell support structures per the ASME Code Section III, Subsection NF. Stress intensity distributions are obtained for all sections of the model. Although the relevant Code section places limits on maximum stresses, the use of a stress intensity based safety factor is used here for convenience. The distribution of stress intensity on the HI-STORM 100 from the bottom end lifting through the inlet vents is shown in Figure 3.D.3. The maximum surface stress intensity, located on the inlet vent plate, is 13,893 psi based on the element distribution used. As seen from Figure 3.D.3, this surface stress intensity bounds the values at all other locations and therefore could be used to provide a bounding safety factor for all sections modeled in this simulation. The nature of the finite element model is such that the surface stress intensity results near discontinuities in loading or in the structure include secondary stress intensity components as well as primary membrane and primary bending. In particular, this stress intensity component includes secondary effects both from the abrupt change in the

applied load and from the joint between the horizontal and vertical plates of the inlet vent. Away from this local region, we can estimate from the distributions plotted in Figure 3.D.3 that the maximum primary membrane plus primary bending stress intensity is approximately 8000 psi.

The distributions of stress intensity on the HI-STORM 100 from the top end lifting through the lifting lugs are shown in Figures 3.D.4a and 3.D.4b, and 3.D.4c. Figures 3.D.4a and 3.D.4b show a cut through the middle surface of the radial rib and rib bolt block. The maximum stress intensity consistent with the finite element discretization, located on the rib plate, is 16,612 psi (Figure 3.D.4b). This stress is localized and represents a mean stress intensity plus secondary membrane stress intensity components introduced from the abrupt geometry change where the rib bolt block is welded to the radial rib. If attention is focused on the radial rib away from the local discontinuity, then the mean stress intensity is approximately 10,000 psi (the iso-stress intensity boundary between yellow and yellow-green in Figure 3.D.4(b)). Figure 3.D.4c shows the "step" (no longer present in the structure) and identifies the local stress intensity amplification that no longer is present.

The stress intensity distribution on the baseplate due to the lifting of HI-STORM 100 through the top end lifting lugs are shown in Figures 3.D.5a, 3.D.5b, and 3.D.5c. These three figures show different views of the components and identify the locations of maximum stress intensity. The maximum stress intensity on the baseplate occurs, as expected, just inboard of the inner shell of the storage overpack and has a maximum value, consistent with the level of discretization, of 10,070 psi (Figure 3.D.5a). It is clear from the distribution that this includes a significant secondary stress intensity component introduced by the inlet vent vertical plate. Away from this local region, the surface stress intensity reduces to approximately 7000 psi. At this location, we consider the result to represent the combined primary membrane plus primary bending stress intensity.

The results of these analyses are summarized as follows (neglecting secondary effects introduced by geometry and load changes):

For the top lift, maximum membrane stress intensity, excluding very localized secondary effects due to geometric discontinuities, is in the radial rib, and has the value 10,000 psi. Since this analysis is based on a 0.5" thickness rather than the actual final plate thickness 0.75", for the purpose of establishing a bounding safety factor, we further reduce this stress intensity by 2/3. Therefore, the appropriate safety factor (SF) is (see Table 3.1.10)

$$\text{SF}(\text{membrane stress intensity in radial rib}) = 17,500 \text{ psi} / (10,000 \text{ psi} \times 2/3) = 2.63$$

For the same top lift, the bounding safety factor for primary membrane plus primary bending

(excluding local discontinuity effects) is computed for the baseplate as:

$$\text{SF}(\text{primary membrane plus primary bending stress intensity in baseplate}) = 26,250\text{psi}/7000\text{psi} = 3.75$$

For the bottom lift,

$$\text{SF}(\text{primary membrane plus primary bending in inlet vent horizontal plate}) = 26,250\text{psi}/8000\text{psi} = 3.28$$

The previous calculations have been based on an applied load of 115% of the lifted load with safety factors developed in accordance with ASME Section III, Subsection NF for Class 3 plate and shell support structures. To also demonstrate compliance with Regulatory Guide 3.61, safety factors based on 33.3% of the material yield strength are presented. These safety factors can be easily derived from the previous results by replacing the allowable stress by 33.3% of the material yield strength (1/3 x 33,150 psi from Table 3.3.2 for SA-516). Therefore, the following bounding results are obtained:

$$\text{SF}(\text{membrane} - 3W) = 2.63 \times 33,150\text{psi}/(3 \times 17,500 \text{psi}) = 1.66$$

$$\text{SF}(\text{membrane plus bending} - 3W) = 3.28 \times 33,150 \text{psi}/(3 \times 26,250 \text{psi}) = 1.38$$

3.D.6 Bolt and Anchor Block Thread Stress Analysis under Three Times Lifted Load

In this section, the threads of the bolt and the bolt anchor block are analyzed under three times the lifted load. The thread system is modeled as a cylindrical area of material under an axial load. The diameter of the cylinder area is the basic pitch diameter of the threads, and the length of the cylinder is the length of engagement of the threads. See Holtec HI-STORM 100 drawing numbers 14954 (sheets 2 and 3) and 1561 (sheet 2) for details.

3.D.6.1 Geometry

The basic pitch diameter of the threads is: $d_p = 3.08762\text{-}838"$

The thread engagement length is: $L = 3 \text{ in.}$

The shear area of the cylinder that represents the threads: $A = 3.14159 \times L \times d_p$

The shear stress on this cylinder under three times the load is: $3W \times 1.15/nA = 10,670\text{-}608 \text{ psi}$

where, the total weight, W , and the number of lift points, n , are 360,000 pounds and 4, respectively, and the 1.15 represents the inertia amplification.

3.D.6.2 Stress Evaluation

The yield strength of the anchor block material at 350 degrees F is taken as 32,700 psi per Table 3.3.3. Assuming the yield strength in shear to be 60% of the yield strength in tension gives the thread shear stress safety factor under three times the lifted load as:

$$\text{SF}(\text{thread shear} - 3 \times \text{lifted load}) = .6 \times 32,700 / 10,670 = 1.84169$$

The lifting stud material is SA564 630 (age hardened at 1075 degrees F). The yield strength of the stud material at 350 degrees F is 108,800 psi per Table 3.3.4.

The load per lift stud is $P = 3W/4 \times 1.15 = 310,500 \text{ lb}$.

The stud tensile *stress* area is (see *Machinery's Handbook, 23rd Edition, p. 1484*) computed using the mean diameter of the threads

$$A = 7.1063258 \text{ sq. inch.}$$

Therefore, the tensile stress in the stud under three times the lifted load is

$$\text{Stress} = P/A = 43,7339,085 \text{ psi}$$

The factor of safety on tensile stress in the lifting stud, based on three times the lifted load, is:

$$\text{SF}(\text{stud tension} - 3 \times \text{lifted load}) = 108,800 / 43,7339,085 = 2.49217$$

It is concluded that thread shear in the anchor block governs the design.

3.D.7 Weld Evaluation

In this section, weld stress evaluations are performed for the weldments considered to be in the primary load path during lifting operations. The allowable stress for the welds is obtained from Reference [3].

3.D.7.1 Anchor Block-to-Radial Rib (Lift from Top)

There are double sided fillet welds that attach the anchor block to the radial ribs (see drawings 1495, sheet 3 and 1561 sheet 2). The following dimensions are used for analysis:

Total Length of weld = $L = 12" + 5"$ (Continuous weld along sides and bottom - see drawing 1561 sheet 2)

Weld leg size = $t = 0.75"$

Weld throat allowable shear stress = $S_a = 0.3S_u$ where S_u is the ultimate strength of the base metal (per [3]) = $.3 \times 65,650$ psi (Table 3.3.3 gives the ultimate strength of the anchor block base material).

$S_a = 19,695$ psi

The following calculations provide a safety factor for the weld in accordance with the requirements of the ASME Code, Section III, Subsection NF for Class 3 plate and shell supports:

Allowable load per anchor block (2 welds) = $S_a \times 2 \times 0.7071 \times t \times L = 355,072$ lb.

Calculated Load (including 15% inertia amplification) = $360,000$ lb $\times 1.15/4 = 103,500$ lb.

SF(ASME Code) = $355,072$ lb./ $103,500$ lb. = 3.43

The following calculations provide a safety factor for the weld in accordance with the requirements of Regulatory Guide 3.61 (here we use the yield strength at 300 degrees F since the weld is buried in the concrete (Table 2.2.3)):

Allowable load per anchor block (2 welds) = $0.6 \times 32,700 \times 2 \times 0.7071 \times t \times L = 353,769$ lb.

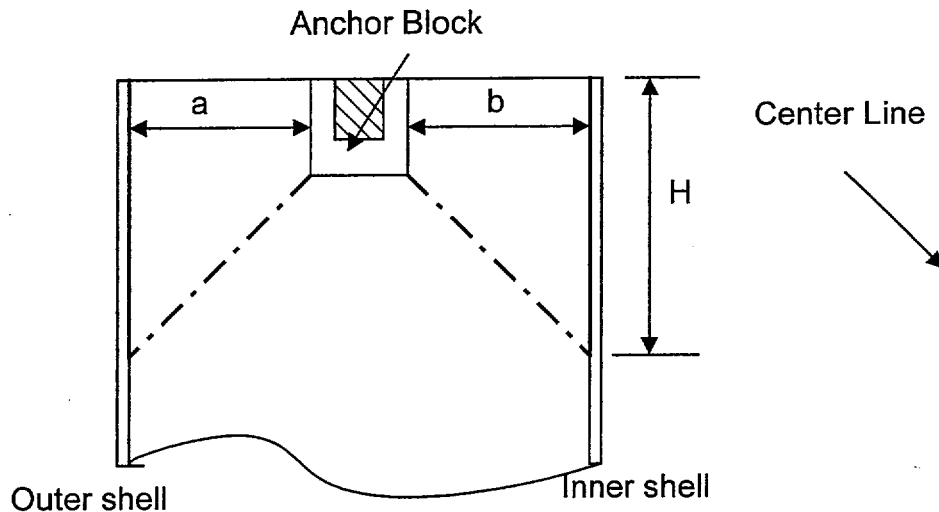
Calculated Load (3 x weight) = $360,000$ lb $\times 3/4 \times 1.15 = 310,500$ lb.

SF(Reg. Guide 3.61) = $353,769$ lb./ $310,500$ lb. = 1.14

3.D.7.2 Radial Rib-to-Inner and Outer Shell (Lift from Top)

The load transferred to the radial ribs from the bolt anchor blocks is dispersed through the rib and also transferred to the inner and outer shell of the storage overpacks. A conservative estimate of the safety factors inherent in the vertical welds connecting the radial ribs to the

inner and outer shells is obtained by assuming that the entire load is dispersed into the shells. The length of weld assumed to act in the load transfer is based on a dispersion angle of 45 degrees as shown in the sketch below:



From the geometry of the structure,

$a = 11.5''$ Drawing 1495, sheet 2
 $b = 11.0''$

The depth of the effective weld to each shell is conservatively computed as the depth of the anchor block plus b, or

$H = 6'' + 11'' = 17''$

Since the effective length of the totality of weld assumed effective to transfer the load to the shells (H for each of four ½" welds) is greater than the length of weld already shown to be acceptable at the anchor block-to-radial rib connection, and since the weld size and type is structurally better than or equal to the anchor block weld, we conclude that the anchor block-

to-radial rib weld safety factors conservatively bound from below the safety factors for the radial rib to inner and outer shell welds in this load application.

3.D.7.3 Baseplate-to-Inner Shell (Top Lift (bounds bottom lift))

The weld between the storage overpack baseplate and the storage overpack inner shell is an all-around fillet weld (except at the duct locations (see drawing 1495, sheet 2)). To bound both the top and bottom lift, it is conservatively assumed that this weld supports a lifted load consisting of the weights of the loaded MPC, the pedestal shield concrete and steel, and the MPC baseplate (i.e., the structural action of the weld to the outer shell is conservatively neglected).

Therefore, the weld is subject to the following total load

116,067 lb. (MPC and pedestal shield) + 7967 lb. (baseplate) (from calculation package weight tables)

so that the applied load in the weld is conservatively assumed as:

Load = 124,034 lb

The weld is a one-side fillet weld with weld leg size "t" at diameter $D = 73.5" + 2 \times 1.25"$, or

$t = 0.75"$

$D = 76"$

From the Bill-of-Materials for the HI-STORM 100 storage overpack, the width of each inlet vent is

$w = 16.5"$

Therefore, the total linear length (around the periphery) of fillet weld available to transfer the load is

$L = 3.14159 \times D - 4 \times w = 172.76"$

Therefore, the weld throat area is

$$\text{Area} = 0.7071 \times t \times L = 91.62 \text{ sq. inches}$$

The capacity of the weld per the ASME Code Section III Subsection NF is defined as Lc1

$$\text{Lc1} = 21,000 \text{ psi} \times \text{Area} = 1,924,020 \text{ lb.}$$

The capacity of the weld per Regulatory Guide 3.61 is defined as Lc2

$$\text{Lc2} = .6 \times 33,150 \text{ psi} \times \text{Area} = 1,822,322 \text{ lb.}$$

Since 3 x lifted load bounds 1.15 x lifted load, it is clear that the Regulatory Guide 3.61 criteria produce the minimum safety factor. The calculated safety factor at this location is

$$\text{SF} = \text{Lc2}/(\text{Load} \times 1.15) = 12.78$$

3.D.7.4 Inlet Vent-to Baseplate Weld (Bottom Lift)

Drawing 1561, sheet 3 identifies the weld available to transfer the lifted load to the hydraulic jacks (not part of the HI-STORM 100 System) used in the bottom lift scenario. Load carrying capacity is assigned only to the fillet welds. The weld leg length "t" and the total length of weld available for load transfer "L" (per inlet vent) are given as:

$$t = 0.5''$$

$$L = 2 \times 29.1875'' \text{ (see Bill-of-Materials item 13)} = 58.375''$$

The load capacity of the weld (Lc3), per the more severe Regulatory Guide 3.61 requirement, is

$$\text{Lc3} = 0.6 \times 33,150 \text{ psi} \times (0.7071 \times t \times L) = 410,499 \text{ lb.}$$

Therefore, the safety factor under three times lifted load (including an inertia amplifier) is

$$\text{SF} = 410,499 \text{ lb.}/(3 \times 360,000 \text{ lb.} \times 1.15)/4 = 1.32$$

3.D.8 Stress Analysis of the Pedestal Shield

The pedestal shield concrete serves to support the loaded MPC and the pedestal platform during normal storage. The pedestal shield concrete is confined by the surrounding pedestal shell that serves, during the lifting operation, to resist radial expansion of the concrete cylinder due to the Poisson Ratio effect under the predominate axial compression of the concrete pedestal shield.

The compressive load capacity of the concrete making up the pedestal shield is the compression area x allowable compressive stress. From Table 3.3.5, the allowable compressive stress in the concrete is

$$\sigma_c = 1535 \text{ psi}$$

The concrete cylinder diameter (see Bill-of-Materials, item 24) is

$$D_c = 67.875''$$

Therefore, the load capacity per the ACI 318.1 concrete code (Reference [3.3.2] in Section 3.8 of this FSAR), defined as Lc4, is

$$Lc4 = \sigma_c \times \text{compression area of concrete cylinder} = 1535 \text{ psi} \times 3618 \text{ sq. inch} = 5,554,154 \text{ lb.}$$

The applied load is conservatively assumed as the summed weight of the loaded MPC plus the pedestal platform plus the pedestal concrete shield.

$$W = 90,000 \text{ lb. (Table 3.2.1)} + 5120 \text{ lb. (weight spreadsheet)} + 5339 \text{ lb. (weight spreadsheet)} \\ = 100,459 \text{ lb.}$$

Conservatively applying the Regulatory Guide 3.61 criteria to the concrete (interpret the allowable compressive stress as the "yield stress" for this evaluation) gives a safety factor

$$SF = Lc4/3W*1.15 = 16.03 \quad (\text{Note that the 1.15 accounts for inertia effects during the lift})$$

The pedestal shell is assumed to fully confine the concrete. Therefore, during compression of the concrete, a maximum lateral (radially oriented) pressure is applied to the pedestal shell due to the Poisson Ratio effect. This pressure varies linearly with concrete depth. Assuming the Poisson's Ratio of the concrete to be $\nu = 0.2$, the maximum pressure on the pedestal shell is

$$p_{\text{confine}} = \nu/(1-\nu) \times (3W \times 1.15/\text{compression area of concrete cylinder}) = 0.25 \times 27.77 \text{ psi} \\ = 7.98 \text{ psi}$$

Conservatively neglecting variations with depth of concrete, the hoop stress in the confining pedestal shell is obtained as follows:

$$t = \text{pedestal shell thickness} = 0.25''$$

$$R = \text{pedestal shell mean radius} = (0.5 \times 68.375" + .5 \times 0.25") = 34.3125"$$

$$\text{Hoop Stress} = p_{\text{confine}} \times R/t = 1,095 \text{ psi}$$

This gives a safety factor based on the Regulatory Guide 3.61 criteria equal to

$$\text{SF} = 33,150 \text{ psi/Hoop Stress} = 30.27$$

This results is bounding for the HI-STORM 100S since the height and weight of the concrete pedestal is reduced.

3.D.9 Conclusion

The design of the HI-STORM 100 is adequate for the bottom end lift through the inlet vents. The design of the HI-STORM 100 is also adequate for the top end lift through the lifting lugs. Safety factors are established based on requirements of the ASME Code Section III, Subsection NF for Class 3 plate and shell supports and also on the requirements of USNRC Regulatory Guide 3.61. *The conclusions also apply to the HI-STORM 100S.*

3.D.10 References

1. ANSYS 5.3, A General Purpose Finite Element Code, ANSYS, Inc.
2. Crane Manufacturer's Association of America (CMAA), Specification #70, 1988, Section 3.3.
3. ASME Code Section III, Subsection NF-3324.5, Table NF-3324.5(a)-1, 1995

APPENDIX 3.I: HI-TRAC FREE THERMAL EXPANSIONS

3.I.1 Scope

In this calculation, estimates of operating gaps, both radially and axially, are computed for the fuel basket-to-MPC shell, and for the MPC shell-to-HI-TRAC. The temperature distribution used as input is derived from a hypothetical worst case MPC thermal load. This calculation is in support of the results presented in Section 3.4.4.2.

3.I.2 Methodology

Bounding temperatures are used to construct temperature distributions that will permit calculation of differential thermal expansions both radially and axially for the basket-to-MPC gaps, and for the MPC-to-HI-TRAC gaps. Reference temperatures are set at 70°F for all components. Temperature distributions are computed at the axial location of the HI-TRAC System where the temperatures are highest. A comprehensive nomenclature listing is provided in Section 3.I.6.

3.I.3 References

[3.I.1] Boley and Weiner, Theory of Thermal Stresses, John Wiley, 1960, Sec. 9.10, pp. 288-291.

[3.I.2] Burgreen, Elements of Thermal Stress Analysis, Arcturus Publishers, Cherry Hill NJ, 1988.

3.I.4 Calculations for Hot Components (Middle of System)

3.I.4.1 Input Data

Based on thermal calculations in Chapter 4, the following temperatures are appropriate at the hottest location of the HI-TRAC (see Figure 3.I.1 and Table 4.5.2).

The temperature change at the inside surface of the HI-TRAC, $\Delta T_{1h} := 322 - 70$

The temperature change at the inside of the water jacket, $\Delta T_{2h} := 314 - 70$

The temperature change at the mean radius of the MPC shell, $\Delta T_{3h} := 455 - 70$

The temperature change at the outside of the MPC basket, $\Delta T_{4h} := (600 - 70) \cdot 1.1$

The temperature change at the center of the basket, $\Delta T_{5h} := 852 - 70$

Note that the outer basket temperature is conservatively amplified by 10% to insure a bounding parabolic distribution. This conservatism serves to maximize the growth of the basket. The geometry of the components are as follows (referring to Figure 3.I.1)

The outer radius of the outer shell, $b := 40.625 \cdot \text{in}$

The inner radius of the HI-TRAC, $a := 34.375 \cdot \text{in}$

The mean radius of the MPC shell, $R_{\text{mpc}} := \frac{68.375 \cdot \text{in} - 0.5 \cdot \text{in}}{2}$ $R_{\text{mpc}} = 33.938 \text{ in}$

The initial MPC-to-overpack minimal radial clearance, $RC_{\text{mo}} := .5 \cdot (68.75 - 68.5) \cdot \text{in}$

$$RC_{\text{mo}} = 0.125 \text{ in}$$

For axial growth calculations of the MPC-to-HI-TRAC top flange clearance, the axial length of the HI-TRAC is defined as the distance from the bottom flange to the top flange, and the axial length of the MPC is defined as the overall MPC height.

The axial length of the HI-TRAC, $L_{\text{ovp}} := 191.25 \cdot \text{in}$

The axial length of the MPC, $L_{\text{mpc}} := 190.5 \cdot \text{in}$

The initial MPC-to-HI-TRAC nominal axial clearance, $AC_{\text{mo}} := L_{\text{ovp}} - L_{\text{mpc}}$

$$AC_{\text{mo}} = 0.75 \text{ in}$$

For growth calculations for the fuel basket-to-MPC shell clearances, the axial length of the basket is defined as the total length of the basket and the outer radius of the basket is defined as the mean radius of the MPC shell minus one-half of the shell thickness minus the initial basket-to-shell radial clearance.

The axial length of the basket, $L_{\text{bas}} := 176.5 \cdot \text{in}$

The initial basket-to-MPC lid nominal axial clearance, $AC_{\text{bm}} := 1.8125 \cdot \text{in}$

The initial basket-to-MPC shell nominal radial clearance, $RC_{\text{bm}} := 0.1875 \cdot \text{in}$

The outer radius of the basket, $R_b := R_{\text{mpc}} - \frac{0.5}{2} \cdot \text{in} - RC_{\text{bm}}$ $R_b = 33.5 \text{ in}$

The coefficients of thermal expansion used in the subsequent calculations are based on the mean temperatures of the MPC shell and a bounding mean temperature for the basket.

The coefficient of thermal expansion for the MPC shell, $\alpha_{\text{mpc}} := 9.338 \cdot 10^{-6}$

The coefficient of thermal expansion for the basket, $\alpha_{\text{bas}} := 9.90 \cdot 10^{-6}$ 800 deg. F

3.I.4.2 Thermal Growth of the Overpack

Results for thermal expansion deformation and stress in the overpack are obtained here. The system is replaced by a equivalent uniform hollow cylinder with approximated average properties.

Based on the given inside and outside surface temperatures, the temperature solution in the cylinder is given in the form:

$$C_a + C_b \cdot \ln\left(\frac{r}{a}\right)$$

where,

$$C_a := \Delta T_{1h} \quad C_a = 252$$

$$C_b := \frac{\Delta T_{2h} - \Delta T_{1h}}{\ln\left(\frac{b}{a}\right)} \quad C_b = -47.889$$

Next, form the integral relationship:

$$Int := \int_a^b \left[C_a + C_b \cdot \ln\left(\frac{r}{a}\right) \right] \cdot r \, dr$$

The Mathcad program, which was used to create this appendix, is capable of evaluating the integral "Int" either numerically or symbolically. To demonstrate that the results are equivalent, the integral is evaluated both ways in order to qualify the accuracy of any additional integrations that are needed.

The result obtained through numerical integration, $Int = 5.807 \times 10^4 \text{ in}^2$

To perform a symbolic evaluation of the solution the integral "Ints" is defined. This integral is then evaluated using the Maple symbolic math engine built into the Mathcad program as:

$$Int_s := \int_a^b \left[C_a + C_b \cdot \ln\left(\frac{r}{a}\right) \right] \cdot r \, dr$$

$$Int_s := \frac{1}{2} \cdot C_b \cdot \ln\left(\frac{b}{a}\right) \cdot b^2 + \frac{1}{2} \cdot C_a \cdot b^2 - \frac{1}{4} \cdot C_b \cdot b^2 + \frac{1}{4} \cdot C_b \cdot a^2 - \frac{1}{2} \cdot C_a \cdot a^2 \quad Int_s = 5.807 \times 10^4 \text{ in}^2$$

We note that the values of Int and Ints are identical. The average temperature in the overpack cylinder (T_{bar}) is therefore determined as:

$$T_{\text{bar}} := \frac{2}{(b^2 - a^2)} \cdot \text{Int}$$

$$T_{\text{bar}} = 247.778$$

We estimate the average coefficient of thermal expansion for the HI-TRAC by weighting the volume of the various layers. A total of three layers are identified for this calculation. They are:

- 1) the inner shell
- 2) the radial lead shield
- 3) the outer shell

Thermal properties are based on estimated temperatures in the component and coefficient of thermal expansion values taken from the tables in Chapter 3. The following averaging calculation involves the thicknesses (t) of the various components, and the estimated coefficients of thermal expansion at the components' mean radial positions. The results of the weighted average process yields an effective coefficient of linear thermal expansion for use in computing radial growth of a solid cylinder (the overpack).

The thicknesses of each component are defined as:

$$t_1 := 0.75 \cdot \text{in}$$

$$t_2 := 4.5 \cdot \text{in}$$

$$t_3 := 1.0 \cdot \text{in}$$

and the corresponding mean radii can therefore be defined as:

$$r_1 := a + .5 \cdot t_1$$

$$r_2 := r_1 + .5 \cdot t_1 + .5 \cdot t_2$$

$$r_3 := r_2 + .5 \cdot t_2 + .5 \cdot t_3$$

To check the accuracy of these calculations, the outer radius of the HI-TRAC is calculated from r_3 and t_3 , and the result is compared with the previously defined value (b).

$$b_1 := r_3 + 0.5 \cdot t_3$$

$$b_1 = 40.625 \text{ in}$$

$$b = 40.625 \text{ in}$$

We note that the calculated value b_1 is identical to the previously defined value b . The coefficients of thermal expansion for each component, estimated based on the temperature gradient, are defined as:

$$\begin{aligned}\alpha_1 &:= 6.3382 \cdot 10^{-6} \\ \alpha_2 &:= 17.2 \cdot 10^{-6} \quad @300 \text{ deg F} \\ \alpha_3 &:= 6.311 \cdot 10^{-6}\end{aligned}$$

Thus, the average coefficient of thermal expansion of the HI-TRAC is determined as:

$$\begin{aligned}\alpha_{avg} &:= \frac{r_1 \cdot t_1 \cdot \alpha_1 + r_2 \cdot t_2 \cdot \alpha_2 + r_3 \cdot t_3 \cdot \alpha_3}{\frac{a+b}{2} \cdot (t_1 + t_2 + t_3)} \\ \alpha_{avg} &= 1.413 \times 10^{-5}\end{aligned}$$

Reference 3.I.1 gives an expression for the radial deformation due to thermal growth. At the inner radius of the HI-TRAC ($r = a$), the radial growth is determined as:

$$\Delta R_{ah} := \alpha_{avg} \cdot a \cdot T_{bar} \quad \Delta R_{ah} = 0.12 \text{ in}$$

Similarly, an overestimate of the axial growth of the HI-TRAC can be determined by applying the average temperature (T_{bar}) over the entire length of the overpack as:

$$\begin{aligned}\Delta L_{ovph} &:= L_{ovp} \cdot \alpha_{avg} \cdot T_{bar} \\ \Delta L_{ovph} &= 0.669 \text{ in}\end{aligned}$$

Estimates of the secondary thermal stresses that develop in the HI-TRAC due to the radial temperature variation are determined using a conservatively high value of E as based on the temperature of the steel. The circumferential stress at the inner and outer surfaces (σ_{ca} and σ_{cb} , respectively) are determined as:

The Young's Modulus of the material, $E := 28600000 \cdot \text{psi}$

$$\sigma_{ca} := \alpha_{avg} \cdot \frac{E}{a^2} \cdot \left[2 \cdot \frac{a^2}{(b^2 - a^2)} \cdot \text{Int} - (C_a) \cdot a^2 \right] \quad \sigma_{ca} = -1706 \text{ psi}$$

$$\sigma_{cb} := \alpha_{avg} \cdot \frac{E}{b^2} \cdot \left[2 \cdot \frac{b^2}{(b^2 - a^2)} \cdot \text{Int} - \left[C_a + C_b \cdot \left(\ln \left(\frac{b}{a} \right) \right) \right] \cdot b^2 \right] \quad \sigma_{cb} = 1526 \text{ psi}$$

The radial stress due to the temperature gradient is zero at both the inner and outer surfaces of the HI-TRAC. The radius where a maximum radial stress is expected, and the corresponding radial stress, are determined by trial and error as:

$$N := 0.47$$

$$r := a \cdot (1 - N) + N \cdot b$$

$$r = 37.313 \text{ in}$$

$$\sigma_r := \alpha_{avg} \cdot \frac{E}{r} \cdot \left[\frac{r^2 - a^2}{2} \cdot T_{bar} - \int_a^r \left[C_a + C_b \cdot \left(\ln \left(\frac{y}{a} \right) \right) \right] \cdot y \, dy \right]$$

$$\sigma_r = -67.389 \text{ psi}$$

The axial stress developed due to the temperature gradient is equal to the sum of the radial and tangential stresses at any radial location. (see eq. 9.10.7) of [3.I.1]. Therefore, the axial stresses are available from the above calculations. The stress intensities in the HI-TRAC due to the temperature distribution are below the Level A membrane stress.

3.I.4.3 Thermal Growth of the MPC Shell

The radial and axial growth of the MPC shell (ΔR_{mpch} and ΔL_{mpch} , respectively) are determined as:

$$\Delta R_{mpch} := \alpha_{mpc} \cdot R_{mpc} \cdot \Delta T_{3h}$$

$$\Delta R_{mpch} = 0.122 \text{ in}$$

$$\Delta L_{mpch} := \alpha_{mpc} \cdot L_{mpc} \cdot \Delta T_{3h}$$

$$\Delta L_{mpch} = 0.685 \text{ in}$$

3.I.4.4 Clearances Between the MPC Shell and HI-TRAC

The final radial and axial MPC shell-to-HI-TRAC clearances (RG_{moh} and AG_{moh} , respectively) are determined as:

$$RG_{moh} := RC_{mo} + \Delta R_{ah} - \Delta R_{mpch}$$

$$RG_{moh} = 0.123 \text{ in}$$

$$AG_{moh} := AC_{mo} + \Delta L_{ovph} - \Delta L_{mpch}$$

$$AG_{moh} = 0.735 \text{ in}$$

Note that this axial clearance (AG_{moh}) is based on the temperature distribution at the top end of the system.

3.I.4.5 Thermal Growth of the MPC Basket

Using formulas given in [3.I.2] for a solid body of revolution, and assuming a parabolic temperature distribution in the radial direction with the center and outer temperatures given previously, the following relationships can be developed for free thermal growth.

$$\text{Define } \Delta T_{bas} := \Delta T_{5h} - \Delta T_{4h}$$

$$\Delta T_{bas} = 199$$

$$\text{Then the mean temperature can be defined as } T_{bar} := \frac{2}{R_b^2} \cdot \int_0^{R_b} \left(\Delta T_{5h} - \Delta T_{bas} \cdot \frac{r^2}{R_b^2} \right) \cdot r \, dr$$

Using the Maple symbolic engine again, the closed form solution of the integral is:

$$T_{bar} := \frac{2}{R_b^2} \cdot \left(\frac{-1}{4} \cdot \Delta T_{bas} \cdot R_b^2 + \frac{1}{2} \cdot \Delta T_{5h} \cdot R_b^2 \right)$$

$$T_{bar} = 682.5$$

The corresponding radial growth at the periphery (ΔR_{bh}) is therefore determined as:

$$\Delta R_{bh} := \alpha_{bas} \cdot R_b \cdot T_{bar} \quad \Delta R_{bh} = 0.226 \text{ in}$$

and the corresponding axial growth (ΔL_{bas}) is determined from [3.I.2] as:

$$\Delta L_{bh} := \Delta R_{bh} \cdot \frac{L_{bas}}{R_b} \quad \Delta L_{bh} = 1.193 \text{ in}$$

Note that the coefficient of thermal expansion for the hottest basket temperature has been used, and the results are therefore conservative.

3.I.4.6 Clearances Between the Fuel Basket and MPC Shell

The final radial and axial fuel basket-to-MPC shell and lid clearances (RG_{bmh} and AG_{bmh} , respectively) are determined as:

$$RG_{bmh} := RC_{bm} - \Delta R_{bh} + \Delta R_{mpch}$$

$$RG_{bmh} = 0.083 \text{ in}$$

$$AG_{bmh} := AC_{bm} - \Delta L_{bh} + \Delta L_{mpch}$$

$$AG_{bmh} = 1.305 \text{ in}$$

3.I.5 Summary of Results

The previous results are summarized here.

MPC Shell-to-HI-TRAC

$$RG_{moh} = 0.123 \text{ in}$$

$$AG_{moh} = 0.735 \text{ in}$$

Fuel Basket-to-MPC Shell

$$RG_{bmh} = 0.083 \text{ in}$$

$$AG_{bmh} = 1.305 \text{ in}$$

3.I.6 Nomenclature

a is the inner radius of the HI-TRAC

AC_{bm} is the initial fuel basket-to-MPC axial clearance.

AC_{mo} is the initial MPC-to-HI-TRAC axial clearance.

AG_{bmh} is the final fuel basket-to-MPC shell axial gap for the hot components.

AG_{moh} is the final MPC shell-to-HI-TRAC axial gap for the hot components.

b is the outer radius of the HI-TRAC

L_{bas} is the axial length of the fuel basket.

L_{mpc} is the axial length of the MPC.

L_{ovp} is the axial length of the HI-TRAC.

r_1 (r_2, r_3) is mean radius of the HI-TRAC inner shell (radial lead shield, outer shell).

R_b is the outer radius of the fuel basket.

R_{mpc} is the mean radius of the MPC shell.

RC_{bm} is the initial fuel basket-to-MPC radial clearance.

RC_{mo} is the initial MPC shell-to-HI-TRAC radial clearance.

RG_{bmh} is the final fuel basket-to-MPC shell radial gap for the hot components.

RG_{moh} is the final MPC shell-to-HI-TRAC radial gap for the hot components.

t_1 (t_2, t_3) is the thickness of the HI-TRAC inner shell (radial lead shield, outer shell).

T_{bar} is the average temperature of the HI-TRAC cylinder.

α_1 (α_2, α_3) is the coefficient of thermal expansion of the HI-TRAC inner shell (radial lead shield, outer shell).

α_{avg} is the average coefficient of thermal expansion of the HI-TRAC.

α_{bas} is the coefficient of thermal expansion of the HI-TRAC.

α_{mpc} is the coefficient of thermal expansion of the MPC.

ΔL_{bh} is the axial growth of the fuel basket for the hot components.

ΔL_{mpch} is the axial growth of the MPC for the hot components.
 ΔL_{ovph} is the axial growth of the HI-TRAC for the hot components.
 ΔR_{ah} is the radial growth of the HI-TRAC inner radius for the hot components.
 ΔR_{bh} is the radial growth of the fuel basket for the hot components.
 ΔR_{mpch} is the radial growth of the MPC shell for the hot components.
 ΔT_{1h} is the temperature change at the HI-TRAC inside surface for hot components.
 ΔT_{2h} is the temperature change at the inside of the water jackets for hot components.
 ΔT_{3h} is the temperature change at the MPC shell mean radius for hot components.
 ΔT_{4h} is the temperature change at the MPC basket periphery for hot components.
 ΔT_{5h} is the temperature change at the MPC basket centerline for hot components.
 ΔT_{bas} is the fuel basket centerline-to-periphery temperature gradient.
 σ_{ca} is the circumferential stress at the HI-TRAC inner surface.
 σ_{cb} is the circumferential stress at the HI-TRAC outer surface.
 σ_r is the maximum radial stress of the HI-TRAC.

APPENDIX 3.M VERTICAL DROP OF OVERPACK

3.M.1 Introduction

The fully loaded HI-STORM 100 storage overpack, with the top lid in place, is assumed to fall vertically from a limiting carry height (see Appendix 3.A) onto the ISFSI pad and is brought to rest with a vertical deceleration of 45 g's. This appendix evaluates the stresses induced on the various elements in the load path as a result of this handling accident. Appendix 3.D has considered vertical handling of the storage overpack; where applicable, results from that analysis are simply amplified by appropriate factors to simulate the loads induced by the vertical drop. The load path in the HI-STORM 100S is "simpler"; an analysis of the HI-STORM 100S top lid bending is also included in this appendix conservatively assuming that the entire lid amplified weight is supported by the lower of the two lid plates.

3.M.2 Methodology

Strength of materials formulations are used to establish the state of stress in the various components of the load path. The structural components of the storage overpack considered here as potentially limiting are:

- Lid bottom plate
- Lid shell
- Lid top plate
- Inner shell
- Inlet vent horizontal plates
- Inlet vent vertical plates
- Pedestal shield
- Pedestal shell
- Structural welds in the load path

Except for direct compression, the shielding material is assumed to have no structural resistance. The decelerated mass of the shield is imposed as a load on the supporting member.

3.M.3 Analyses

3.M.3.1 Lid Bottom Plate

The shell thickness is less than the bottom plate thickness and provides some degree of clamping action. Conservatively evaluate the state of stress in this plate by assuming simple support conditions at the outer periphery where the connection is made to the lid shell. This analysis leads to the maximum stress occurring at the center of the lid bottom plate. Figure 3.M.1 is a sketch of the configuration to be analyzed.

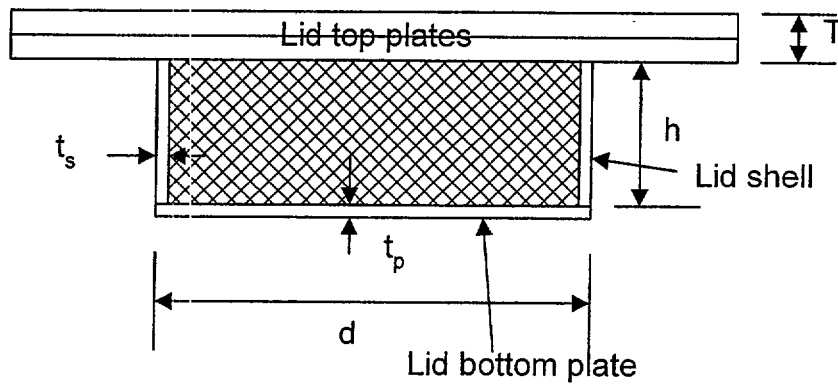


FIGURE 3.M.1 Geometry of Lid Shield

Input Data: (from BM-1575 and Appendix 3.K)

$d := 69\text{-in}$ $t_p := 1.25\text{-in}$ $t_s := 1\text{-in}$

$h := 10.5\text{-in}$ $T := 4\text{-in}$

The weight of the shield material is $W_{\text{shield}} := 3213\text{-lbf}$

The weight of the bottom plate is $W_{\text{bot}} := 1323\text{-lbf}$

see calculations in Appendix 3.K

The weight of the lid shell is

$$W_{\text{shell}} := 0.283 \cdot \frac{\text{lbf}}{\text{in}^3} \cdot \pi \cdot (d - t_s) \cdot h \cdot t_s$$

$W_{\text{shell}} = 634.796\text{ lbf}$

Design basis deceleration $G := 45$ Table 2.2.8

For the Level D event, the allowable stress intensity of SA-516 Grade 70, at 350 degrees F, is obtained from Table 3.1.12.

$S_a := 59650\text{-psi}$ Primary membrane plus primary bending

$S_{\text{apm}} := 39750\text{-psi}$ Primary membrane only

The ultimate strength of the material is

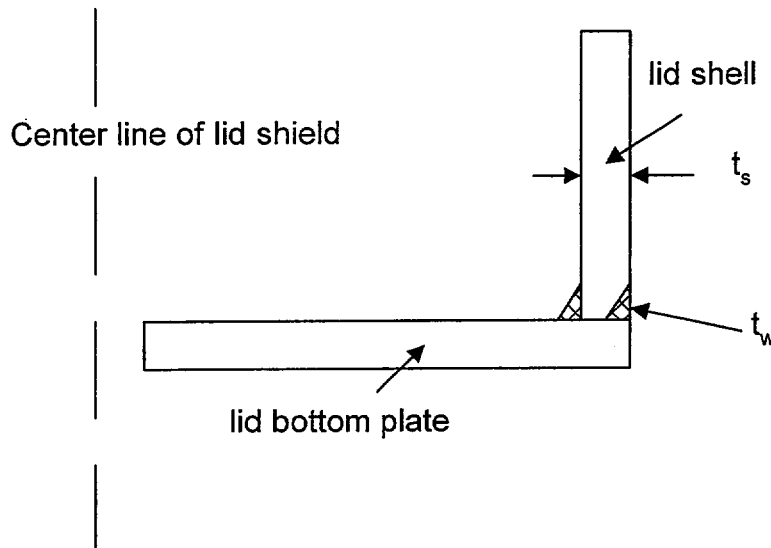
$$S_u := 70000 \cdot \text{psi}$$

The amplified lateral pressure load on the plate under the vertical handling event is computed as:

$$p := G \cdot \frac{(W_{\text{shield}} + W_{\text{bot}})}{\left(\frac{\pi \cdot d^2}{4}\right)} \quad p = 54.588 \text{ psi}$$

The lid bottom plate and the lid shell are connected by peripheral welds. These welds are sized to insure that they have the same moment capacity as the shell (the thinner of the two components). With this insured, then full credit can be assured for moment transfer at the joint. The weld calculation is given below:

It is required to determine the weld leg size that insures the moment carrying capacity of the following configuration:



Unit circumferential width

$$b := 1 \cdot \text{in}$$

The moment in the lid shell when the extreme fiber stress equals the allowable stress is

$$M_p := \frac{b \cdot t_s^2}{6} \cdot S_a$$

The weld area is (conservatively assume fillet welds)

$$A_w := .7071 \cdot t_w \cdot b$$

The moment capacity of the pair of fillet welds is

$$M_w := .42 \cdot S_u \cdot (A_w) \cdot t_s \quad \text{where the moment arm is } t_s \text{ and Table 3.3.2 gives } S_u$$

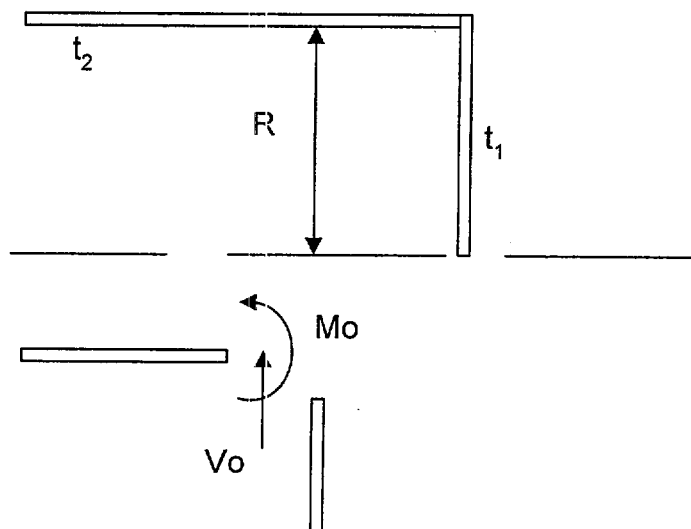
Equating the two moment expressions and solving for the weld size gives

$$t_w := \frac{S_a \cdot t_s}{6 \cdot (.42 \cdot .7071) \cdot S_u} \quad t_w = 0.478 \text{ in}$$

The specified weld size on the drawing 1561, sheet 2 meets the requirement. Therefore, the connection can fully support moment transfer.

To obtain the joint moment, we conservatively consider the lid bottom plate and the lid shell as the closed end of a pressure vessel and use a classical plate-shell solution to determine the shear force and bending moment at the joint. The "internal pressure" is taken as the amplified pressure due to the weight of the shield and the lid bottom plate. Note that this assumption loads the shell with a larger internal pressure than actually occurs.

The solution comes from Table XIII, Case 30 of the text "Formulas for Stress and Strain", R. Roark, McGraw Hill, 4th Edition. The configuration is shown below with nomenclature per the referenced case:



Following the reference text, define

$$E := 28000000 \cdot \text{psi} \quad \text{Young's Modulus of SA-516 Grade 70 @ 350 degrees F}$$

$$R := \frac{d}{2} - \frac{t_s}{2}$$

$$R = 34 \text{ in}$$

$$\nu := 0.3$$

Poisson's Ratio

$$t_2 := t_s$$

$$t_2 = 1 \text{ in}$$

$$t_1 := t_p$$

$$t_1 = 1.25 \text{ in}$$

$$D_1 := \frac{E \cdot t_1^3}{12 \cdot (1 - \nu^2)}$$

$$D_2 := \frac{E \cdot t_2^3}{12 \cdot (1 - \nu^2)}$$

$$\lambda := \left[3 \cdot \frac{(1 - \nu^2)}{R^2 \cdot t_2^2} \right]^{.25}$$

$$\lambda = 0.22 \text{ in}^{-1}$$

Compute the following quantities in accordance with Roark's text

$$x_1 := \frac{p \cdot R^3 \cdot \lambda^2 \cdot D_2}{4 \cdot D_1 \cdot (1 + \nu)}$$

$$x_2 := \frac{2 \cdot p \cdot R^2 \cdot \lambda^3 \cdot t_1 \cdot D_2}{t_2 \cdot (1 - .5 \cdot \nu) \cdot [E \cdot t_1 + 2 \cdot R \cdot D_2 \cdot \lambda^3 \cdot (1 - \nu)]}$$

$$x_3 := 2 \cdot \lambda$$

$$x_4 := \frac{2 \cdot R \cdot \lambda^2 \cdot D_2}{D_1 \cdot (1 + \nu)}$$

$$x_5 := \frac{\lambda \cdot E \cdot t_1}{E \cdot t_1 + 2 \cdot D_2 \cdot \lambda^3 \cdot R \cdot (1 - \nu)}$$

$$x_6 := 2 \cdot \lambda + \frac{2 \cdot R \cdot \lambda^2 \cdot D_2}{D_1 \cdot (1 + \nu)}$$

$$x_7 := \frac{p \cdot R^3 \cdot \lambda^2 \cdot D_2}{4 \cdot D_1 \cdot (1 + \nu)}$$

Then M_o and V_o are computed as

$$M_o := \frac{x_1 + x_2}{x_3 + x_4 - x_5}$$

$$M_o = 6.802 \times 10^3 \text{ in} \cdot \frac{\text{lbf}}{\text{in}}$$

$$V_o := M_o \cdot x_6 - x_7$$

$$V_o = 1.586 \times 10^3 \frac{\text{lbf}}{\text{in}}$$

Stress in the lid shell:

a. due to pressure

$$t_2 = 1 \text{ in}$$

$$\sigma_{xp} := \frac{p \cdot R}{2 \cdot t_2}$$

$$\sigma_{xp} = 927.995 \text{ psi}$$

$$t_1 = 1.25 \text{ in}$$

$$\sigma_{\theta} := 2 \cdot \sigma_{xp}$$

$$\sigma_{\theta} = 1.856 \times 10^3 \text{ psi}$$

b. due to Mo

$$\sigma_{xmo} := \frac{6 \cdot Mo}{t_2^2} \quad \sigma_{xmo} = 4.081 \times 10^4 \text{ psi} \quad \text{bending stress}$$

$$\sigma_w := \sigma_{xmo} \quad \text{defined for later use}$$

$$\sigma_{\theta mo} := \frac{2 \cdot Mo}{t_2} \cdot \lambda \cdot R \quad \sigma_{\theta mo} = 2.248 \times 10^4 \text{ psi} \quad \text{membrane stress}$$

$$\sigma_{\theta b} := \nu \cdot \sigma_{xmo} \quad \sigma_{\theta b} = 1.224 \times 10^4 \text{ psi} \quad \text{bending stress}$$

c. due to Vo - away from the end a distance $\frac{\pi}{4 \cdot \lambda} = 3.563 \text{ in}$

$$\sigma_{xvo} := \frac{1.932 \cdot Vo}{(\lambda \cdot t_2^2)} \quad \sigma_{xvo} = 1.39 \times 10^4 \text{ psi} \quad \text{bending stress}$$

$$\sigma_{\theta vo} := \frac{2 \cdot Vo}{t_2} \cdot \lambda \cdot R \quad \sigma_{\theta vo} = 2.377 \times 10^4 \text{ psi} \quad \text{membrane stress}$$

$$\sigma_{\theta b} := \nu \cdot \sigma_{xvo} \quad \sigma_{\theta b} = 4.17 \times 10^3 \text{ psi} \quad \text{bending stress}$$

The shell stresses at the joint are considered as secondary stress in ASME parlance; they are not required to meet any limits under a Level D event (per Appendix F, F1332). It is noted, however, that the sum of the maximum extreme fiber stresses are less than the limits for primary membrane plus bending stress per Table 3.1.12.

Stress in the lid bottom plate (stresses evaluated on shield side surface, positive value is compression):

a. due to pressure (stress at center of plate - x means radial stress in the plate)

$$W := p \cdot \pi \cdot R^2 \quad W = 1.982 \times 10^5 \text{ lbf} \quad m := \frac{1}{\nu} \quad t_1 = 1.25 \text{ in}$$

$$\sigma_{xp} := 3 \cdot \frac{W}{8 \cdot \pi \cdot m \cdot t_1^2} \cdot (3 \cdot m + 1) \quad \sigma_{xp} = 4.998 \times 10^4 \text{ psi}$$

$$\sigma_{\theta} := \sigma_{xp} \quad \sigma_{\theta} = 4.998 \times 10^4 \text{ psi}$$

b. due to Mo (any radial location (shield side of plate))

$$\sigma_{xmo} := \frac{-6 \cdot Mo}{t_1^2} \quad \sigma_{xmo} = -2.612 \times 10^4 \text{ psi} \quad \text{bending stress}$$

$$\sigma_{\theta b} := 1 \cdot \sigma_{xmo} \quad \sigma_{\theta b} = -2.612 \times 10^4 \text{ psi} \quad \text{bending stress}$$

c. due to Vo - uniform tensile radial stress

$$\sigma_{xvo} := \frac{Vo}{t_1} \quad \sigma_{xvo} = 1.269 \times 10^3 \text{ psi} \quad \text{membrane stress}$$

The lid bottom plate stresses at the joint are considered as "primary" in ASME parlance; they are required to meet the limits under a Level D event given in Table 3.1.12 at 350 degrees F.

The maximum stress at the center of the lid bottom plate is

$$\sigma_1 := \sigma_{xp} + \sigma_{xmo} \quad \sigma_1 = 2.386 \times 10^4 \text{ psi}$$

The maximum stress at the outside radius of the lid bottom plate is

$$\sigma_1 := \sigma_{xmo} \quad \sigma_1 = -2.612 \times 10^4 \text{ psi}$$

Therefore, the safety factor for the lid bottom plate is

$$SF_{\text{lidbot}} := \frac{S_a}{-\sigma_1} \quad SF_{\text{lidbot}} = 2.284$$

3.M.3.2 Lid Shell Weld to Lid Bottom Plate and to Lid Top Plate

3.M.3.2.1 Lid Bottom Plate-to Lid Shell Weld

By virtue of the calculations in the previous section where we demonstrate that the weld can support the developed moment, the safety factor in the weld is equal to the safety factor in the shell if we consider the stress due to Mo as a primary bending stress for a Level D event. Thus

$$SF_{\text{weld1}} := \frac{S_a}{\sigma_w} \quad SF_{\text{weld1}} = 1.462$$

The actual weld stress induced to support the bending moment is

$$\tau_1 := \frac{.42 \cdot S_u}{SF_{\text{weld1}}} \quad \tau_1 = 2.012 \times 10^4 \text{ psi}$$

The weld stress due to the shear force V_o is computed as follows. The weld area of each of the fillet welds is

$$A_w := .7071 \cdot t_w \cdot b \qquad A_w = 0.338 \text{ in}^2 \qquad \text{for a 1" circumferential width}$$

Therefore

$$\tau_2 := \frac{V_o \cdot b}{2 \cdot A_w} \qquad \tau_2 = 2.345 \times 10^3 \text{ psi}$$

The weld stress due to the total vertical load W is

$$\tau_3 := \frac{W}{2\pi \cdot R} \cdot b \cdot \frac{1}{2 \cdot A_w} \qquad \tau_3 = 1.372 \times 10^3 \text{ psi}$$

Thus the final safety factor, after accounting for all weld shear stresses, is

$$SF_{\text{weld1}} := \frac{.42 \cdot S_u}{\sqrt{(\tau_1 + \tau_3)^2 + \tau_2^2}} \qquad SF_{\text{weld1}} = 1.36$$

The weld shear stresses due to V_o and due to direct vertical load are small compared to the weld stress.

3.M.3.2.2 Lid Top Plate-to Lid Shell Weld

This weld is an outside fillet weld attaching the lid shell to the top plate. The weld leg size is "tf" where

$$tf := \frac{5}{16} \cdot \text{in} \qquad \text{Drawing 1561, sheet 2}$$

The total load applied to the weld from the postulated drop consists of the total weight of the shield material, the lid bottom plate, and the lid shell, all amplified by the design basis deceleration.

$$\text{Load} := G \cdot (W_{\text{shield}} + W_{\text{bot}} + W_{\text{shell}}) \qquad \text{Load} = 2.327 \times 10^5 \text{ lbf}$$

This load is supported by the lid shell-bottom plate fillet weld acting in shear. The weld shear stress is computed as

$$\tau_{\text{weld_shear}} := \frac{\text{Load}}{\pi \cdot (d + .667 \cdot tf) \cdot (0.7071 \cdot tf)} \qquad \tau_{\text{weld_shear}} = 4.843 \times 10^3 \text{ psi}$$

For the postulated Level D drop event, the allowable weld stress is based upon the ultimate strength of the base material. Therefore, the safety factor, SF, for this weld is

$$SF := .42 \cdot \frac{S_u}{\tau_{\text{weld_shear}}} \quad SF = 6.07$$

This weld does not provide the minimum safety factor under this condition.

3.M.3.3 Lid Shell (conservatively considered as a membrane shell and neglecting end effects)

The circumferential membrane stress away from supports is

$$\sigma_c := p \cdot \frac{R}{t_2} \quad \sigma_c = 1.856 \times 10^3 \text{ psi}$$

The axial membrane stress away from supports is

$$\sigma_a := .5 \cdot \sigma_c \quad \sigma_a = 927.995 \text{ psi}$$

The safety factor on primary stress intensity is

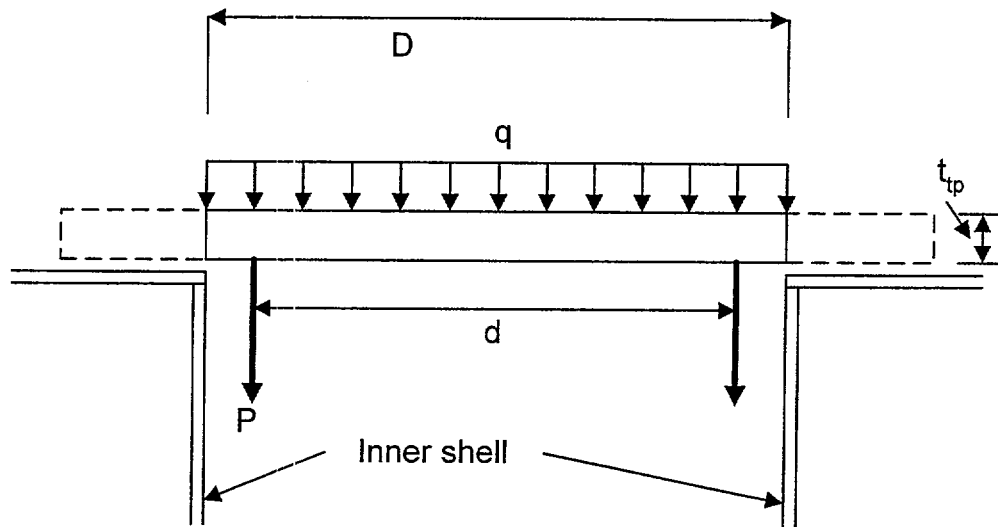
$$SF_{Is} := \frac{S_{apm}}{\sigma_c} \quad SF_{Is} = 21.417$$

3.M.3.4 Lid Top Plates - HI-STORM 100

The lid top plates are two separate components each of thickness

$$t_{tp} := .5 \cdot T \quad t_{tp} = 2 \text{ in}$$

Under the postulated handling event, the lower of the two plates will deflect more than the upper plate because the total load is greater (the lid shield and surrounding steel weighs more than the shield block and its surrounding steel (see Appendix 3.K, subsections 3.K.4.2 and 3.K.4.3). Therefore, we focus the stress analysis on the lower of the two lid top plates. The configuration is analyzed as a simply supported plate with diameter equal to the outer diameter of the inner shell of the HI-STORM 100 storage overpack. The overhanging part of the top plate is conservatively neglected since the overhanging weight will give stresses that reduce the stress in the central section of the top plate. The configuration is shown below:



$D := 73.5\text{-in} + 1.5\text{-in}$ DWG. 1495, sheet 2

$d = 69\text{ in}$

The weight of the lid shell (see appendix 3.K) is $W_{\text{lidshell}} := 634.8\text{-lbf}$

Therefore, the load P (per unit circumferential length) is

$$P := \frac{G \cdot (W_{\text{shield}} + W_{\text{bot}} + W_{\text{lidshell}})}{\pi \cdot d} \quad P = 1.073 \times 10^3 \frac{\text{lbf}}{\text{in}}$$

The amplified pressure due to the the lid plate self weight is

$$q := G \cdot 283 \cdot \frac{\text{lbf}}{\text{in}^3} \cdot t_{\text{tp}} \quad q = 25.47\text{ psi} \quad (\text{density from Subsection 3.3.1.1})$$

The maximum stress in the top lid plate occurs at the center of the plate. Using Timoshenko and Woinowsky-Krieger, Theory of shells (second edition, p. 64), calculate

$$a := \frac{D}{2} \quad c := \frac{d}{2} \quad \nu = 0.3 \quad Q := 2 \cdot \pi \cdot c \cdot P$$

$$M_1 := (1 - \nu) \cdot Q \cdot \frac{(c^2 - a^2)}{8 \cdot \pi \cdot a^2} - \frac{(1 + \nu) \cdot Q \cdot \log\left(\frac{c}{a}\right)}{4 \cdot \pi} \quad M_1 = -123.768\text{ lbf}$$

$$\sigma_1 := 6 \cdot \frac{M_1}{t_{tp}^2}$$

$$\sigma := \frac{3 \cdot (3 + \nu)}{8} \cdot q \cdot \left(\frac{D}{2 \cdot t_{tp}} \right)^2 - \sigma_1$$

$$\sigma = 1.127 \times 10^4 \text{ psi}$$

The safety factor is

$$SF_{lid_top_plate} := \frac{S_a}{\sigma}$$

$$SF_{lid_top_plate} = 5.294$$

Note that the lid remains in the elastic range under this loading; therefore, there is no potential for an impact with the MPC and no effect on continued retrievability of the MPC.

3.M.3.5 Inner Shell

The inner shell is conservatively assumed to resist the reaction load from the top plate plus its own amplified weight (including the shield shell), plus a linearly varying pressure from radial expansion of the concrete due to a Poisson ratio effect. In the following, the potential for overstress and compression buckling under the load is examined.

Input data

Inner shell thickness $t_{is} := 1.25 \cdot \text{in}$ BM-1575

Inside diameter of inner shell $d_{inner} := 73.5 \cdot \text{in}$ DWG 1495 sheet 2

Shield shell thickness $t_{ss} := 0.75 \cdot \text{in}$ BM-1575

Length of inner shell $L_{is} := 224.5 \cdot \text{in}$

The amplified load applied through the lid top plate is conservatively assumed as the bounding weight of the top lid as listed in Table 3.2.1 and it is conservatively assumed that the inner shell supports the entire load.

$$W_{total} := 23000 \cdot \text{Ibf} \cdot G \quad W_{total} = 1.035 \times 10^6 \text{ Ibf}$$

The load per unit mean circumferential length at the top of the of the inner shell is

$$P_{mean} := \frac{W_{total}}{\pi \cdot (d_{inner} + t_{is})} \quad P_{mean} = 4.407 \times 10^3 \frac{\text{Ibf}}{\text{in}}$$

This results in a constant compressive stress in the inner shell equal to

$$\sigma_{mean} := \frac{P_{mean}}{t_{is}} \quad \sigma_{mean} = 3.526 \times 10^3 \text{ psi}$$

An amplified bounding weight of the shells adds an additional stress to the above value at the bottom of the storage overpack inner shell as follows:

$$W_{\text{shells}} := 0.283 \cdot \frac{\text{lbf}}{\text{in}^3} \cdot \frac{\pi}{4} \cdot \left[(d_{\text{inner}} + 2 \cdot t_{\text{is}} + 2 \cdot t_{\text{ss}})^2 - d_{\text{inner}}^2 \right] \cdot L_{\text{is}} \quad W_{\text{shells}} = 3.014 \times 10^4 \text{ lbf}$$

$$\sigma_{\text{meanw}} := \frac{W_{\text{shells}} \cdot G}{\pi \cdot (d_{\text{inner}} + t_{\text{is}}) \cdot t_{\text{is}}} \quad \sigma_{\text{meanw}} = 4.62 \times 10^3 \text{ psi}$$

This stress component is zero at the top of the inner shell and varies linearly until it reaches the maximum value given above at the bottom of the inner shell.

Finally, there is an amplified pressure on the outer surface of the inner shell imposed by the Poisson ratio effect from the compression of the concrete in the radial shield. The maximum value of this radial stress is

$$\sigma_{\text{radial}} := \frac{\nu_c}{1 - \nu_c} \cdot \sigma_c \quad \nu_c := 0.2$$

where σ_c is the compressive stress in the concrete at the baseplate. This stress is linearly varying from the top of the inner shell to the baseplate. The concrete compressive stress, at the base, is estimated as follows:

The weight density of concrete is $\gamma_c := 150 \cdot \frac{\text{lbf}}{\text{ft}^3}$

Using the length of the inner shell as the height of the concrete column gives

$$\sigma_c := \gamma_c \cdot L_{\text{is}} \cdot G \quad \sigma_c = 876.952 \text{ psi}$$

Note that this is below the allowable compressive stress in the concrete (Table 3.3.5). Therefore, the maximum value of the radial(external) pressure imposed on the inner shell is

$$\sigma_{\text{radial}} := \frac{\nu_c}{1 - \nu_c} \cdot \sigma_c \quad \sigma_{\text{radial}} = 219.238 \text{ psi}$$

Appendix 3.AK examines the structural integrity of the inner shell under this loading in accordance with ASME Code Case N-284, which has been used in the HI-STAR 100 TSAR and SAR to examine stability issues and is accepted by the NRC for these kind of evaluations. Both stability and yielding are examined and it is concluded that buckling of the inner shell is not credible

The safety factor is

$$\text{SF} := \frac{1.34}{.341} \quad \text{SF} = 3.93$$

The preceding analysis has computed vertical compressive stress acting on the inner shell above the inlet vents for the primary purpose of evaluating stability of the inner shell under the combination of external pressure plus compressive axial stress. On a cross section below the inlet vents, there will be an increase in the compressive stress level due to the reduction in metal area. Section 3.4.4.3.2.1 provides the reduced area calculation. The net metal area reduction for the inner and outer shells is

$$\text{Reduction_factor_inner_shell} := \frac{211.04}{293.54} \qquad \text{Reduction_factor_outer_shell} := \frac{260.93}{310.43}$$

Therefore, the increased mean compressive primary stress on a section of the inner shell below the inlet duct is

$$\sigma_{\text{mcsi}} := \frac{\sigma_{\text{mean}} + \sigma_{\text{meanw}}}{\text{Reduction_factor_inner_shell}} \qquad \sigma_{\text{mcsi}} = 1.133 \times 10^4 \text{ psi}$$

Comparing the stress intensity with the allowable mean stress intensity for the inner shell under Level D conditions (Table 3.1.12) defines the safety factor

$$\text{SF}_{\text{mcs}} := \frac{S_{\text{apm}}}{\sigma_{\text{mcsi}}} \qquad \text{SF}_{\text{mcs}} = 3.508$$

3.M.3.6 Outer Shell

The geometry of the outer shell is obtained from BM-1575.

$$d_{\text{outer}} := 132.5\text{-in} \qquad t_{\text{outer}} := 0.75\text{-in} \qquad L_{\text{outer}} := 224.5\text{-in}$$

The compressive stress developed at the base of the outer shell (just above the inlet vent) is

$$W_{\text{shells}} := 0.283 \cdot \frac{\text{lbf}}{\text{in}^3} \cdot \frac{\pi}{4} \cdot \left[d_{\text{outer}}^2 - (d_{\text{outer}} - 2 \cdot t_{\text{outer}})^2 \right] \cdot L_{\text{outer}} \qquad W_{\text{shells}} = 1.972 \times 10^4 \text{ lbf}$$

$$\sigma_{\text{meanw}} := \frac{W_{\text{shells}} \cdot G}{\pi \cdot (d_{\text{outer}} - t_{\text{outer}}) \cdot t_{\text{outer}}} \qquad \sigma_{\text{meanw}} = 2.859 \times 10^3 \text{ psi}$$

Below the inlet duct, this mean stress is amplified to the value

$$\sigma_{\text{mcs}} := \frac{\sigma_{\text{meanw}}}{\text{Reduction_factor_outer_shell}} \qquad \sigma_{\text{mcs}} = 3.401 \times 10^3 \text{ psi}$$

The safety factor for Level D mean stress in the outer shell is

$$SF_{mcs} := \frac{S_{apm}}{\sigma_{mcs}} \qquad SF_{mcs} = 11.686$$

Instability of the outer shell is examined in Appendix 3.AK and is found to be not credible

3.M.3.7 Inlet Vent Horizontal Plates

The inlet vent horizontal plate is subject to the amplified weight of the concrete and is exposed to the pressure from the column of concrete above the plate. This pressure is

$$P_{ip} := \sigma_c \qquad P_{ip} = 876.952 \text{ psi}$$

The dimensions of this plate are given in BM-1575. The length, width, and thickness, are

$$L_{ip} := 30.25\text{-in} \qquad w_{ip} := 16.5\text{-in} \qquad t_{ip} := 2\text{-in}$$

Under the vertical handling accident, the bending stress in this item is determined by treating the plate as simply supported on all four sides and using classical plate theory. From the text "Theory of Plates and Shells", Timoshenko and Woinowsky-Krieger, McGraw-Hill, 1959 (2nd Edition), the solution is found in Section 30, Table 8. Using the nomenclature of the referenced text,

$$b := L_{ip} \qquad a := w_{ip} \qquad \frac{b}{a} = 1.833$$

From the table, the maximum bending moment factor is

$$\beta := 0.096 \qquad \text{and}$$

$$M_x := \beta \cdot P_{ip} \cdot a^2 \qquad M_x = 2.292 \times 10^4 \text{ in} \cdot \frac{\text{lb} \cdot \text{f}}{\text{in}}$$

The maximum bending stress is

$$\sigma_{ip} := 6 \cdot \frac{M_x}{2 t_{ip}} \qquad \sigma_{ip} = 3.438 \times 10^4 \text{ psi}$$

The safety factor is conservatively computed for this Level D condition as

$$SF_{ip} := \frac{S_a}{\sigma_{ip} + P_{ip}} \qquad SF_{ip} = 1.692$$

The total vertical reaction load is conservatively assumed to be resisted only by the inlet vent vertical plates.

3.M.3.8 Inlet Vent Vertical Plates

Consistent with the assumptions used to qualify the inlet vent horizontal plate, the inlet vent vertical plate is analyzed for the mean compressive stress developed. From BM-1575, the inlet vent vertical plates have thickness, depth, and length given as

$$t_{ivp} := 0.75 \cdot \text{in} \quad c := 10 \cdot \text{in} \quad L_{ivp} := 29.1875 \cdot \text{in}$$

The compressive stress developed is conservatively calculated as

$$\sigma_{ivp} := \frac{P_{ip} \cdot L_{ip} \cdot w_{ip}}{2 \cdot t_{ivp} \cdot L_{ivp}} \quad \sigma_{ivp} = 9.998 \times 10^3 \text{ psi}$$

The safety factor is

$$SF := \frac{S_{apm}}{\sigma_{ivp}} \quad SF = 3.976$$

Because of the backing provided by the concrete, and the short span of this plate, an elastic instability is not credible

3.M.3.8 Pedestal Shield and Pedestal Shell

The results obtained for this component in Appendix 3.D, specifically sub-section 3.D.8, are used here to establish safety factors under the postulated handling accident event. The following results are found in Appendix 3.D for the pedestal shield and pedestal shell under 3 x 1.15 times the load from a loaded MPC.

$$SF_{\text{shield}} := 16.03 \quad \text{Concrete compression}$$

$$SF_{\text{pedestal_shell}} := 30.27 \quad \text{Hoop stress in shell}$$

For the vertical handling accident condition of storage, the safety factors are reduced to

$$SF_{\text{pshield}} := SF_{\text{shield}} \cdot \frac{3 \cdot 1.15}{G} \quad SF_{\text{pshield}} = 1.229$$

$$SF_{\text{pshell}} := SF_{\text{pedestal_shell}} \cdot \frac{3 \cdot 1.15}{G} \quad SF_{\text{pshell}} = 2.321$$

3.M.3.9 Weld in the Load Path

The only structural weld that is subject to significant stress and needs evaluation under this accident event is the weld connecting the lid bottom plate to the lid shell. We have demonstrated earlier that this weld is adequately sized (see section 3.M.3.1). The remaining welds serve only to insure that lateral connections of the shells to adjoining flat sections are maintained. The load transfer is by metal-to-metal compression contact; the connection welds are not needed to maintain equilibrium. Nevertheless, weld capacities of other connecting welds are examined to demonstrate that confinement of the shielding is maintained.

3.M.3.9.1 Outer Shell-to-Baseplate Circumferential Weld

$$t_w := 0.375 \text{ in} \quad \text{weld size (fillet)} \quad (\text{Drawing 1495})$$

$$\text{Allowable weld stress} \quad \tau_{\text{allow}} := 0.42 \cdot S_u \quad \tau_{\text{allow}} = 2.94 \times 10^4 \text{ psi}$$

Under this load condition, the weld need only resist radial loading from the "hydrostatic" radial pressure from the concrete shielding.

$$d_{\text{outer}} = 132.5 \text{ in} \quad t_{\text{outer}} = 0.75 \text{ in}$$

The shear force per unit of periphery is computed by considering the shell to be subjected to uniform internal pressure, and completely restrained from radial displacement by the weld. The solution for the shear force is obtained by superposition of two classical shell solutions (internal pressure in a long shell, and end shear applied to an otherwise unloaded shell). Enforcing zero displacement at the end of the shell leads to the following expression for the shear force per unit of shell periphery.

$$E = 2.8 \times 10^7 \text{ psi} \quad \nu = 0.3$$

$$D := \frac{E \cdot t_{\text{outer}}^3}{12 \cdot (1 - \nu^2)} \quad \lambda := \left[\frac{3 \cdot (1 - \nu^2)}{(.5 \cdot d_{\text{outer}} \cdot t_{\text{outer}})^2} \right]^{.25}$$

The shear force is

$$V_o := 2 \cdot D \cdot \lambda^3 \cdot P_{\text{radial}} \cdot \frac{(.5 \cdot d_{\text{outer}})^2}{E \cdot t_{\text{outer}}} \cdot (2 - \nu) \quad V_o = 1.022 \times 10^3 \frac{\text{lbf}}{\text{in}}$$

The weld capacity over the same 1" width is

$$\text{Weld_Capacity} := \tau_{\text{allow}} \cdot .7071 \cdot t_w \quad \text{Weld_Capacity} = 7.796 \times 10^3 \frac{\text{lbf}}{\text{in}}$$

Therefore the safety factor on the outer shell to baseplate weld is

$$SF_{\text{weldo}} := \frac{\text{Weld_Capacity}}{V_o} \quad SF_{\text{weldo}} = 7.629$$

3.M.3.9.2 Inner Shell-to-Baseplate Circumferential Weld

$$t_w := 0.75 \cdot \text{in} \quad \text{weld size (fillet)}$$

$$\text{Allowable weld stress} \quad \tau_{\text{allow}} := 0.42 \cdot S_u \quad \tau_{\text{allow}} = 2.94 \times 10^4 \text{ psi}$$

Under this load condition, the weld need only resist radial loading from the "hydrostatic" radial pressure from the concrete shielding. However, for added conservatism, we also assume that the weld supports a portion of the the mean compressive stress developed.

$$d_{\text{inner}} = 73.5 \text{ in} \quad t_{\text{is}} = 1.25 \text{ in}$$

The shear force per unit of periphery is computed by considering the shell to be subjected to uniform internal pressure, and completely restrained from radial displacement by the weld. The solution for the shear force is obtained by superposition of two classical shell solutions (internal pressure in a long shell, and end shear applied to an otherwise unloaded shell). Enforcing zero displacement at the end of the shell leads to the following expression for the shear force per unit of shell periphery.

$$E = 2.8 \times 10^7 \text{ psi} \quad \nu = 0.3$$

$$D := \frac{E \cdot t_{\text{is}}^3}{12 \cdot (1 - \nu^2)} \quad \lambda := \left[\frac{3 \cdot (1 - \nu^2)}{(.5 \cdot d_{\text{inner}} \cdot t_{\text{is}})^2} \right]^{.25}$$

The shear force is

$$V_o := 2 \cdot D \cdot \lambda^3 \cdot P_{\text{radial}} \cdot \frac{(.5 \cdot d_{\text{inner}})^2}{E \cdot t_{\text{is}}} \cdot (2 - \nu) \quad V_o = 982.604 \frac{\text{lbf}}{\text{in}}$$

The weld shear stress to support V_o is

$$\tau_1 := \frac{V_o}{.7071 \cdot t_w} \quad \tau_1 = 1.853 \times 10^3 \text{ psi}$$

Assuming a portion of the compressive load (ratio of weld leg size to total contact length with baseplate) on the inner shell is transferred through the weld gives a weld shear stress component

$$\tau_2 := (\sigma_{\text{mcsi}} \cdot t_{\text{is}}) \cdot \left(\frac{1}{t_{\text{is}} + 1 \cdot t_w} \right) \quad \tau_2 = 7.082 \times 10^3 \text{ psi}$$

The weld safety factor is

$$SF_{\text{weldi}} := \frac{\tau_{\text{allow}}}{\sqrt{\tau_1^2 + \tau_2^2}} \quad SF_{\text{weldi}} = 4.016$$

3.M.3.9.3 Pedestal Shell-to-Baseplate Circumferential Weld

$$t_w := 0.25 \cdot \text{in} \quad \text{weld size (fillet)}$$

$$\text{Allowable weld stress} \quad \tau_{\text{allow}} := 0.42 \cdot S_u \quad \tau_{\text{allow}} = 2.94 \times 10^4 \text{ psi}$$

Under this load condition, the weld need only resist radial loading from the "hydrostatic" radial pressure from the concrete shielding. However, for added conservatism, we also assume that the weld supports a portion of the the mean compressive stress developed.

$$d_{ps} := 68.375 \cdot \text{in} \quad t_{ps} := 0.25 \cdot \text{in} \quad \text{BM-1575}$$

From Appendix 3.D, the lateral "hydrostatic" pressure from the compressed shield material is

$$P_{\text{shield}} := 7.98 \cdot \text{psi} \quad \text{under a load amplifier } 3 \times 1.15$$

Therefore, for the drop condition studied in this appendix, where 45 G is the amplifier, the pressure on the pedestal shell is

$$p_s := \frac{P_{\text{shield}} \cdot G}{3 \cdot 1.15} \quad p_s = 104.087 \text{ psi}$$

The shear force per unit of periphery is computed by considering the shell to be subjected to uniform internal pressure, and completely restrained from radial displacement by the weld. The solution for the shear force is obtained by superposition of two classical shell solutions (internal pressure in a long shell, and end shear applied to an otherwise unloaded shell). Enforcing zero displacement at the end of the shell leads to the following expression for the shear force per unit of shell periphery.

$$E = 2.8 \times 10^7 \text{ psi} \quad \nu = 0.3$$

$$D := \frac{E \cdot t_{ps}^3}{12 \cdot (1 - \nu^2)} \quad \lambda := \left[\frac{3 \cdot (1 - \nu^2)}{(5 \cdot d_{ps} \cdot t_{ps})^2} \right]^{.25}$$

The shear force is

$$V_o := 2 \cdot D \cdot \lambda^3 \cdot p_s \cdot \frac{(5 \cdot d_{ps})^2}{E \cdot t_{ps}} \cdot (2 - \nu) \quad V_o = 201.224 \frac{\text{lb}}{\text{in}}$$

The weld shear stress to support V_o is

$$\tau_1 := \frac{V_o}{.7071 \cdot t_w} \quad \tau_1 = 1.138 \times 10^3 \text{ psi}$$

The weld capacity over the same unit width is

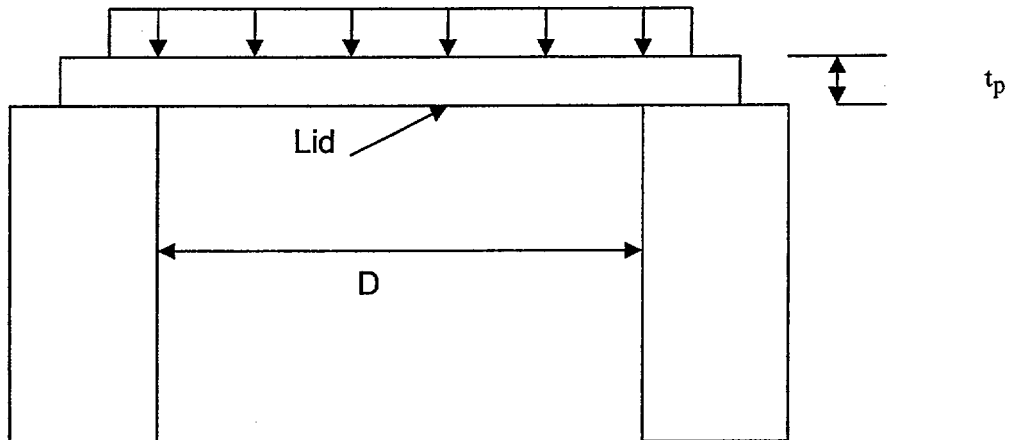
$$\text{Weld_Capacity} := \tau_{\text{allow}} \cdot .7071 \cdot t_w \quad \text{Weld_Capacity} = 5.197 \times 10^3 \frac{\text{lbf}}{\text{in}}$$

Therefore the safety factor on the pedestal shell-to-baseplate weld is

$$\text{SF}_{\text{weld}} := \frac{\text{Weld_Capacity}}{V_o} \quad \text{SF}_{\text{weld}} = 25.828$$

3.M.4 Analysis of Bending of HI-STORM 100S Top Lid

Consider the following configuration for analysis (the upper of the two lid plates is most heavily loaded):



The thickness of the upper of two lids is

$$t_{tp} = 2 \text{ in}$$

$$D := 73.5 \text{ in} \quad \text{Assume the pinned support is at the inner edge.}$$

The weight of the shield block concrete and the surrounding metal shell is obtained from the detailed weight analysis archived in the calculation package. The total weight of this component is

$$W := 5716 \text{ lbf}$$

The equivalent uniform pressure is

$$q1 := \frac{W \cdot G}{\left(\frac{\pi \cdot D^2}{4} \right)} \quad q1 = 60.623 \text{ psi}$$

The amplified pressure due to the lid plate self weight is

$$q2 := G \cdot 283 \cdot \frac{\text{lb}}{\text{in}^3} \cdot t_{tp} \quad q2 = 25.47 \text{ psi} \quad (\text{density from Subsection 3.3.1.1})$$

Therefore, the total amplified pressure on the upper of two top lids (conservatively assume it carries all of the load from the shield block and neglect any resisting interface pressure from the lower plate) is

$$q := q1 + q2$$

The bending stress in the center of the plate is

$$\sigma := \frac{3 \cdot (3 + \nu)}{8} \cdot q \cdot \left(\frac{D}{2 \cdot t_{tp}} \right)^2 \quad \sigma = 3.597 \times 10^4 \text{ psi}$$

$$SF_{\text{lid_top_plate}} := \frac{S_a}{\sigma} \quad SF_{\text{lid_top_plate}} = 1.658$$

3.M.4 Conclusion

The HI-STORM 100 storage overpack meets Level D requirements for Load Case 02.a in Table 3.1.5. Even under the postulated accident condition loads, the calculated stress levels do not imply that any significant deformations occur that would preclude removal of a loaded MPC. Thus ready retrievability of fuel is maintained after such an event. The results for the HI-STORM 100 will bound the results for the HI-STORM 100S.

Appendix 3.N

Intentionally Deleted

Appendix 3.O

Intentionally Deleted

Appendix 3.P

Intentionally Deleted

Appendix 3.Q

Intentionally Deleted

Appendix 3.R

Intentionally Deleted

Appendix 3.S

Intentionally Deleted

Appendix 3.T

Intentionally Deleted

APPENDIX 3.U: HI-STORM 100 COMPONENT THERMAL EXPANSIONS; MPC-24

3.U.1 Scope

In this calculation, estimates of operating gaps, both radially and axially, are computed for the fuel basket-to-MPC shell, and for the MPC shell-to-overpack. This calculation is in support of the results presented in Section 3.4.4.2.

3.U.2 Methodology

Bounding temperatures are used to construct temperature distributions that will permit calculation of differential thermal expansions both radially and axially for the basket-to-MPC gaps, and for the MPC-to-overpack gaps. Reference temperatures are set at 70°F for all components.

Temperature distributions are computed at the hottest cross section of the HI-STORM 100. A comprehensive nomenclature listing is provided in Section 3.U.6.

3.U.3 References

[3.U.1] Boley and Weiner, Theory of Thermal Stresses, John Wiley, 1960, Sec. 9.10, pp. 288-291.

[3.U.2] Burgreen, Elements of Thermal Stress Analysis, Arcturus Publishers, Cherry Hill NJ, 1988.

3.U.4 Calculations for Hot Components (Middle of System)

3.U.4.1 Input Data

Based on thermal calculations in Chapter 4, the following temperatures are appropriate at the hottest location of the cask (see Figure 3.U.1 and Tables 4.4.9 and 4.4.36).

The temperature change at the overpack inner shell, $\Delta T_{1h} := 199 - 70$

The temperature change at the overpack outer shell, $\Delta T_{2h} := 145 - 70$

The temperature change at the mean radius of the MPC shell, $\Delta T_{3h} := 344 - 70$

The temperature change at the outside of the MPC basket, $\Delta T_{4h} := (486 - 70) \cdot 1.1$

The temperature change at the center of the basket (helium gas), $\Delta T_{5h} := 650 - 70$

Note that the outer basket temperature is conservatively amplified by 10% to insure a bounding parabolic distribution. This conservatism serves to maximize the growth of the basket.

The geometry of the components are as follows (referring to Figure 3.U.1)

The outer radius of the overpack, $b := 66.25 \cdot \text{in}$

The minimum inner radius of the overpack, $a := 34.75 \cdot \text{in}$

The mean radius of the MPC shell, $R_{\text{mpc}} := \frac{68.375 \cdot \text{in} - 0.5 \cdot \text{in}}{2}$ $R_{\text{mpc}} = 33.938 \text{ in}$

The initial MPC-to-overpack radial clearance, $RC_{\text{mo}} := .5 \cdot (69.5 - 68.5) \cdot \text{in}$
 $RC_{\text{mo}} = 0.5 \text{ in}$

This initial radial clearance value, used to perform a radial growth check, is conservatively based on the channel radius (see Dwg. 1495, Sh. 5) and the maximum MPC diameter. For axial growth calculations for the MPC-to-overpack lid clearance, the axial length of the overpack is defined as the distance from the top of the pedestal platform to the bottom of the lid bottom plate, and the axial length of the MPC is defined as the overall MPC height.

The axial length of the overpack, $L_{\text{ovp}} := 191.5 \cdot \text{in}$

The axial length of the MPC, $L_{\text{mpc}} := 190.5 \cdot \text{in}$

The initial MPC-to-overpack nominal axial clearance, $AC_{\text{mo}} := L_{\text{ovp}} - L_{\text{mpc}}$

$$AC_{\text{mo}} = 1 \text{ in}$$

For growth calculations for the fuel basket-to-MPC shell clearances, the axial length of the basket is defined as the total length of the basket and the outer radius of the basket is defined as the mean radius of the MPC shell minus one-half of the shell thickness minus the initial basket-to-shell radial clearance.

The axial length of the basket, $L_{\text{bas}} := 176.5 \cdot \text{in}$

The initial basket-to-MPC lid nominal axial clearance, $AC_{\text{bm}} := 1.8125 \cdot \text{in}$

The initial basket-to-MPC shell nominal radial clearance, $RC_{\text{bm}} := 0.1875 \cdot \text{in}$

The outer radius of the basket, $R_b := R_{\text{mpc}} - \frac{0.5}{2} \cdot \text{in} - RC_{\text{bm}}$ $R_b = 33.5 \text{ in}$

The coefficients of thermal expansion used in the subsequent calculations are based on the mean temperatures of the MPC shell and the basket (conservatively estimated high).

The coefficient of thermal expansion for the MPC shell, $\alpha_{\text{mpc}} := 9.015 \cdot 10^{-6}$

The coefficient of thermal expansion for the basket, $\alpha_{\text{bas}} := 9.60 \cdot 10^{-6} \text{ 600 deg. F}$

3.U.4.2 Thermal Growth of the Overpack

Results for thermal expansion deformation and stress in the overpack are obtained here. The system is replaced by a equivalent uniform hollow cylinder with approximated average properties.

Based on the given inside and outside surface temperatures, the temperature solution in the cylinder is given in the form:

$$C_a + C_b \cdot \ln\left(\frac{r}{a}\right)$$

where

$$C_a := \Delta T_{1h} \quad C_a = 129$$

$$C_b := \frac{\Delta T_{2h} - \Delta T_{1h}}{\ln\left(\frac{b}{a}\right)} \quad C_b = -83.688$$

Next, form the integral relationship:

$$\text{Int} := \int_a^b \left[C_a + C_b \cdot \ln\left(\frac{r}{a}\right) \right] \cdot r \, dr$$

The Mathcad program, which was used to create this appendix, is capable of evaluating the integral "Int" either numerically or symbolically. To demonstrate that the results are equivalent, the integral is evaluated both ways in order to qualify the accuracy of any additional integrations that are needed.

The result obtained through numerical integration, $\text{Int} = 1.533 \times 10^5 \text{ in}^2$

To perform a symbolic evaluation of the solution the integral "Ints" is defined. This integral is then evaluated using the Maple symbolic math engine built into the Mathcad program as:

$$\text{Int}_s := \int_a^b \left[C_a + C_b \cdot \ln\left(\frac{r}{a}\right) \right] \cdot r \, dr$$

$$\text{Int}_s := \frac{1}{2} \cdot C_b \cdot \ln\left(\frac{b}{a}\right) \cdot b^2 + \frac{1}{2} \cdot C_a \cdot b^2 - \frac{1}{4} \cdot C_b \cdot b^2 + \frac{1}{4} \cdot C_b \cdot a^2 - \frac{1}{2} \cdot C_a \cdot a^2$$

$$\text{Int}_s = 1.533 \times 10^5 \text{ in}^2$$

We note that the values of Int and Ints are identical. The average temperature in the overpack cylinder (T_{bar}) is therefore determined as:

$$T_{\text{bar}} := \frac{2}{(b^2 - a^2)} \cdot \text{Int} \quad T_{\text{bar}} = 96.348$$

We estimate the average coefficient of thermal expansion for the overpack by weighting the volume of the various layers. A total of four layers are identified for this calculation. They are:

- 1) the inner shell
- 2) the shield shell
- 3) the radial shield
- 4) the outer shell

Thermal properties are based on estimated temperatures in the component and coefficient of thermal expansion values taken from the tables in Chapter 3. The following averaging calculation involves the thicknesses (t) of the various components, and the estimated coefficients of thermal expansion at the components' mean radial positions. The results of the weighted average process yields an effective coefficient of linear thermal expansion for use in computing radial growth of a solid cylinder (the overpack).

The thicknesses of each component are defined as:

$$t_1 := 1.25 \cdot \text{in}$$

$$t_2 := 0.75 \cdot \text{in}$$

$$t_3 := 26.75 \cdot \text{in}$$

$$t_4 := 0.75 \cdot \text{in}$$

and the corresponding mean radii can therefore be defined as:

$$r_1 := a + .5 \cdot t_1 + 2.0 \cdot \text{in} \quad (\text{add the channel depth})$$

$$r_2 := r_1 + .5 \cdot t_1 + .5 \cdot t_2$$

$$r_3 := r_2 + .5 \cdot t_2 + .5 \cdot t_3$$

$$r_4 := r_3 + .5 \cdot t_3 + .5 \cdot t_4$$

To check the accuracy of these calculations, the outer radius of the overpack is calculated from r_4 and t_4 , and the result is compared with the previously defined value (b).

$$b_1 := r_4 + 0.5 \cdot t_4$$

$$b_1 = 66.25 \text{ in}$$

$$b = 66.25 \text{ in}$$

We note that the calculated value b_1 is identical to the previously defined value b . The coefficients of thermal expansion for each component, estimated based on the temperature gradient, are defined as:

$$\alpha_1 := 5.782 \cdot 10^{-6}$$

$$\alpha_2 := 5.782 \cdot 10^{-6}$$

$$\alpha_3 := 5.5 \cdot 10^{-6}$$

$$\alpha_4 := 5.638 \cdot 10^{-6}$$

Thus, the average coefficient of thermal expansion of the overpack is determined as:

$$\alpha_{\text{avg}} := \frac{r_1 \cdot t_1 \cdot \alpha_1 + r_2 \cdot t_2 \cdot \alpha_2 + r_3 \cdot t_3 \cdot \alpha_3 + r_4 \cdot t_4 \cdot \alpha_4}{\frac{a+b}{2} \cdot (t_1 + t_2 + t_3 + t_4)}$$
$$\alpha_{\text{avg}} = 5.628 \times 10^{-6}$$

Reference 3.U.1 gives an expression for the radial deformation due to thermal growth. At the inner radius of the overpack ($r = a$), the radial growth is determined as:

$$\Delta R_{\text{ah}} := \alpha_{\text{avg}} \cdot a \cdot T_{\text{bar}}$$

$$\Delta R_{\text{ah}} = 0.019 \text{ in}$$

Similarly, an overestimate of the axial growth of the overpack can be determined by applying the average temperature (T_{bar}) over the entire length of the overpack as:

$$\Delta L_{\text{ovph}} := L_{\text{ovp}} \cdot \alpha_{\text{avg}} \cdot T_{\text{bar}}$$

$$\Delta L_{\text{ovph}} = 0.104 \text{ in}$$

Estimates of the secondary thermal stresses that develop in the overpack due to the radial temperature variation are determined using a conservatively high value of E as based on the temperature of the steel. The circumferential stress at the inner and outer surfaces (σ_{ca} and σ_{cb} , respectively) are determined as:

The Young's Modulus of the material, $E := 28300000 \text{ psi}$

$$\sigma_{ca} := \alpha_{avg} \cdot \frac{E}{a^2} \cdot \left[2 \cdot \frac{a^2}{(b^2 - a^2)} \cdot \text{Int} - (C_a) \cdot a^2 \right]$$

$$\sigma_{ca} = -5200 \text{ psi}$$

$$\sigma_{cb} := \alpha_{avg} \cdot \frac{E}{b^2} \cdot \left[2 \cdot \frac{b^2}{(b^2 - a^2)} \cdot \text{Int} - \left[C_a + C_b \cdot \left(\ln \left(\frac{b}{a} \right) \right) \right] \cdot b^2 \right]$$

$$\sigma_{cb} = 3400 \text{ psi}$$

The radial stress due to the temperature gradient is zero at both the inner and outer surfaces of the overpack. The radius where a maximum radial stress is expected, and the corresponding radial stress, are determined by trial and error as:

$$N := 0.37$$

$$r := a \cdot (1 - N) + N \cdot b$$

$$r = 46.405 \text{ in}$$

$$\sigma_r := \alpha_{avg} \cdot \frac{E}{r^2} \cdot \left[\frac{r^2 - a^2}{2} \cdot T_{bar} - \int_a^r \left[C_a + C_b \cdot \left(\ln \left(\frac{y}{a} \right) \right) \right] \cdot y \, dy \right]$$

$$\sigma_r = -678.201 \text{ psi}$$

The axial stress developed due to the temperature gradient is equal to the sum of the radial and tangential stresses at any radial location. (see eq. 9.10.7) of [3.U.1]. Therefore, the axial stresses are available from the above calculations. The stress intensities in the overpack due to the temperature distribution are below the Level A membrane stress.

3.U.4.3 Thermal Growth of the MPC Shell

The radial and axial growth of the MPC shell (ΔR_{mpch} and ΔL_{mpch} , respectively) are determined as:

$$\Delta R_{mpch} := \alpha_{mpc} \cdot R_{mpc} \cdot \Delta T_{3h}$$

$$\Delta R_{mpch} = 0.084 \text{ in}$$

$$\Delta L_{mpch} := \alpha_{mpc} \cdot L_{mpc} \cdot \Delta T_{3h}$$

$$\Delta L_{mpch} = 0.471 \text{ in}$$

3.U.4.4 Clearances Between the MPC Shell and Overpack

The final radial and axial MPC shell-to-overpack clearances (RG_{moh} and AG_{moh} , respectively) are determined as:

$$RG_{moh} := RC_{mo} + \Delta R_{ah} - \Delta R_{mpch}$$

$$RG_{moh} = 0.435 \text{ in}$$

$$AG_{moh} := AC_{mo} + \Delta L_{ovph} - \Delta L_{mpch}$$

$$AG_{moh} = 0.633 \text{ in}$$

Note that this axial clearance (AG_{moh}) is based on the temperature distribution at the hottest cross section.

3.U.4.5 Thermal Growth of the MPC-24 Basket

Using formulas given in [3.U.2] for a solid body of revolution, and assuming a parabolic temperature distribution in the radial direction with the center and outer temperatures given previously, the following relationships can be developed for free thermal growth.

Define $\Delta T_{bas} := \Delta T_{5h} - \Delta T_{4h}$ $\Delta T_{bas} = 122.4$

Then the mean temperature can be defined as $T_{bar} := \frac{2}{R_b^2} \int_0^{R_b} \left(\Delta T_{5h} - \Delta T_{bas} \cdot \frac{r^2}{R_b^2} \right) \cdot r \, dr$

Using the Maple symbolic engine again, the closed form solution of the integral is:

$$T_{bar} := \frac{2}{R_b^2} \cdot \left(\frac{-1}{4} \cdot \Delta T_{bas} \cdot R_b^2 + \frac{1}{2} \cdot \Delta T_{5h} \cdot R_b^2 \right)$$
$$T_{bar} = 518.8$$

The corresponding radial growth at the periphery (ΔR_{bh}) is therefore determined as:

$$\Delta R_{bh} := \alpha_{bas} \cdot R_b \cdot T_{bar}$$
$$\Delta R_{bh} = 0.167 \text{ in}$$

and the corresponding axial growth (ΔL_{bas}) is determined from [3.U.2] as:

$$\Delta L_{bh} := \Delta R_{bh} \cdot \frac{L_{bas}}{R_b}$$
$$\Delta L_{bh} = 0.879 \text{ in}$$

Note that the coefficient of thermal expansion for the hottest basket temperature has been used, and the results are therefore conservative.

3.U.4.6 Clearances Between the Fuel Basket and MPC Shell

The final radial and axial fuel basket-to-MPC shell and lid clearances (RG_{bms} and AG_{bms} , respectively) are determined as:

$$RG_{bms} := RC_{bm} - \Delta R_{bh} + \Delta R_{mpch}$$

$$RG_{bms} = 0.104 \text{ in}$$

$$AG_{bms} := AC_{bm} - \Delta L_{bh} + \Delta L_{mpch}$$

$$AG_{bms} = 1.404 \text{ in}$$

3.U.5 Summary of Results

The previous results are summarized here.

MPC Shell-to-Overpack

$$RG_{moh} = 0.435 \text{ in}$$

$$AG_{moh} = 0.633 \text{ in}$$

Fuel Basket-to-MPC Shell

$$RG_{bms} = 0.104 \text{ in}$$

$$AG_{bms} = 1.404 \text{ in}$$

3.U.6 Nomenclature

a is the inner radius of the overpack

AC_{bm} is the initial fuel basket-to-MPC axial clearance.

AC_{mo} is the initial MPC-to-overpack axial clearance.

AG_{bmh} is the final fuel basket-to-MPC shell axial gap for the hot components.

AG_{moh} is the final MPC shell-to-overpack axial gap for the hot components.

b is the outer radius of the overpack.

L_{bas} is the axial length of the fuel basket.

L_{mpc} is the axial length of the MPC.

L_{ovp} is the axial length of the overpack.

r_1 (r_2, r_3, r_4) is mean radius of the overpack inner shell (shield shell, concrete, outer shell).

R_b is the outer radius of the fuel basket.

R_{mpc} is the mean radius of the MPC shell.

RC_{bm} is the initial fuel basket-to-MPC radial clearance.

RC_{mo} is the initial MPC shell-to-overpack radial clearance.

RG_{bmh} is the final fuel basket-to-MPC shell radial gap for the hot components.

RG_{moh} is the final MPC shell-to-overpack radial gap for the hot components.

t_1 (t_2, t_3, t_4) is the thickness of the overpack inner shell (shield shell, concrete, outer shell).

T_{bar} is the average temperature of the overpack cylinder.

α_1 ($\alpha_2, \alpha_3, \alpha_4$) is the coefficient of thermal expansion of the overpack inner shell (shield shell, concrete, outer shell).

α_{avg} is the average coefficient of thermal expansion of the overpack.

α_{bas} is the coefficient of thermal expansion of the overpack.

α_{mpc} is the coefficient of thermal expansion of the MPC.

ΔL_{bh} is the axial growth of the fuel basket for the hot components.

ΔL_{mpch} is the axial growth of the MPC for the hot components.
 ΔL_{ovph} is the axial growth of the overpack for the hot components.
 ΔR_{ah} is the radial growth of the overpack inner radius for the hot components.
 ΔR_{bh} is the radial growth of the fuel basket for the hot components.
 ΔR_{mpch} is the radial growth of the MPC shell for the hot components.
 ΔT_{1h} is the temperature change at the overpack inner shell for hot components.
 ΔT_{2h} is the temperature change at the overpack outer shell for hot components.
 ΔT_{3h} is the temperature change at the MPC shell mean radius for hot components.
 ΔT_{4h} is the temperature change at the MPC basket periphery for hot components.
 ΔT_{5h} is the temperature change at the MPC basket centerline for hot components.
 ΔT_{bas} is the fuel basket centerline-to-periphery temperature gradient.
 σ_{ca} is the circumferential stress at the overpack inner surface.
 σ_{cb} is the circumferential stress at the overpack outer surface.
 σ_r is the maximum radial stress of the overpack.
 σ_{zi} is the axial stress at the fuel basket centerline.
 σ_{zo} is the axial stress at the fuel basket periphery.

APPENDIX 3.V: HI-STORM 100 COMPONENT THERMAL EXPANSIONS; MPC-32

3.V.1 Scope

In this calculation, estimates of operating gaps, both radially and axially, are computed for the fuel basket-to-MPC shell, and for the MPC shell-to-overpack. This calculation is in support of the results presented in Section 3.4.4.2.

3.V.2 Methodology

Bounding temperatures are used to construct temperature distributions that will permit calculation of differential thermal expansions both radially and axially for the basket-to-MPC gaps, and for the MPC-to-overpack gaps. Reference temperatures are set at 70°F for all components. Temperature distributions are computed at the axial location of the HI-STORM 100 System where the temperatures are highest. A comprehensive nomenclature listing is provided in Section 3.V.6.

3.V.3 References

[3.V.1] Boley and Weiner, Theory of Thermal Stresses, John Wiley, 1960, Sec. 9.10, pp. 288-291.

[3.V.2] Burgreen, Elements of Thermal Stress Analysis, Arcturus Publishers, Cherry Hill NJ, 1988.

3.V.4 Calculations for Hot Components (Middle of System)

3.V.4.1 Input Data

Based on calculations in Chapter 4, the following temperatures are appropriate at the hottest axial location of the cask (see Figure 3.V.1 and Tables 4.4.26 and 4.4.36).

The temperature change at the overpack inner shell, $\Delta T_{1h} := 199 - 70$

The temperature change at the overpack outer shell, $\Delta T_{2h} := 145 - 70$

The temperature change at the mean radius of the MPC shell, $\Delta T_{3h} := 351 - 70$

The temperature change at the outside of the MPC basket, $\Delta T_{4h} := (496 - 70) \cdot 1.1$

The temperature change at the center of the basket (helium gas), $\Delta T_{5h} := 660 - 70$

Note that the outer basket temperature is conservatively amplified by 10% to insure a bounding parabolic distribution. This conservatism serves to maximize the growth of the basket.

The geometry of the components are as follows (referring to Figure 3.V.1)

The outer radius of the overpack, $b := 66.25 \cdot \text{in}$

The inner radius of the overpack, $a := 34.75 \cdot \text{in}$

The mean radius of the MPC shell, $R_{\text{mpc}} := \frac{68.375 \cdot \text{in} - 0.5 \cdot \text{in}}{2}$ $R_{\text{mpc}} = 33.938 \text{ in}$

The initial MPC-to-overpack nominal radial clearance, $RC_{\text{mo}} := .5 \cdot (69.5 - 68.5) \cdot \text{in}$
 $RC_{\text{mo}} = 0.5 \text{ in}$

This initial radial clearance value, used to perform a radial growth check, is conservatively based on the channel radius and the maximum MPC diameter. For axial growth calculations for the MPC-to-overpack lid clearance, the axial length of the overpack is defined as the distance from the top of the pedestal platform to the bottom of the lid bottom plate, and the axial length of the MPC is defined as the overall MPC height.

The axial length of the overpack, $L_{\text{ovp}} := 191.5 \cdot \text{in}$

The axial length of the MPC, $L_{\text{mpc}} := 190.5 \cdot \text{in}$

The initial MPC-to-overpack nominal axial clearance, $AC_{\text{mo}} := L_{\text{ovp}} - L_{\text{mpc}}$

$$AC_{\text{mo}} = 1 \text{ in}$$

For growth calculations for the fuel basket-to-MPC shell clearances, the axial length of the basket is defined as the total length of the basket and the outer radius of the basket is defined as the mean radius of the MPC shell minus one-half of the shell thickness minus the initial basket-to-shell radial clearance.

The axial length of the basket, $L_{\text{bas}} := 176.5 \cdot \text{in}$

The initial basket-to-MPC lid nominal axial clearance, $AC_{\text{bm}} := 1.8125 \cdot \text{in}$

The initial basket-to-MPC shell nominal radial clearance, $RC_{\text{bm}} := 0.1875 \cdot \text{in}$

The outer radius of the basket, $R_b := R_{\text{mpc}} - \frac{0.5}{2} \cdot \text{in} - RC_{\text{bm}}$ $R_b = 33.5 \text{ in}$

The coefficients of thermal expansion used in the subsequent calculations are based on the mean temperatures of the MPC shell and the basket (conservatively estimated high).

The coefficient of thermal expansion for the MPC shell, $\alpha_{\text{mpc}} := 9.015 \cdot 10^{-6}$

The coefficient of thermal expansion for the basket, $\alpha_{\text{bas}} := 9.60 \cdot 10^{-6} \text{ } 600 \text{ deg. F}$

3.V.4.2 Thermal Growth of the Overpack

Results for thermal expansion deformation and stress in the overpack are obtained here. The system is replaced by a equivalent uniform hollow cylinder with approximated average properties.

Based on the given inside and outside surface temperatures, the temperature solution in the cylinder is given in the form:

$$C_a + C_b \cdot \ln\left(\frac{r}{a}\right)$$

where

$$C_a := \Delta T_{1h} \quad C_a = 129$$

$$C_b := \frac{\Delta T_{2h} - \Delta T_{1h}}{\ln\left(\frac{b}{a}\right)} \quad C_b = -83.688$$

Next, form the integral relationship:

$$Int := \int_a^b \left[C_a + C_b \cdot \ln\left(\frac{r}{a}\right) \right] \cdot r \, dr$$

The Mathcad program, which was used to create this appendix, is capable of evaluating the integral "Int" either numerically or symbolically. To demonstrate that the results are equivalent, the integral is evaluated both ways in order to qualify the accuracy of any additional integrations that are needed.

The result obtained through numerical integration, $Int = 1.533 \times 10^5 \text{ in}^2$

To perform a symbolic evaluation of the solution the integral "Ints" is defined. This integral is then evaluated using the Maple symbolic math engine built into the Mathcad program as:

$$Int_s := \int_a^b \left[C_a + C_b \cdot \ln\left(\frac{r}{a}\right) \right] \cdot r \, dr$$

$$Int_s := \frac{1}{2} \cdot C_b \cdot \ln\left(\frac{b}{a}\right) \cdot b^2 + \frac{1}{2} \cdot C_a \cdot b^2 - \frac{1}{4} \cdot C_b \cdot b^2 + \frac{1}{4} \cdot C_b \cdot a^2 - \frac{1}{2} \cdot C_a \cdot a^2$$

$$Int_s = 1.533 \times 10^5 \text{ in}^2$$

We note that the values of Int and Int_s are identical. The average temperature in the overpack cylinder (T_{bar}) is therefore determined as:

$$T_{\text{bar}} := \frac{2}{(b^2 - a^2)} \cdot \text{Int} \quad T_{\text{bar}} = 96.348$$

We estimate the average coefficient of thermal expansion for the overpack by weighting the volume of the various layers. A total of four layers are identified for this calculation. They are:

- 1) the inner shell
- 2) the shield shell
- 3) the radial shield
- 4) the outer shell

Thermal properties are based on estimated temperatures in the component and coefficient of thermal expansion values taken from the tables in Chapter 3. The following averaging calculation involves the thicknesses (t) of the various components, and the estimated coefficients of thermal expansion at the components' mean radial positions. The results of the weighted average process yields an effective coefficient of linear thermal expansion for use in computing radial growth of a solid cylinder (the overpack).

The thicknesses of each component are defined as:

$$t_1 := 1.25 \cdot \text{in}$$

$$t_2 := 0.75 \cdot \text{in}$$

$$t_3 := 26.75 \cdot \text{in}$$

$$t_4 := 0.75 \cdot \text{in}$$

and the corresponding mean radii can therefore be defined as:

$$r_1 := a + .5 \cdot t_1 + 2 \cdot \text{in}$$

$$r_2 := r_1 + .5 \cdot t_1 + .5 \cdot t_2$$

$$r_3 := r_2 + .5 \cdot t_2 + .5 \cdot t_3$$

$$r_4 := r_3 + .5 \cdot t_3 + .5 \cdot t_4$$

To check the accuracy of these calculations, the outer radius of the overpack is calculated from r_4 and t_4 , and the result is compared with the previously defined value (b).

$$b_1 := r_4 + 0.5 \cdot t_4$$

$$b_1 = 66.25 \text{ in}$$

$$b = 66.25 \text{ in}$$

We note that the calculated value b_1 is identical to the previously defined value b . The coefficients of thermal expansion for each component, estimated based on the temperature gradient, are defined as:

$$\alpha_1 := 5.782 \cdot 10^{-6}$$

$$\alpha_2 := 5.782 \cdot 10^{-6}$$

$$\alpha_3 := 5.5 \cdot 10^{-6}$$

$$\alpha_4 := 5.638 \cdot 10^{-6}$$

Thus, the average coefficient of thermal expansion of the overpack is determined as:

$$\alpha_{\text{avg}} := \frac{r_1 \cdot t_1 \cdot \alpha_1 + r_2 \cdot t_2 \cdot \alpha_2 + r_3 \cdot t_3 \cdot \alpha_3 + r_4 \cdot t_4 \cdot \alpha_4}{\frac{a+b}{2} \cdot (t_1 + t_2 + t_3 + t_4)}$$

$$\alpha_{\text{avg}} = 5.628 \times 10^{-6}$$

Reference 3.V.1 gives an expression for the radial deformation due to thermal growth. At the inner radius of the overpack ($r = a$), the radial growth is determined as:

$$\Delta R_{\text{ah}} := \alpha_{\text{avg}} \cdot a \cdot T_{\text{bar}}$$

$$\Delta R_{\text{ah}} = 0.019 \text{ in}$$

Similarly, an overestimate of the axial growth of the overpack can be determined by applying the average temperature (T_{bar}) over the entire length of the overpack as:

$$\Delta L_{\text{ovph}} := L_{\text{ovp}} \cdot \alpha_{\text{avg}} \cdot T_{\text{bar}}$$

$$\Delta L_{\text{ovph}} = 0.104 \text{ in}$$

Estimates of the secondary thermal stresses that develop in the overpack due to the radial temperature variation are determined using a conservatively high value of E as based on the temperature of the steel. The circumferential stress at the inner and outer surfaces (σ_{ca} and σ_{cb} , respectively) are determined as:

The Young's Modulus of the material, $E := 28300000 \cdot \text{psi}$

$$\sigma_{ca} := \alpha_{avg} \cdot \frac{E}{a^2} \cdot \left[2 \cdot \frac{a^2}{(b^2 - a^2)} \cdot \text{Int} - (C_a) \cdot a^2 \right]$$

$$\sigma_{ca} = -5200 \text{ psi}$$

$$\sigma_{cb} := \alpha_{avg} \cdot \frac{E}{b^2} \cdot \left[2 \cdot \frac{b^2}{(b^2 - a^2)} \cdot \text{Int} - \left[C_a + C_b \cdot \left(\ln \left(\frac{b}{a} \right) \right) \right] \cdot b^2 \right]$$

$$\sigma_{cb} = 3400 \text{ psi}$$

The radial stress due to the temperature gradient is zero at both the inner and outer surfaces of the overpack. The radius where a maximum radial stress is expected, and the corresponding radial stress, are determined by trial and error as:

$$N := 0.37$$

$$r := a \cdot (1 - N) + N \cdot b$$

$$r = 46.405 \text{ in}$$

$$\sigma_r := \alpha_{avg} \cdot \frac{E}{r^2} \cdot \left[\frac{r^2 - a^2}{2} \cdot T_{bar} - \int_a^r \left[C_a + C_b \cdot \left(\ln \left(\frac{y}{a} \right) \right) \right] \cdot y \, dy \right]$$

$$\sigma_r = -678.201 \text{ psi}$$

The axial stress developed due to the temperature gradient is equal to the sum of the radial and tangential stresses at any radial location. (see eq. 9.10.7) of [3.V.1]. Therefore, the axial stresses are available from the above calculations. The stress intensities in the overpack due to the temperature distribution are below the Level A membrane stress.

3.V.4.3 Thermal Growth of the MPC Shell

The radial and axial growth of the MPC shell (ΔR_{mpch} and ΔL_{mpch} , respectively) are determined as:

$$\Delta R_{mpch} := \alpha_{mpc} \cdot R_{mpc} \cdot \Delta T_{3h} \qquad \Delta R_{mpch} = 0.086 \text{ in}$$

$$\Delta L_{mpch} := \alpha_{mpc} \cdot L_{mpc} \cdot \Delta T_{3h} \qquad \Delta L_{mpch} = 0.483 \text{ in}$$

3.V.4.4 Clearances Between the MPC Shell and Overpack

The final radial and axial MPC shell-to-overpack clearances (RG_{moh} and AG_{moh} , respectively) are determined as:

$$RG_{moh} := RC_{mo} + \Delta R_{ah} - \Delta R_{mpch}$$

$$RG_{moh} = 0.433 \text{ in}$$

$$AG_{moh} := AC_{mo} + \Delta L_{ovph} - \Delta L_{mpch}$$

$$AG_{moh} = 0.621 \text{ in}$$

Note that this axial clearance (AG_{moh}) is based on the temperature distribution at the middle of the system.

3.V.4.5 Thermal Growth of the MPC-32 Basket

Using formulas given in [3.V.2] for a solid body of revolution, and assuming a parabolic temperature distribution in the radial direction with the center and outer temperatures given previously, the following relationships can be developed for free thermal growth.

Define $\Delta T_{bas} := \Delta T_{5h} - \Delta T_{4h}$ $\Delta T_{bas} = 121.4$

Then the mean temperature can be defined as
$$T_{bar} := \frac{2}{R_b^2} \int_0^{R_b} \left(\Delta T_{5h} - \Delta T_{bas} \cdot \frac{r^2}{R_b^2} \right) \cdot r \, dr$$

Using the Maple symbolic engine again, the closed form solution of the integral is:

$$T_{bar} := \frac{2}{R_b^2} \cdot \left(\frac{-1}{4} \cdot \Delta T_{bas} \cdot R_b^2 + \frac{1}{2} \cdot \Delta T_{5h} \cdot R_b^2 \right)$$

$$T_{bar} = 529.3$$

The corresponding radial growth at the periphery (ΔR_{bh}) is therefore determined as:

$$\Delta R_{bh} := \alpha_{bas} \cdot R_b \cdot T_{bar}$$

$$\Delta R_{bh} = 0.17 \text{ in}$$

and the corresponding axial growth (ΔL_{bas}) is determined from [3.V.2] as:

$$\Delta L_{bh} := \Delta R_{bh} \cdot \frac{L_{bas}}{R_b}$$

$$\Delta L_{bh} = 0.897 \text{ in}$$

Note that the coefficient of thermal expansion for the hottest basket temperature has been used, and the results are therefore conservative.

3.V.4.6 Clearances Between the Fuel Basket and MPC Shell

The final radial and axial fuel basket-to-MPC shell and lid clearances (RG_{bms} and AG_{bms} , respectively) are determined as:

$$RG_{bms} := RC_{bm} - \Delta R_{bh} + \Delta R_{mpch}$$

$$RG_{bms} = 0.103 \text{ in}$$

$$AG_{bms} := AC_{bm} - \Delta L_{bh} + \Delta L_{mpch}$$

$$AG_{bms} = 1.398 \text{ in}$$

3.V.5 Summary of Results

The previous results are summarized here.

MPC Shell-to-Overpack

$$RG_{moh} = 0.433 \text{ in}$$

$$AG_{moh} = 0.621 \text{ in}$$

Fuel Basket-to-MPC Shell

$$RG_{bms} = 0.103 \text{ in}$$

$$AG_{bms} = 1.398 \text{ in}$$

3.V.6 Nomenclature

a is the inner radius of the overpack

AC_{bm} is the initial fuel basket-to-MPC axial clearance.

AC_{mo} is the initial MPC-to-overpack axial clearance.

AG_{bmh} is the final fuel basket-to-MPC shell axial gap for the hot components.

AG_{moh} is the final MPC shell-to-overpack axial gap for the hot components.

b is the outer radius of the overpack.

L_{bas} is the axial length of the fuel basket.

L_{mpc} is the axial length of the MPC.

L_{ovp} is the axial length of the overpack.

r_1 (r_2, r_3, r_4) is mean radius of the overpack inner shell (shield shell, concrete, outer shell).

R_b is the outer radius of the fuel basket.

R_{mpc} is the mean radius of the MPC shell.

RC_{bm} is the initial fuel basket-to-MPC radial clearance.

RC_{mo} is the initial MPC shell-to-overpack radial clearance.

RG_{bmh} is the final fuel basket-to-MPC shell radial gap for the hot components.

RG_{moh} is the final MPC shell-to-overpack radial gap for the hot components.

t_1 (t_2, t_3, t_4) is the thickness of the overpack inner shell (shield shell, concrete, outer

shell).

\bar{t}_{shell} is the average temperature of the overpack cylinder.

α_1 ($\alpha_2, \alpha_3, \alpha_4$) is the coefficient of thermal expansion of the overpack inner shell (shield shell, concrete, outer shell).

α_{avg} is the average coefficient of thermal expansion of the overpack.

α_{bas} is the coefficient of thermal expansion of the overpack.

α_{mpc} is the coefficient of thermal expansion of the MPC.

ΔL_{bh} is the axial growth of the fuel basket for the hot components.

ΔL_{mpch} is the axial growth of the MPC for the hot components.
 ΔL_{ovph} is the axial growth of the overpack for the hot components.
 ΔR_{ah} is the radial growth of the overpack inner radius for the hot components.
 ΔR_{bh} is the radial growth of the fuel basket for the hot components.
 ΔR_{mpch} is the radial growth of the MPC shell for the hot components.
 ΔT_{1h} is the temperature change at the overpack inner shell for hot components.
 ΔT_{2h} is the temperature change at the overpack outer shell for hot components.
 ΔT_{3h} is the temperature change at the MPC shell mean radius for hot components.
 ΔT_{4h} is the temperature change at the MPC basket periphery for hot components.
 ΔT_{5h} is the temperature change at the MPC basket centerline for hot components.
 ΔT_{bas} is the fuel basket centerline-to-periphery temperature gradient.
 σ_{ca} is the circumferential stress at the overpack inner surface.
 σ_{cb} is the circumferential stress at the overpack outer surface.
 σ_r is the maximum radial stress of the overpack.
 σ_{zi} is the axial stress at the fuel basket centerline.
 σ_{zo} is the axial stress at the fuel basket periphery.

APPENDIX 3.W: HI-STORM 100 COMPONENT THERMAL EXPANSIONS; MPC-68

3.W.1 Scope

In this calculation, estimates of operating gaps, both radially and axially, are computed for the fuel basket-to-MPC shell, and for the MPC shell-to-overpack. This calculation is in support of the results presented in Section 3.4.4.2.

3.W.2 Methodology

Bounding temperatures are used to construct temperature distributions that will permit calculation of differential thermal expansions both radially and axially for the basket-to-MPC gaps, and for the MPC-to-overpack gaps. Reference temperatures are set at 70°F for all components. Temperature distributions are computed at the location of the HI-STORM 100 System where the temperatures are highest. A comprehensive nomenclature listing is provided in Section 3.W.6.

3.W.3 References

[3.W.1] Boley and Weiner, Theory of Thermal Stresses, John Wiley, 1960, Sec. 9.10, pp. 288-291.

[3.W.2] Burgreen, Elements of Thermal Stress Analysis, Arcturus Publishers, Cherry Hill NJ, 1988.

3.W.4 Calculations for Hot Components (Middle of System)

3.W.4.1 Input Data

Based on thermal calculations in Chapter 4, the following temperatures are appropriate at the hottest location of the cask (see Figure 3.W.1 and Tables 4.4.10 and 4.4.36).

The temperature change at the overpack inner shell, $\Delta T_{1h} := 199 - 70$

The temperature change at the overpack outer shell, $\Delta T_{2h} := 145 - 70$

The temperature change at the mean radius of the MPC shell, $\Delta T_{3h} := 347 - 70$

The temperature change at the outside of the MPC basket, $\Delta T_{4h} := (501 - 70) \cdot 1.1$

The temperature change at the center of the basket (helium gas), $\Delta T_{5h} := 720 - 70$

Note that the outer basket temperature is conservatively amplified by 10% to insure a bounding parabolic distribution. This conservatism serves to maximize the growth of the basket. The geometry of the components are as follows (referring to Figure 3.W.1)

The outer radius of the overpack, $b := 66.25\text{-in}$

The inner radius of the overpack, $a := 34.75\text{-in}$

The mean radius of the MPC shell, $R_{\text{mpc}} := \frac{68.375\text{-in} - 0.5\text{-in}}{2}$ $R_{\text{mpc}} = 33.938\text{ in}$

The initial MPC-to-overpack nominal radial clearance, $RC_{\text{mo}} := .5 \cdot (69.5 - 68.5)\text{-in}$
 $RC_{\text{mo}} = 0.5\text{ in}$

This initial radial clearance value, used to perform a radial growth check, is conservatively based on the channel radius (see Dwg. 1495, Sh. 5) and the maximum MPC diameter. For axial growth calculations for the MPC-to-overpack lid clearance, the axial length of the overpack is defined as the distance from the top of the pedestal platform to the bottom of the lid bottom plate, and the axial length of the MPC is defined as the overall MPC height.

The axial length of the overpack, $L_{\text{ovp}} := 191.5\text{-in}$

The axial length of the MPC, $L_{\text{mpc}} := 190.5\text{-in}$

The initial MPC-to-overpack nominal axial clearance, $AC_{\text{mo}} := L_{\text{ovp}} - L_{\text{mpc}}$

$$AC_{\text{mo}} = 1\text{ in}$$

For growth calculations for the fuel basket-to-MPC shell clearances, the axial length of the basket is defined as the total length of the basket and the outer radius of the basket is defined as the mean radius of the MPC shell minus one-half of the shell thickness minus the initial basket-to-shell radial clearance.

The axial length of the basket, $L_{\text{bas}} := 176.5\text{-in}$

The initial basket-to-MPC lid nominal axial clearance, $AC_{\text{bm}} := 1.8125\text{-in}$

The initial basket-to-MPC shell nominal radial clearance, $RC_{\text{bm}} := 0.1875\text{-in}$

The outer radius of the basket, $R_b := R_{\text{mpc}} - \frac{0.5}{2}\text{-in} - RC_{\text{bm}}$ $R_b = 33.5\text{ in}$

The coefficients of thermal expansion used in the subsequent calculations are based on the mean temperatures of the MPC shell and the basket (conservatively estimated high).

The coefficient of thermal expansion for the MPC shell, $\alpha_{\text{mpc}} := 9.015 \cdot 10^{-6}$

The coefficient of thermal expansion for the basket, $\alpha_{\text{bas}} := 9.60 \cdot 10^{-6}$ 600 deg. F

3.W.4.2 Thermal Growth of the Overpack

Results for thermal expansion deformation and stress in the overpack are obtained here. The system is replaced by a equivalent uniform hollow cylinder with approximated average properties.

Based on the given inside and outside surface temperatures, the temperature solution in the cylinder is given in the form:

$$C_a + C_b \cdot \ln\left(\frac{r}{a}\right)$$

where

$$C_a := \Delta T_{1h} \quad C_a = 129$$

$$C_b := \frac{\Delta T_{2h} - \Delta T_{1h}}{\ln\left(\frac{b}{a}\right)} \quad C_b = -83.688$$

Next, form the integral relationship:

$$\text{Int} := \int_a^b \left[C_a + C_b \cdot \left(\ln\left(\frac{r}{a}\right) \right) \right] \cdot r \, dr$$

The Mathcad program, which was used to create this appendix, is capable of evaluating the integral "Int" either numerically or symbolically. To demonstrate that the results are equivalent, the integral is evaluated both ways in order to qualify the accuracy of any additional integrations that are needed.

The result obtained through numerical integration, $\text{Int} = 1.533 \times 10^5 \text{ in}^2$

To perform a symbolic evaluation of the solution the integral "Ints" is defined. This integral is then evaluated using the Maple symbolic math engine built into the Mathcad program as:

$$\text{Int}_s := \int_a^b \left[C_a + C_b \cdot \left(\ln\left(\frac{r}{a}\right) \right) \right] \cdot r \, dr$$

$$\text{Int}_s := \frac{1}{2} \cdot C_b \cdot \ln\left(\frac{b}{a}\right) \cdot b^2 + \frac{1}{2} \cdot C_a \cdot b^2 - \frac{1}{4} \cdot C_b \cdot b^2 + \frac{1}{4} \cdot C_b \cdot a^2 - \frac{1}{2} \cdot C_a \cdot a^2$$

$$\text{Int}_s = 1.533 \times 10^5 \text{ in}^2$$

We note that the values of Int and Ints are identical. The average temperature in the overpack cylinder (T_{bar}) is therefore determined as:

$$T_{\text{bar}} := \frac{2}{(b^2 - a^2)} \cdot \text{Int} \quad T_{\text{bar}} = 96.348$$

We estimate the average coefficient of thermal expansion for the overpack by weighting the volume of the various layers. A total of four layers are identified for this calculation. They are:

- 1) the inner shell
- 2) the shield shell
- 3) the radial shield
- 4) the outer shell

Thermal properties are based on estimated temperatures in the component and coefficient of thermal expansion values taken from the tables in Chapter 3. The following averaging calculation involves the thicknesses (t) of the various components, and the estimated coefficients of thermal expansion at the components' mean radial positions. The results of the weighted average process yields an effective coefficient of linear thermal expansion for use in computing radial growth of a solid cylinder (the overpack).

The thicknesses of each component are defined as:

$$t_1 := 1.25 \cdot \text{in}$$

$$t_2 := 0.75 \cdot \text{in}$$

$$t_3 := 26.75 \cdot \text{in}$$

$$t_4 := 0.75 \cdot \text{in}$$

and the corresponding mean radii can therefore be defined as:

$$r_1 := a + .5 \cdot t_1 + 2.0 \cdot \text{in} \quad (\text{add the channel depth})$$

$$r_2 := r_1 + .5 \cdot t_1 + .5 \cdot t_2$$

$$r_3 := r_2 + .5 \cdot t_2 + .5 \cdot t_3$$

$$r_4 := r_3 + .5 \cdot t_3 + .5 \cdot t_4$$

To check the accuracy of these calculations, the outer radius of the overpack is calculated from r_4 and t_4 , and the result is compared with the previously defined value (b).

$$b_1 := r_4 + 0.5 \cdot t_4$$

$$b_1 = 66.25 \text{ in}$$

$$b = 66.25 \text{ in}$$

We note that the calculated value b_1 is identical to the previously defined value b . The coefficients of thermal expansion for each component, estimated based on the temperature gradient, are defined as:

$$\alpha_1 := 5.782 \cdot 10^{-6}$$

$$\alpha_2 := 5.782 \cdot 10^{-6}$$

$$\alpha_3 := 5.5 \cdot 10^{-6}$$

$$\alpha_4 := 5.638 \cdot 10^{-6}$$

Thus, the average coefficient of thermal expansion of the overpack is determined as:

$$\alpha_{avg} := \frac{r_1 \cdot t_1 \cdot \alpha_1 + r_2 \cdot t_2 \cdot \alpha_2 + r_3 \cdot t_3 \cdot \alpha_3 + r_4 \cdot t_4 \cdot \alpha_4}{\frac{a+b}{2} \cdot (t_1 + t_2 + t_3 + t_4)}$$
$$\alpha_{avg} = 5.628 \times 10^{-6}$$

Reference 3.W.1 gives an expression for the radial deformation due to thermal growth. At the inner radius of the overpack ($r = a$), the radial growth is determined as:

$$\Delta R_{ah} := \alpha_{avg} \cdot a \cdot T_{bar}$$

$$\Delta R_{ah} = 0.019 \text{ in}$$

Similarly, an overestimate of the axial growth of the overpack can be determined by applying the average temperature (T_{bar}) over the entire length of the overpack as:

$$\Delta L_{ovph} := L_{ovp} \cdot \alpha_{avg} \cdot T_{bar}$$

$$\Delta L_{ovph} = 0.104 \text{ in}$$

Estimates of the secondary thermal stresses that develop in the overpack due to the radial temperature variation are determined using a conservatively high value of E as based on the temperature of the steel. The circumferential stress at the inner and outer surfaces (σ_{ca} and σ_{cb} , respectively) are determined as:

The Young's Modulus of the material, $E := 28300000 \cdot \text{psi}$

$$\sigma_{ca} := \alpha_{avg} \cdot \frac{E}{a^2} \left[2 \cdot \frac{a^2}{(b^2 - a^2)} \cdot \text{Int} - (C_a) \cdot a^2 \right]$$

$$\sigma_{ca} = -5200 \text{ psi}$$

$$\sigma_{cb} := \alpha_{avg} \cdot \frac{E}{b^2} \left[2 \cdot \frac{b^2}{(b^2 - a^2)} \cdot \text{Int} - \left[C_a + C_b \cdot \left(\ln \left(\frac{b}{a} \right) \right) \right] \cdot b^2 \right]$$

$$\sigma_{cb} = 3400 \text{ psi}$$

The radial stress due to the temperature gradient is zero at both the inner and outer surfaces of the overpack. The radius where a maximum radial stress is expected, and the corresponding radial stress, are determined by trial and error as:

$$N := 0.38$$

$$r := a \cdot (1 - N) + N \cdot b$$

$$r = 46.72 \text{ in}$$

$$\sigma_r := \alpha_{avg} \cdot \frac{E}{r^2} \left[\frac{r^2 - a^2}{2} \cdot T_{bar} - \int_a^r \left[C_a + C_b \cdot \left(\ln \left(\frac{y}{a} \right) \right) \right] \cdot y \, dy \right]$$

$$\sigma_r = -677.823 \text{ psi}$$

The axial stress developed due to the temperature gradient is equal to the sum of the radial and tangential stresses at any radial location. (see eq. 9.10.7) of [3.W.1]. Therefore, the axial stresses are available from the above calculations. The stress intensities in the overpack due to the temperature distribution are below the Level A membrane stress.

3.W.4.3 Thermal Growth of the MPC Shell

The radial and axial growth of the MPC shell (ΔR_{mpch} and ΔL_{mpch} , respectively) are determined as:

$$\Delta R_{mpch} := \alpha_{mpc} \cdot R_{mpc} \cdot \Delta T_{3h} \qquad \Delta R_{mpch} = 0.085 \text{ in}$$

$$\Delta L_{mpch} := \alpha_{mpc} \cdot L_{mpc} \cdot \Delta T_{3h} \qquad \Delta L_{mpch} = 0.476 \text{ in}$$

3.W.4.4 Clearances Between the MPC Shell and Overpack

The final radial and axial MPC shell-to-overpack clearances (RG_{moh} and AG_{moh} , respectively) are determined as:

$$RG_{moh} := RC_{mo} + \Delta R_{ah} - \Delta R_{mpch}$$

$$RG_{moh} = 0.434 \text{ in}$$

$$AG_{moh} := AC_{mo} + \Delta L_{ovph} - \Delta L_{mpch}$$

$$AG_{moh} = 0.628 \text{ in}$$

Note that this axial clearance (AG_{moh}) is based on the temperature distribution at the middle of the system.

3.W.4.5 Thermal Growth of the MPC-68 Basket

Using formulas given in [3.W.2] for a solid body of revolution, and assuming a parabolic temperature distribution in the radial direction with the center and outer temperatures given previously, the following relationships can be developed for free thermal growth.

$$\text{Define } \Delta T_{bas} := \Delta T_{5h} - \Delta T_{4h} \quad \Delta T_{bas} = 175.9$$

$$\text{Then the mean temperature can be defined as } T_{bar} := \frac{2}{R_b^2} \int_0^{R_b} \left(\Delta T_{5h} - \Delta T_{bas} \cdot \frac{r^2}{R_b^2} \right) \cdot r \, dr$$

Using the Maple symbolic engine again, the closed form solution of the integral is:

$$T_{bar} := \frac{2}{R_b^2} \cdot \left(\frac{-1}{4} \cdot \Delta T_{bas} \cdot R_b^2 + \frac{1}{2} \cdot \Delta T_{5h} \cdot R_b^2 \right)$$

$$T_{bar} = 562.05$$

The corresponding radial growth at the periphery (ΔR_{bh}) is therefore determined as:

$$\Delta R_{bh} := \alpha_{bas} \cdot R_b \cdot T_{bar}$$

$$\Delta R_{bh} = 0.181 \text{ in}$$

and the corresponding axial growth (ΔL_{bas}) is determined from [3.W.2] as:

$$\Delta L_{bh} := \Delta R_{bh} \frac{L_{bas}}{R_b}$$

$$\Delta L_{bh} = 0.952 \text{ in}$$

Note that the coefficient of thermal expansion for the hottest basket temperature has been used, and the results are therefore conservative.

3.W.4.6 Clearances Between the Fuel Basket and MPC Shell

The final radial and axial fuel basket-to-MPC shell and lid clearances (RG_{bmh} and AG_{bmh} , respectively) are determined as:

$$RG_{bmh} := RC_{bm} - \Delta R_{bh} + \Delta R_{mpch}$$

$$RG_{bmh} = 0.091 \text{ in}$$

$$AG_{bmh} := AC_{bm} - \Delta L_{bh} + \Delta L_{mpch}$$

$$AG_{bmh} = 1.336 \text{ in}$$

3.W.5 Summary of Results

The previous results are summarized here.

MPC Shell-to-Overpack

$$RG_{moh} = 0.434 \text{ in}$$

$$AG_{moh} = 0.628 \text{ in}$$

Fuel Basket-to-MPC Shell

$$RG_{bmh} = 0.091 \text{ in}$$

$$AG_{bmh} = 1.336 \text{ in}$$

3.W.6 Nomenclature

a is the inner radius of the overpack

AC_{bm} is the initial fuel basket-to-MPC axial clearance.

AC_{mo} is the initial MPC-to-overpack axial clearance.

AG_{bmh} is the final fuel basket-to-MPC shell axial gap for the hot components.

AG_{moh} is the final MPC shell-to-overpack axial gap for the hot components.

b is the outer radius of the overpack.

L_{bas} is the axial length of the fuel basket.

L_{mpc} is the axial length of the MPC.

L_{ovp} is the axial length of the overpack.

r_1 (r_2, r_3, r_4) is mean radius of the overpack inner shell (shield shell, concrete, outer shell).

R_b is the outer radius of the fuel basket.

R_{mpc} is the mean radius of the MPC shell.

RC_{bm} is the initial fuel basket-to-MPC radial clearance.

RC_{mo} is the initial MPC shell-to-overpack radial clearance.

RG_{bmh} is the final fuel basket-to-MPC shell radial gap for the hot components.

RG_{moh} is the final MPC shell-to-overpack radial gap for the hot components.

t_1 (t_2, t_3, t_4) is the thickness of the overpack inner shell (shield shell, concrete, outer shell).

T_{bar} is the average temperature of the overpack cylinder.

α_1 ($\alpha_2, \alpha_3, \alpha_4$) is the coefficient of thermal expansion of the overpack inner shell (shield shell, concrete, outer shell).

α_{avg} is the average coefficient of thermal expansion of the overpack.

α_{bas} is the coefficient of thermal expansion of the overpack.

α_{mpc} is the coefficient of thermal expansion of the MPC.

ΔL_{bh} is the axial growth of the fuel basket for the hot components.

ΔL_{mpch} is the axial growth of the MPC for the hot components.
 ΔL_{ovph} is the axial growth of the overpack for the hot components.
 ΔR_{ah} is the radial growth of the overpack inner radius for the hot components.
 ΔR_{bh} is the radial growth of the fuel basket for the hot components.
 ΔR_{mpch} is the radial growth of the MPC shell for the hot components.
 ΔT_{1h} is the temperature change at the overpack inner shell for hot components.
 ΔT_{2h} is the temperature change at the overpack outer shell for hot components.
 ΔT_{3h} is the temperature change at the MPC shell mean radius for hot components.
 ΔT_{4h} is the temperature change at the MPC basket periphery for hot components.
 ΔT_{5h} is the temperature change at the MPC basket centerline for hot components.
 ΔT_{bas} is the fuel basket centerline-to-periphery temperature gradient.
 σ_{ca} is the circumferential stress at the overpack inner surface.
 σ_{cb} is the circumferential stress at the overpack outer surface.
 σ_r is the maximum radial stress of the overpack.
 σ_{zi} is the axial stress at the fuel basket centerline.
 σ_{zo} is the axial stress at the fuel basket periphery.

APPENDIX 3.Y: MISCELLANEOUS CALCULATIONS

3.Y.1 CALCULATION FOR THE FILLET WELDS IN THE FUEL BASKET

The fillet welds in the fuel basket honeycomb are made by an autogenous operation that has been shown to produce highly consistent and porosity free weld lines. However, Subsection NG of the ASME Code permits only 40% quality credit on double fillet welds which can be only visually examined (Table NG-3352-1). Subsection NG, however, fails to provide a specific stress limit on such fillet welds. In the absence of a Code mandated limit, Holtec International's standard design procedure requires that the weld section possess as much load resistance capability as the parent metal section. Since the loading on the honeycomb panels is essentially that of section bending, it is possible to develop a closed form expression for the required weld throat t corresponding to panel thickness h .

We refer to Figure 3.Y.1 that shows a unit depth of panel-to-panel joint subjected to moment M .

The stress distribution in the panel is given by the classical Kirchoff beam formula

$$s_p = \frac{6M}{h^2}$$

or

$$M = \frac{s_p h^2}{6}$$

s_p is the extreme fiber stress in the panel.

Assuming that the panel edge-to-panel contact region develops no resistive pressure, Figure 3.Y.1(c) shows the free body of the dual fillet welds. F is the net compressive or tensile force acting on the surface of the leg of the weld.

From moment equilibrium

$$M = F(h + t)$$

Following standard weld design practice, we assume that the shear stress on the throat of the weld is equal to the force F divided by the weld throat area. If we assume 40% weld efficiency, minimum weld throat, and define S_w as the average shear stress on the weld throat, then for a unit depth of weld,

$$F = S_w (0.707) (0.4) t$$

$$F = 0.283 S_w t$$

Then, from Eq. 3.Y.2,

$$M = 0.283 S_w t (h + t)$$

Comparing the two foregoing expressions for M , we have

$$0.283 S_w (ht + t^2) = \frac{S_p h \text{sup } 2}{6}$$

This is to be solved for the weld thickness t that is required for a panel thickness h . The relationship between S_p and S_w is evaluated using the most limiting hypothetical accident condition.

Specific stress levels appropriate for fillet welds for service conditions are found only in Subsection NF where 30% of the ultimate strength of the material is mandated (Table NF-3324.5(a)-1). For the Level D (faulted) condition appropriate to the most limiting drop or accident condition, Appendix F provides no specific limits for welds. Accordingly, Holtec set the

weld stress limit for Level D conditions to be the weld stress limit for Level A conditions amplified by the ratio of the membrane stress limits set forth in Subsection NG for Level D and Level A, respectively.

Table 2.2.11 sets limits on S_p (primary membrane plus bending stress). Table 3.1.14 gives

$$S_p = 55,450 \text{ psi at } 725^\circ \text{F}$$

The appropriate limit for the weld stress is set as

$$S_w = 0.42 S_u$$

Table 3.3.1 gives a value for the ultimate strength of the base metal as 62,350 psi at 725degreesF. The weld metal used at the panel connections is one grade higher in ultimate tensile stress than the adjacent base metal (80,000 psi at room temperature compared with 75,000 for the base metal at room temperature).

The strength of the weld is assumed to decrease with temperature the same as the base metal.

$$S_w = .42 \times 80,000 \left(\frac{62,350}{75,000} \right) = 27,930 \text{ psi}$$

Therefore, the corresponding limit stress on the weld throat is

$$h^2 = (0.283) (6) \frac{S_w}{S_p} (ht + t^2)$$

$$h^2 = 1.698 \frac{S_w}{S_p} (ht + t^2)$$

The equation given above establishes the relationship between the weld size "t", the fuel basket panel wall thickness "h", and the ratio of allowable weld strength "S_w" to base metal allowable strength "S_p". We now apply this formula to establish the minimum fillet weld size to be specified on

the design drawings to insure a factor of safety of 1.0 subsequent to incorporation of the appropriate dynamic load amplifier. Table 3.4.6 gives fuel basket safety factors "SF" for primary membrane plus bending stress intensities corresponding to the base metal allowable strength S_p at 725 degrees F. As noted in Subsection 3.4.4.4.1, the reported safety factors are conservatively low because of the conservative assumptions in modeling. Appendix 3.X provides dynamic amplification factors "DAF" for *typical* fuel basket types. To establish the minimum permissible weld size, S_p is replaced in the above formula by $(S_p \times (DAF/SF \times 1.1))$, and t/h computed for each basket. The additional 10% increase in safety factor is a conservative accounting that factors in the known conservatism in the finite element solution and the results from the simplified evaluation in Subsection 3.4.4.4.1. The following results are obtained:

MINIMUM WELD SIZE FOR FUEL BASKETS					
Item	SF (Table 3.4.6) x 1.1	DAF (<i>Bounding Values</i>)	t/h	h (inch)	t (inch)
MPC-24	1.41	1.077	0.57	10/32	0.178
MPC-68	1.58	1.06	0.516	8/32	0.129
MPC-32	1.40828	1.08	0.57	9/32	0.160
MPC-24E	1.903	1.08	0.455	10/32	0.142

Sheathing Weld Capacity

Theory:

Simple Force equilibrium relationships are used to demonstrate that the sheathing weld is adequate to support a 45g deceleration load applied vertically and horizontally to the sheathing and to the confined Boral. We perform the analysis assuming the weld is continuous and then modify the results to reflect the amplification due to intermittent welding.

Definitions

h = length of weld line (in.) (long side of sheathing)

w = width of weld line (in.) (short edge of sheathing)

t_w = weld size

e = 0.3 = quality factor for single fillet weld (from subsection NG, Table NG-3352-1)

W_b = weight of a Boral panel (lbf)

W_s = weight of sheathing confining a Boral panel (lbf)

G = 45

S_w = weld shear stress (psi)

Equations

Weld area = $2 (0.707 t_w e) (h)$ (neglect the top and bottom of the sheathing)

Load on weld = $(W_b + W_s) G$ (either horizontal or vertical)

Weld stress from combined action of vertical plus horizontal load in each of the two directions.

$$S_w = \frac{G (W_b + W_s) \sqrt{3}}{2 (.707) e t_w (h)}$$

For a PWR panel, the weights are calculated as

$$W_b = 11.35 \text{ lb.}$$

$$W_s = 28.0 \text{ lb.}$$

The weld size is conservatively assumed as a 1/16" fillet weld, and the length and width of the weld line is

$$h = 156 \text{ in.}$$

$$w = 7.5 \text{ in.}$$

Therefore,

$$S_w = \frac{45 \times (11.35 + 28) \times 1.732}{1.414 \times 0.3 \times (1/16) (156)} = 742 \text{ psi}$$

For an MPC-68 panel, the corresponding values are

$$W_b = 7.56 \text{ lb.}$$

$$W_s = 17.48 \text{ lb.}$$

$$h = 139 \text{ in.}$$

$$w = 5 \text{ in.}$$

$$S_w = \frac{45 \times (7.56 + 17.48) \times 1.732}{1.414 \times 0.3 \times (1/16 \text{ in.}) (139 \text{ in.})} = 530 \text{ psi}$$

The actual welding specified along the length of a sheathing panel is 2" weld on 8" pitch. The effect of the intermittent weld is to raise the average weld shear stress by a factor of 4. From the above results, it is concluded that the sheathing weld stress is negligible during the most severe drop accident condition. *This conclusion is valid for any and all fuel baskets.*

3.Y.2 Calculation for MPC Cover Plates in MPC Lid

The MPC cover plates are welded to the MPC lid during loading operations. The cover plates are part of the confinement boundary for the MPC. No credit is taken for the pressure retaining abilities of the quick disconnect couplings for the MPC vent and drain. Therefore, the MPC cover plates must meet ASME Code, Section III, Subsection NB limits for normal, off-normal, and accident conditions.

The normal and off-normal condition design basis MPC internal pressure is 100 psi. The accident condition design basis MPC internal pressure is 125 psi. Conservatively, the accident condition pressure loading is applied and it is demonstrated that the Level A limits for Subsection NB are met.

The MPC cover plate is depicted in the Design Drawings. The cover plate is stepped and has a maximum and minimum thickness of 0.38 inches and 0.1875 inches, respectively. Conservatively, the minimum thickness is utilized for these calculations.

To verify the MPC cover plate maintains the MPC internal pressure while meeting the ASME Code, Subsection NB limits, the cover plate bending stress and shear stress, and weld stress are calculated and compared to allowables.

Definitions

P = accident condition MPC internal pressure (psi) = 125 psi

r = cover plate radius (in.) = 2 in.

t = cover plate minimum thickness (in.) = 0.1875 in.

t_w = weld size (in.) = 0.1875 in.

The design temperature of the MPC cover plate is conservatively taken as equal to the MPC lid, 550°F. The peak temperature of the MPC lid is experienced on the internal portion of the MPC lid, and the actual operating temperature of the top surface is less than 400°F.

For the design temperature of 550°F, the Alloy X allowable membrane stress intensity is

$$S_m = 16,950 \text{ psi}$$

The allowable weld shear stress is 0.3 S_u per Subsection NF of the ASME Code for Level A conditions.

Equations

Using Timoshenko, Strength of Materials, Part II, Advanced Theory and Problems, Third Edition, Page 99, the formula for the bending stress in the coverplate is

:

$$S_b = \frac{(9.9)(P)(r^2)}{(8)(t^2)} \quad (\nu = 0.3)$$

$$S_b = \frac{(9.9)(125 \text{ psi})(2 \text{ in})^2}{(8)(0.1875 \text{ in})^2}$$

$$S_b = 17,600 \text{ psi}$$

The allowable bending stress is $1.5S_m$.

Therefore, $S_b < 1.5S_m$ (i.e., $17,600 \text{ psi} < 24,425 \text{ psi}$)

The shear stress due to the accident condition MPC internal pressure is calculated as follows:

$$\tau = \frac{P \pi r^2}{2 \pi r t}$$

$$\tau = \frac{(125 \text{ psi})(\pi)(2 \text{ in})^2}{(2)(\pi)(2 \text{ in})(0.1875 \text{ in})}$$

$$\tau = 667 \text{ psi}$$

This shear stress in the cover plate is less than the Level A limit of $0.4S_m = 6,780 \text{ psi}$.

The stress in the weld is calculated by dividing the shear stress in the cover plate by 0.707 and applying a quality factor 0.3. The weld size is equal to the minimum cover plate thickness and therefore the weld stress can be calculated from the cover plate shear stress.

$$S_w = \frac{\tau}{0.707 \times 0.3} = \frac{667 \text{ psi}}{0.707 \times 0.3}$$

$$S_w = 3,145 \text{ psi}$$

$$S_w < 0.3 S_u = 0.3 \times 63,300 \text{ psi} = 18,990 \text{ psi}$$

The Level A weld stress limit of 30% of the ultimate strength (at 550°F) has been taken from

Section NF of the ASME Code, the only section that specifically addresses stress limits for welds.

The stress developed as a result of the accident condition MPC internal pressure has been conservatively shown to be below the Level A, Subsection NB, ASME Code limits. The MPC cover plates meet the stress limits for normal, off-normal, and accident loading conditions at design temperature.

3.Y.3 Fuel Basket Angle Support Stress Calculations

The fuel basket internal to the MPC canister is supported by a combination of angle fuel basket supports and flat plate or solid bar fuel basket supports. These fuel basket supports are subject to significant load only when a lateral acceleration is applied to the fuel basket and the contained fuel. The quasi-static finite element analyses of the MPC's, under lateral inertia loading, focused on the structural details of the fuel basket and the MPC shell. Basket supports were modeled in less detail which served only to properly model the load transfer path between fuel basket and canister. Safety factors reported for the fuel basket supports from the finite element analyses, are overly conservative, and do not reflect available capacity of the fuel basket angle support. A more detailed stress analysis of the fuel basket angle supports is performed herein. We perform a strength of materials analysis of the fuel basket angle supports that complements the finite element results. We compute weld stresses at the support-to-shell interface, and membrane and bending stresses in the basket support angle plate itself. Using this strength of materials approach, we demonstrate that the safety factors for the fuel basket angle supports are larger than indicated by the finite element analysis.

The fuel basket supports of interest are angled plate components that are welded to the MPC shell using continuous single fillet welds. The design drawings and bill of materials in Section 1.5 of this submittal define the location of these supports for all MPC constructions. These basket supports experience no loading except when the fuel assembly basket and contained fuel is subject to lateral deceleration loads either from normal handling or accident events.

In this section, the analysis proceeds in the following manner. The fuel basket support loading is obtained by first computing the fuel basket weight (cell walls plus Boral plus sheathing) and adding to it the fuel weight. To maximize the support load, the MPC is assumed to be fully populated with fuel assemblies. This total calculated weight is then amplified by the design basis deceleration load and divided by the length of the fuel basket support. The resulting value is the load per unit length that must be resisted by all of the fuel basket supports. We next conservatively estimate, from the drawings for each MPC, the number of cells in a direct line (in the direction of the deceleration) that is resisted by the most highly loaded fuel basket angle support. We then compute the resisting load on the particular support induced by the inertia load from this number of cells. Force equilibrium on a simplified model of the fuel basket angle support then provides the weld load and the axial force and bending moment in the fuel basket support. The computation of safety factors is performed for a 45G load that bounds the non-mechanistic tip-over accident in HI-STORM and the deceleration load experienced by the MPC in a HI-TRAC side drop.

This section of Appendix 3.Y has been written using Mathcad; The notation ":= " is an equality.

We first establish as input data common to all MPC's, the allowable weld shear stress. In section 3.Y.1, the allowable weld stress for a Level D accident event defined. We further reduce this allowable stress by an appropriate weld efficiency obtained from the ASME Code, Section III, Subsection NG, Table NG-3352-1.

Weld efficiency $e := 0.35$ (single fillet weld, visual inspection only)

The fuel support brackets are constructed from Alloy "X". At the canister interface,

Ultimate Strength $S_u := 64000 \cdot \text{psi}$ Alloy X @ 450 degrees F (Table 3.3.1)

Note that here we use the design temperature for the MPC shell under normal conditions (Table 2.2.3) since the fire accident temperature is not applicable during the tip-over. The allowable weld shear stress, incorporating the weld efficiency is (use the base metal ultimate strength for additional conservatism) determined as:

$$\tau_{\text{all}} := .42 \cdot S_u \cdot e \quad \tau_{\text{all}} = 9.408 \times 10^3 \text{ psi}$$

For the non-mechanistic tip-over, the design basis deceleration in "g's" is

$G := 45$ (Table 3.1.2)

The total load to be resisted by the fuel basket supports is obtained by first computing the moving weight, relative to the MPC canister, for each MPC. The fuel basket weight is obtained from the weight calculation (dated 11/11/97) in HI-971656, HI-STAR 100 Structural Calculation Package.

The weights of the fuel baskets and total fuel load are (the notation "lbf" = "pound force")

Fuel Basket	Fuel	
$W_{\text{mpc32}} := 11875 \cdot \text{lbf}$	$W_{\text{f32}} := 53760 \cdot \text{lbf}$	MPC-32
$W_{\text{mpc68}} := 15263 \cdot \text{lbf}$	$W_{\text{f68}} := 47600 \cdot \text{lbf}$	MPC-68
$W_{\text{mpc24}} := 17045 \cdot \text{lbf}$	$W_{\text{f24}} := 40320 \cdot \text{lbf}$	MPC-24
$W_{\text{mpc24e}} := 21496 \cdot \text{lbf}$	$W_{\text{f24}} := 40320 \cdot \text{lbf}$	MPC-24E

Since the MPC24E is heavier, we assign a bounding weight to the MPC24 basket equal to that of the MPC24E in the following calculation.

$$W_{\text{mpc24}} := W_{\text{mpc24e}}$$

The minimum length of the fuel basket support is $L := 168\text{-in}$

Dwg. 1396, sheet 1 Note that for the MPC-68, the support length is increased by 1/2"

Therefore, the load per unit length that acts along the line of action of the deceleration, and is resisted by the total of all supports, is computed as

$$Q_{32} := \frac{(W_{\text{mpc}32} + W_{f32}) \cdot G}{(L + 0.5 \cdot \text{in})} \quad Q_{32} = 1.753 \times 10^4 \frac{\text{lbf}}{\text{in}}$$

$$Q_{68} := \frac{(W_{\text{mpc}68} + W_{f68}) \cdot G}{(L + 0.5 \cdot \text{in})} \quad Q_{68} = 1.679 \times 10^4 \frac{\text{lbf}}{\text{in}}$$

$$Q_{24} := \frac{(W_{\text{mpc}24} + W_{f24}) \cdot G}{L} \quad Q_{24} = 1.656 \times 10^4 \frac{\text{lbf}}{\text{in}}$$

$$Q_{24e} := \frac{(W_{\text{mpc}24e} + W_{f24}) \cdot G}{L} \quad Q_{24e} = 1.656 \times 10^4 \frac{\text{lbf}}{\text{in}}$$

The subscript associated with the above items is used as the identifier for the particular MPC.

An examination of the MPC construction drawings 1392, 1395, 1401, (sheet 1 of each drawing) indicates that the deceleration load is supported by shims and by fuel basket angle supports. By inspection of the relevant drawing, we can determine that the most highly loaded fuel basket angle support will resist the deceleration load from "NC" cells where NC for each basket type is obtained by counting the cells and portions of cells "above" the support in the direction of the deceleration. The following values for NC are used in the subsequent computation of fuel basket angle support stress:

$$NC_{32} := 6$$

$$NC_{68} := 8$$

$$NC_{24} := 7$$

The total normal load per unit length on the fuel basket support for each MPC type is therefore computed as:

$$P_{32} := Q_{32} \cdot \frac{NC_{32}}{32} \qquad P_{32} = 3.287 \times 10^3 \frac{\text{lb}}{\text{in}}$$

$$P_{68} := Q_{68} \cdot \frac{NC_{68}}{68} \qquad P_{68} = 1.975 \times 10^3 \frac{\text{lb}}{\text{in}}$$

$$P_{24} := Q_{24} \cdot \frac{NC_{24}}{24} \qquad P_{24} = 4.829 \times 10^3 \frac{\text{lb}}{\text{in}}$$

$$P_{24e} := Q_{24e} \cdot \frac{NC_{24}}{24} \qquad P_{24e} = 4.829 \times 10^3 \frac{\text{lb}}{\text{in}}$$

Here again, the subscript notation identifies the particular MPC.

Figure 3.Y.2 shows a typical fuel basket support with the support reactions at the base of the leg. The applied load and the loads necessary to put the support in equilibrium is not subscripted since the figure is meant to be typical of any MPC fuel basket angle support. The free body is drawn in a conservative manner by assuming that the load P is applied at the quarter point of the top flat portion. In reality, as the load is applied, the top flat portion deforms and the load shifts completely to the outer edges of the top flat section of the support. From the design drawings, we use the appropriate dimensions and perform the following analyses (subscripts are introduced as necessary as MPC identifiers):

The free body diagram shows the bending moment that will arise at the location where the idealized top flat section and the angled support are assumed to meet. Compatibility of joint rotation at the connection between the top flat and the angled portion of the support plus force and moment equilibrium equations from classical beam theory provide sufficient equations to solve for the bending moment at the connection (point O in Figure 3.Y.2), the load R at the weld, and the bending moment under the load P/2.

$$M_o := \frac{9}{16} \cdot \frac{Pw^2}{(S + 3 \cdot w)} \quad \blacksquare$$

Note that the small block after the equation indicates that this is a text equation rather than an evaluated equation. This is a Mathcad identifier.

The load in the weld, R, is expressed in the form

$$R := \frac{P \cdot H}{2 \cdot L} + \frac{M_o}{L}$$

Finally, the bending moment under the load, on the top flat portion, is given as

$$M_p := \frac{P}{2} \cdot \frac{w}{2} - M_o$$

The throat thickness of the fillet weld used between the supports and the MPC shell is

$$t_w := 0.125 \cdot \text{in} \cdot 7071$$

The wall thickness for computation of member stresses is: $t_{\text{wall}} := \frac{5}{16} \cdot \text{in}$

Performing the indicated computations and evaluations for each of the MPC's gives:

MPC-32 (Dwg.1392 sheet 4)

$$\theta_{32} := 9 \cdot \text{deg} \quad L_{32} := 5.6 \cdot \text{in} \quad w_{32} := \left(0.25 + .125 + .5 \cdot \frac{5}{16} \right) \cdot \text{in}$$

Therefore

$$H_{32} := L_{32} \cdot \tan(\theta_{32}) \quad H_{32} = 0.887 \text{ in} \quad w_{32} = 0.531 \text{ in}$$

$$S := \sqrt{L_{32}^2 + H_{32}^2} \quad S = 5.67 \text{ in}$$

$$M_o := \frac{9}{16} \cdot \frac{(P_{32} \cdot w_{32}^2)}{(S + 3 \cdot w_{32})} \quad M_o = 71.832 \text{ lbf} \cdot \frac{\text{in}}{\text{in}}$$

$$R_{32} := \frac{P_{32} \cdot H_{32}}{2 \cdot L_{32}} + \frac{M_o}{L_{32}} \quad R_{32} = 273.102 \frac{\text{lbf}}{\text{in}}$$

$$M_p := \frac{P_{32}}{2} \cdot \frac{w_{32}}{2} - M_o \quad M_p = 364.672 \text{ lbf} \cdot \frac{\text{in}}{\text{in}}$$

The weld stress is

$$\tau_{\text{weld}} := \frac{R_{32}}{t_w} \quad \tau_{\text{weld}} = 3.09 \times 10^3 \text{ psi}$$

For this event, the safety factor on the weld is

$$SF_{\text{weld}} := \frac{\tau_{\text{all}}}{\tau_{\text{weld}}} \quad SF_{\text{weld}} = 3.045$$

The maximum bending stress in the angled member is

$$\sigma_{\text{bending}} := 6 \cdot \frac{M_o}{t_{\text{wall}}^2} \quad \sigma_{\text{bending}} = 4.413 \times 10^3 \text{ psi}$$

The direct stress in the basket support angled section is

$$\sigma_{\text{direct}} := \frac{(R_{32} \cdot \sin(\theta_{32}) + .5 \cdot P_{32} \cdot \cos(\theta_{32}))}{t_{\text{wall}}} \quad \sigma_{\text{direct}} = 5.331 \times 10^3 \text{ psi}$$

From Table 3.1.16, the allowable membrane stress intensity for this condition is

$$S_{\text{membrane}} := 39400 \cdot \text{psi} \quad (\text{use the value at 600 degree F to conservatively bound the Safety Factor})$$

$$SF_{\text{membrane}} := \frac{S_{\text{membrane}}}{\sigma_{\text{direct}}} \quad SF_{\text{membrane}} = 7.391$$

From Table 3.1.16, the allowable combined stress intensity for this accident condition is

$$S_{\text{combined}} := 59100 \cdot \text{psi} \quad (\text{use the value at 600 degree F to conservatively bound the Safety Factor})$$

$$SF_{\text{combined}} := \frac{S_{\text{combined}}}{\sigma_{\text{direct}} + \sigma_{\text{bending}}} \quad SF_{\text{combined}} = 6.065$$

Note that for this model, it is appropriate to compare the computed stress with allowable stress intensities since we are dealing with beams and there are no surface pressure stresses.

The maximum bending stress in the top flat section is

$$\sigma_{\text{bending}} := 6 \cdot \frac{M_p}{t_{\text{wall}}^2} \quad \sigma_{\text{bending}} = 2.241 \times 10^4 \text{ psi}$$

The direct stress in the basket support top flat section is

$$\sigma_{\text{direct}} := \frac{R_{32}}{t_{\text{wall}}} \quad \sigma_{\text{direct}} = 873.926 \text{ psi}$$

Computing the safety factors gives:

$$SF_{\text{membrane}} := \frac{S_{\text{membrane}}}{\sigma_{\text{direct}}} \quad SF_{\text{membrane}} = 45.084$$

$$SF_{\text{combined}} := \frac{S_{\text{combined}}}{\sigma_{\text{direct}} + \sigma_{\text{bending}}} \quad SF_{\text{combined}} = 2.539$$

All safety factors are greater than 1.0; therefore, the design is acceptable

MPC-24 (Dwg.1395 sheet 4)

$$\theta_{24} := 9 \cdot \text{deg} \quad L_{24} := 4 \cdot \text{in} \quad w_{24} := \left(0.25 + .125 + .5 \cdot \frac{5}{16} \right) \cdot \text{in}$$

Therefore

$$H_{24} := L_{24} \cdot \tan(\theta_{24}) \quad H_{24} = 0.634 \text{ in} \quad w_{24} = 0.531 \text{ in}$$

$$S := \sqrt{L_{24}^2 + H_{24}^2} \quad S = 4.05 \text{ in}$$

$$M_o := \frac{9 \cdot (P_{24} \cdot w_{24}^2)}{16 \cdot (S + 3 \cdot w_{24})} * \quad M_o = 135.848 \text{ lbf} \cdot \frac{\text{in}}{\text{in}}$$

$$R_{24} := \frac{P_{24} \cdot H_{24}}{2 \cdot L_{24}} + \frac{M_o}{L_{24}} * \quad R_{24} = 416.411 \frac{\text{lbf}}{\text{in}}$$

$$M_p := \frac{P_{24} \cdot w_{24}}{2} - M_o * \quad M_p = 505.553 \text{ lbf} \cdot \frac{\text{in}}{\text{in}}$$

The weld stress is

$$\tau_{\text{weld}} := \frac{R_{24}}{t_w} \quad \tau_{\text{weld}} = 4.711 \times 10^3 \text{ psi}$$

For this event, the safety factor on the weld is

$$SF_{\text{weld}} := \frac{\tau_{\text{all}}}{\tau_{\text{weld}}} \quad SF_{\text{weld}} = 1.997$$

The maximum bending stress in the angled member is

$$\sigma_{\text{bending}} := 6 \cdot \frac{M_o}{t_{\text{wall}}^2} \quad \sigma_{\text{bending}} = 8.347 \times 10^3 \text{ psi}$$

The direct stress in the basket support angled section is

$$\sigma_{\text{direct}} := \frac{(R_{24} \cdot \sin(\theta_{24}) + .5 \cdot P_{24} \cdot \cos(\theta_{24}))}{t_{\text{wall}}} \quad \sigma_{\text{direct}} = 7.84 \times 10^3 \text{ psi}$$

From Table 3.1.16, the allowable membrane stress intensity for this condition is

$$S_{\text{membrane}} := 39400 \cdot \text{psi} \quad (\text{use the value at 600 degree F to conservatively bound the Safety Factor})$$

$$SF_{\text{membrane}} := \frac{S_{\text{membrane}}}{\sigma_{\text{direct}}} \quad SF_{\text{membrane}} = 5.025$$

From Table 3.1.16, the allowable combined stress intensity for this accident condition is

$$S_{\text{combined}} := 59100 \cdot \text{psi} \quad (\text{use the value at 600 degree F to conservatively bound the Safety Factor})$$

$$SF_{\text{combined}} := \frac{S_{\text{combined}}}{\sigma_{\text{direct}} + \sigma_{\text{bending}}} \quad SF_{\text{combined}} = 3.651$$

Note that for this model, it is appropriate to compare the computed stress with allowable stress intensities since we are dealing with beams and there are no surface pressure stresses.

$$SF_{\text{membrane}} := \frac{S_{\text{membrane}}}{\sigma_{\text{direct}}} \quad SF_{\text{membrane}} = 5.025$$

$$SF_{\text{combined}} := \frac{S_{\text{combined}}}{\sigma_{\text{direct}} + \sigma_{\text{bending}}} \quad SF_{\text{combined}} = 3.651$$

The maximum bending stress in the top flat section is

$$\sigma_{\text{bending}} := 6 \cdot \frac{M_p}{t_{\text{wall}}^2} \quad \sigma_{\text{bending}} = 3.106 \times 10^4 \text{ psi}$$

The direct stress in the basket support top flat section is

$$\sigma_{\text{direct}} := \frac{R_{24}}{t_{\text{wall}}} \quad \sigma_{\text{direct}} = 1.333 \times 10^3 \text{ psi}$$

Computing the safety factors gives:

$$SF_{\text{membrane}} := \frac{S_{\text{membrane}}}{\sigma_{\text{direct}}} \quad SF_{\text{membrane}} = 29.568$$

$$SF_{\text{combined}} := \frac{S_{\text{combined}}}{\sigma_{\text{direct}} + \sigma_{\text{bending}}} \quad SF_{\text{combined}} = 1.824$$

All safety factors are greater than 1.0; therefore, the design is acceptable

MPC-68 (Dwg 1401 sheet 4)

$$\theta_{68} := 12.5 \cdot \text{deg} \quad L_{68} := 4.75 \cdot \text{in} \quad (\text{estimated}) \quad w_{68} := \left(0.75 - .5 \cdot \frac{5}{16}\right) \cdot \text{in}$$

Note that in the MPC-68, there is no real top flat portion to the angle support. "w" is computed as the radius of the bend less 50% of the wall thickness. However, in the remaining calculations, the applied load is assumed a distance w/2 from the center on each side of the support centerline in Figure 3.Y.2.

Therefore

$$H_{68} := L_{68} \cdot \tan(\theta_{68}) \quad H_{68} = 1.053 \text{ in} \quad w_{68} = 0.594 \text{ in}$$

$$S := \sqrt{L_{68}^2 + H_{68}^2} \quad S = 4.865 \text{ in}$$

$$M_o := \frac{9}{16} \cdot \frac{P_{68} \cdot w_{68}^2}{(S + 3 \cdot w_{68})} \quad M_o = 58.928 \text{ lbf} \cdot \frac{\text{in}}{\text{in}}$$

$$R_{68} := \frac{P_{68} \cdot H_{68}}{2 \cdot L_{68}} + \frac{M_o}{L_{68}} * \quad R_{68} = 231.34 \frac{\text{lbf}}{\text{in}}$$

$$M_p := \frac{P_{68}}{2} \cdot \frac{w_{68}}{2} - M_o * \quad M_p = 234.251 \text{ lbf} \cdot \frac{\text{in}}{\text{in}}$$

The weld stress is

$$\tau_{\text{weld}} := \frac{R_{68}}{t_w} \quad \tau_{\text{weld}} = 2.617 \times 10^3 \text{ psi}$$

The safety factor on the weld is

$$SF_{\text{weld}} := \frac{\tau_{\text{all}}}{\tau_{\text{weld}}} \quad SF_{\text{weld}} = 3.594$$

The maximum bending stress in the angled member is

$$\sigma_{\text{bending}} := 6 \cdot \frac{M_o}{t_{\text{wall}}^2} \quad \sigma_{\text{bending}} = 3.621 \times 10^3 \text{ psi}$$

The direct stress in the basket support angled section is

$$\sigma_{\text{direct}} := \frac{(R_{68} \cdot \sin(\theta_{68}) + .5 \cdot P_{68} \cdot \cos(\theta_{68}))}{t_{\text{wall}}} \quad \sigma_{\text{direct}} = 3.245 \times 10^3 \text{ psi}$$

$$SF_{\text{membrane}} := \frac{S_{\text{membrane}}}{\sigma_{\text{direct}}} \quad SF_{\text{membrane}} = 12.14$$

$$SF_{\text{combined}} := \frac{S_{\text{combined}}}{\sigma_{\text{direct}} + \sigma_{\text{bending}}} \quad SF_{\text{combined}} = 8.608$$

The maximum bending stress in the idealized top flat section is

$$\sigma_{\text{bending}} := 6 \cdot \frac{M_p}{t_{\text{wall}}^2} \quad \sigma_{\text{bending}} = 1.439 \times 10^4 \text{ psi}$$

The direct stress in the basket support top flat section is

$$\sigma_{\text{direct}} := \frac{R_{68}}{t_{\text{wall}}} \quad \sigma_{\text{direct}} = 740.289 \text{ psi}$$

$$SF_{\text{membrane}} := \frac{S_{\text{membrane}}}{\sigma_{\text{direct}}} \quad SF_{\text{membrane}} = 53.222$$

$$SF_{\text{combined}} := \frac{S_{\text{combined}}}{\sigma_{\text{direct}} + \sigma_{\text{bending}}} \quad SF_{\text{combined}} = 3.905$$

All safety factors are greater than 1.0; therefore, the design is acceptable

SUMMARY OF RESULTS

The above calculations demonstrate that for all MPC fuel basket angle supports, the minimum safety margin is 1.82 (MPC-24 combined membrane plus bending in the top flat section). This is a larger safety factor than predicted from the finite element solution. The reason for this increase is attributed to the fact that the finite element analysis used a less robust structural model of the supports for stress analysis purposes since the emphasis there was on analysis of the fuel basket itself and the MPC canister.. Therefore, in reporting safety factors, or safety margins, the minimum safety factor of 1.82 should be used for this component in any summary table.

APPENDIX 3.AC - LIFTING CALCULATIONS

3.AC.1 Scope of Appendix

In this Appendix, the attachment locations that are used for lifting various lids are analyzed for strength and engagement length. The mating lifting device is not a part of this submittal but representative catalog items are chosen for analysis to demonstrate that commercially available lifting devices suffice to meet the required safety margins.

3.AC.2 Configuration

The required data for analysis is 1) the number of bolts NB; 2) the bolt diameter db; 3) the lid weight; and 4), the details of the individual bolts.

3.AC.3 Acceptance Criteria

The lifting bolts are considered as part of a special lifting device; therefore, NUREG-0612 applies. The acceptance criteria is that the bolts and the adjacent lid threads must have stress less than $1/3 \times$ material yield strength and $1/5 \times$ material ultimate strength. These reduced requirements are acceptable since the outer diameters of the lifted parts are larger than the inner diameter of the cavity under the lifted parts; therefore, the lifted parts cannot impact stored directly as long as sufficient controls are maintained on carry heights to preclude inordinant rotations in the event of a handling accident.

3.AC.4 Composition of Appendix

This appendix is created using the Mathcad (version 2000) software package. Mathcad uses the symbol ':=' as an assignment operator, and the equals symbol '=' retrieves values for constants or variables.

3.AC.5 References

[3.AC.1] E. Oberg and F.D. Jones, *Machinery's Handbook*, Fifteenth Edition, Industrial Press 1957, pp987-990.

[3.AC.2] FED-STD-H28/2A, *Federal Standard Screw-Thread Standards for Federal Services*, United States Government Printing Office, April, 1984.

3.AC.6 Input Data for Lifting of Overpack Top Lid (HI-STORM 100S bounds)

Lifted Weight (Table 3.2.1): $W_{\text{lift}} := (25500 \cdot 1.15) \cdot \text{lb}$ includes 15% inertia load factor

The following input parameters are taken from Holtec Dwgs. for 100S lid.

Bolt diameter $db := 1.5 \cdot \text{in}$ (Dwg. 3072)

$N := 6 \cdot \frac{1}{\text{in}}$ is the number of threads per inch (UNC)

$L_{\text{eng}} := 1.5 \cdot \text{in}$ is the length of engagement (lower of two 2" top plates, Dwg. 1561).

Number of Bolts $NB := 4$

Lifting of the HI-STORM 100 lid is limited to a straight (90 deg) lift. For conservatism the minimum lift angle (from the horizontal) is assumed to be:

$\text{ang} := 80 \cdot \text{deg}$

$A_d := \pi \cdot \frac{db^2}{4}$ $A_d = 1.767 \text{ in}^2$ is the area of the unthreaded portion of the bolt

$A_{\text{stress}} := 1.405 \cdot \text{in}^2$ is the stress area of the bolt

$d_{\text{pitch}} := 1.3917 \cdot \text{in}$ is the pitch diameter of the bolt

$dm_{\text{ext}} := 1.2955 \cdot \text{in}$ is the minor diameter of the bolt

$dm_{\text{int}} := 1.3196 \cdot \text{in}$ is the minor diameter of the hole

The design temperature of the top lid, located atop the overpack, is 350 deg. F. The lid lifting bolts, will not see this temperature under normal circumstances. For conservatism, the material properties and allowable stresses for the lid used in the qualification are taken at 350 deg F.

The yield and ultimate strengths of the overpack top lid are reduced by factors of 3 and 5, respectively. The eyebolt working load limit(not part of the HI-STORM 100 System) will have a safety factor of 5.

$S_{\text{ulid}} := \frac{70000}{5} \cdot \text{psi}$ (Table 3.3.2) $S_{\text{ylid}} := \frac{33150}{3} \cdot \text{psi}$ (Table 3.3.2)

The yield stress criteria governs the analysis.

3.AC.7 Calculations

3.AC.7.1 Length of Engagement/Strength Calculations

In this section, it is shown that the length of thread engagement is adequate. The method and terminology of Reference 3.AC.2 is followed.

$$p := \frac{1}{N} \quad \text{is the thread pitch}$$

$$H := 4 \cdot 0.21651 \cdot p \quad H = 0.144 \text{ in}$$

$$\text{Depth}_{\text{ext}} := \frac{17}{24} \cdot H \quad \text{Depth}_{\text{ext}} = 0.102 \text{ in}$$

$$\text{Depth}_{\text{int}} := \frac{5}{8} \cdot H \quad \text{Depth}_{\text{int}} = 0.09 \text{ in}$$

$$\text{dmaj}_{\text{ext}} := \text{dm}_{\text{ext}} + 2 \cdot \text{Depth}_{\text{ext}} \quad \text{dmaj}_{\text{ext}} = 1.5 \text{ in}$$

Using page 103 of reference 3.AC.2,

$$\text{Bolt_thrd_shr_A} := \pi \cdot N \cdot L_{\text{eng}} \cdot \text{dm}_{\text{int}} \cdot \left[\frac{1}{2 \cdot N} + .57735 \cdot (d_{\text{pitch}} - \text{dm}_{\text{int}}) \right]$$

$$\text{Bolt_thrd_shr_A} = 4.662 \text{ in}^2$$

$$\text{Ext_thrd_shr_A} := \pi \cdot N \cdot L_{\text{eng}} \cdot \text{dmaj}_{\text{ext}} \cdot \left[\frac{1}{2 \cdot N} + 0.57735 \cdot (\text{dmaj}_{\text{ext}} - d_{\text{pitch}}) \right]$$

$$\text{Ext_thrd_shr_A} = 6.186 \text{ in}^2$$

The normal stress capacities of the bolt, and load capacity of the top lid material, based on yield strength, are (the shear area is taken as the stress area here since the lifting bolt that also fits into this hole is not part of the HI-STORM 100 System. The representative lid lifting bolt specification for the analysis is assumed as equivalent to Crosby S-279, Part Number 9900271):

$$\text{Load_Capacity}_{\text{bolt}} := 21400 \cdot \text{lbf}$$

$$\text{Load_Capacity}_{\text{bolt}} = 2.14 \times 10^4 \text{ lbf}$$

$$\text{Load_Capacity}_{\text{lid}} := (0.577 \cdot S_{y\text{lid}}) \cdot \text{Ext_thrd_shr_A}$$

$$\text{Load_Capacity}_{\text{lid}} = 3.944 \times 10^4 \text{ lbf}$$

Therefore, the lifting capacity of the configuration is based on bolt shear due to lid thread capacity or the actual catalog rated capacity of the bolt adjusted for the angled lift.

$$\text{Max_Lift_Load} := \text{NB} \cdot \text{Load_Capacity}_{\text{lid}}$$

$$\text{Max_Lift_Load} = 1.578 \times 10^5 \text{ lbf}$$

$$\text{SF} := \frac{\text{Max_Lift_Load}}{W_{\text{lift}}}$$

$$\text{SF} = 5.38 > 1$$

Even though a vertical lift is required, the safety factor is consistently and conservatively computed based on the assumed lift angle:

or

$$\text{SF} := \frac{\text{NB} \cdot \text{Load_Capacity}_{\text{bolt}} \cdot 0.844}{W_{\text{lift}}}$$

$$\text{SF} = 2.464 > 1$$

Note that the minimum safety factor based on bolt rated capacity does not include the built-in catalog rated safety factor of 5. The factor of 0.844 is based on an interpolation of the reduction factor stated in the Crosby Catalog (p. 72) for off angle lifts as computed below:

For a 45 degree off-angle, the reduction factor is 0.70; therefore for the assumed 10 degree off-angle,

$$\frac{(90 \cdot \text{deg} - \text{ang})}{45 \cdot \text{deg}} \cdot 0.70 = 0.156$$

$$1 - .156 = 0.844$$

3.AC.8 Input Data for Lifting of HI-TRAC Pool Lid

Lifted Weight: (the HI-TRAC 125 pool lid bounds all other lids - this is the only load)

Weight := 12500·lbf Table 3.2.2. This load bounds all other lids that may be lifted

ang := 45·deg

Minimum Lift Angle from Horizontal (to bound all lifts other than the HI-STORM 100 top lid)

inertia_load_factor := .15

$$W_{\text{lift}} := \text{Weight} \cdot (1.0 + \text{inertia_load_factor})$$

$$W_{\text{lift}} = 1.437 \times 10^4 \text{ lbf} \quad \text{includes any anticipated inertia load factor}$$

The assumed representative lifting bolts used for the analysis herein are High-Load Lifting B per McMaster-Carr Catalog 104, p. 929, Part Number 3026T34.

$$\text{Working_Load} := 17000 \cdot \text{lbf} \quad \text{These lifting bolts are designed for off-vertical lifts}$$

$$\text{Bolt diameter} \quad \text{db} := .875 \cdot \text{in}$$

$$\text{Number of Bolts} \quad \text{NB} := 4$$

$$N := 9 \cdot \frac{1}{\text{in}} \quad \text{is the number of threads per inch}$$

$$L_{\text{eng}} := 1.375 \cdot \text{in} \quad \text{is the length of engagement (per M-C catalog)}$$

The material properties are those of SA 516 Grade 70 @ 350 deg. F. From Table 3.3.2,

$$S_{\text{ulid}} := \frac{70000 \cdot \text{psi}}{5} \quad S_{\text{ylid}} := \frac{33150 \cdot \text{psi}}{3}$$

$$A_{\text{d}} := \pi \cdot \frac{\text{db}^2}{4} \quad A_{\text{d}} = 0.601 \text{ in}^2 \quad \text{is the area of the unthreaded portion of the bolt}$$

$$A_{\text{stress}} := .462 \cdot \text{in}^2 \quad \text{is the stress area of the bolt} \quad \text{Thread properties are from Machinery's Handbook, 23rd Edition, Table 3a, p.1484}$$

$$d_{\text{pitch}} := .8028 \cdot \text{in} \quad \text{is the pitch diameter of the bolt}$$

$$d_{\text{mext}} := .7427 \cdot \text{in} \quad \text{is the major diameter of the bolt}$$

$$d_{\text{mint}} := .7547 \cdot \text{in} \quad \text{is the minor diameter of the threaded hole}$$

3.AC.9 Calculations

Length of Engagement/Strength Calculations

In this section, it is shown that the length of thread engagement is adequate. The method and terminology of reference 3.AC.2 is followed.

$$p := \frac{1}{N} \quad \text{is the thread pitch}$$

$$H := 4 \cdot 0.21651 \cdot p \quad H = 0.096 \text{ in}$$

$$\text{Depth}_{\text{ext}} := \frac{17}{24} \cdot H \quad \text{Depth}_{\text{ext}} = 0.068 \text{ in}$$

$$\text{Depth}_{\text{int}} := \frac{5}{8} \cdot H \quad \text{Depth}_{\text{int}} = 0.06 \text{ in}$$

$$d_{\text{maj}_{\text{ext}}} := d_{\text{ext}} + 2 \cdot \text{Depth}_{\text{ext}} \quad d_{\text{maj}_{\text{ext}}} = 0.879 \text{ in}$$

Using page 103 of reference 3.AC.2,

$$\text{Bolt_thrd_shr_A} := \pi \cdot N \cdot L_{\text{eng}} \cdot d_{\text{mint}} \cdot \left[\frac{1}{2 \cdot N} + .57735 \cdot (d_{\text{pitch}} - d_{\text{mint}}) \right]$$
$$\text{Bolt_thrd_shr_A} = 2.445 \text{ in}^2$$

$$\text{Ext_thrd_shr_A} := \pi \cdot N \cdot L_{\text{eng}} \cdot d_{\text{maj}_{\text{ext}}} \cdot \left[\frac{1}{2 \cdot N} + 0.57735 \cdot (d_{\text{maj}_{\text{ext}}} - d_{\text{pitch}}) \right]$$
$$\text{Ext_thrd_shr_A} = 3.402 \text{ in}^2$$

The load capacity of the lid material based on yield strength is:

$$\text{Load_Capacity}_{\text{lid}} := (0.577 \cdot S_{\text{ylid}}) \cdot \text{Ext_thrd_shr_A}$$
$$\text{Load_Capacity}_{\text{lid}} = 2.169 \times 10^4 \text{ lbf}$$

Therefore, the lifting capacity of the configuration, based on lid shear, is:

$$\text{Max_Lift_Load}_{\text{lidshear}} := N \cdot \text{Load_Capacity}_{\text{lid}}$$

$$\text{Max_Lift_Load}_{\text{lidshear}} = 8.677 \times 10^4 \text{ lbf}$$

The safety factor is defined as

$$\text{SF} := \frac{\text{Max_Lift_Load}_{\text{lidshear}}}{W_{\text{lift}}} \quad \text{SF} = 6.036 > 1$$

The safety factor, based on the working load limit specified in the McMaster-Carr Catalog,

$$\text{SF}_b := \frac{\text{Working_Load}}{0.25 \cdot W_{\text{lift}}} \quad \text{SF}_b = 4.73$$

3.AC.10 Input Data for Lifting of HI-TRAC Top Lid

Lifted Weight: (the HI-TRAC 125 top lid bounds all other lids - this is the only load)

$$\text{Weight} := 2750 \cdot \text{lbf} \quad \text{Table 3.2.2}$$

$$\text{ang} := 45 \cdot \text{deg} \quad \text{Minimum Lift Angle from Horizontal (to bound all lifts other than the HI-STORM 100 top lid)}$$

$$\text{inertia_load_factor} := .15$$

$$W_{\text{lift}} := \text{Weight} \cdot (1.0 + \text{inertia_load_factor})$$

$$W_{\text{lift}} = 3.163 \times 10^3 \text{ lbf} \quad \text{includes any anticipated inertia load factor}$$

The lifting bolts assumed as representative for the analysis herein are High-Load Lifting Bolt per McMaster-Carr Catalog 104, p. 929, Part Number 3026T32.

$$\text{Working_Load} := 9000 \cdot \text{lbf} \quad \text{These lifting bolts are designed for off-vertical lifts}$$

$$\text{Bolt diameter} \quad \text{db} := .625 \cdot \text{in}$$

$$\text{Number of Bolts} \quad \text{NB} := 4$$

$$N := 11 \cdot \frac{1}{\text{in}} \quad \text{is the number of threads per inch}$$

$L_{eng} := 1.0 \cdot \text{in}$ is the length of engagement (per M-C catalog)

For , the material properties are those of SA 516 Grade 70 @ 350 deg. F. From Table 3.3.2,

$$S_{ulid} := \frac{70000 \cdot \text{psi}}{5} \qquad S_{ylid} := \frac{33150 \cdot \text{psi}}{3}$$

$$A_d := \pi \cdot \frac{d_b^2}{4} \qquad A_d = 0.307 \text{ in}^2 \qquad \text{is the area of the unthreaded portion of the bolt}$$

$$A_{stress} := .226 \cdot \text{in}^2 \qquad \text{is the stress area of the bolt} \qquad \text{Thread properties are from}$$

$$d_{pitch} := .566 \cdot \text{in} \qquad \text{is the pitch diameter of the bolt} \qquad \text{Machinery's Handbook, 23rd Edition, Table 3a, p.1484}$$

$$d_{m_{ext}} := .5168 \cdot \text{in} \qquad \text{is the major diameter of the bolt}$$

$$d_{m_{int}} := .5266 \cdot \text{in} \qquad \text{is the minor diameter of the threaded hole}$$

3.AC.11 Calculations

Length of Engagement/Strength Calculations

In this section, it is shown that the length of thread engagement is adequate The method ar terminology of reference 3.AC.2 is followed.

$$p := \frac{1}{N} \qquad \text{is the thread pitch}$$

$$H := 4 \cdot 0.21651 \cdot p \qquad H = 0.079 \text{ in}$$

$$\text{Depth}_{ext} := \frac{17}{24} \cdot H \qquad \text{Depth}_{ext} = 0.056 \text{ in}$$

$$\text{Depth}_{int} := \frac{5}{8} \cdot H \qquad \text{Depth}_{int} = 0.049 \text{ in}$$

$$d_{maj_{ext}} := d_{m_{ext}} + 2 \cdot \text{Depth}_{ext} \qquad d_{maj_{ext}} = 0.628 \text{ in}$$

Using page 103 of reference 3.AC.2,

$$\text{Bolt_thrd_shr_A} := \pi \cdot N \cdot L_{\text{eng}} \cdot d_{\text{m}_{\text{int}}} \left[\frac{1}{2 \cdot N} + .57735 \cdot (d_{\text{pitch}} - d_{\text{m}_{\text{int}}}) \right]$$

$$\text{Bolt_thrd_shr_A} = 1.241 \text{ in}^2$$

$$\text{Ext_thrd_shr_A} := \pi \cdot N \cdot L_{\text{eng}} \cdot d_{\text{m}_{\text{aj}_{\text{ext}}}} \left[\frac{1}{2 \cdot N} + 0.57735 \cdot (d_{\text{m}_{\text{aj}_{\text{ext}}}} - d_{\text{pitch}}) \right]$$

$$\text{Ext_thrd_shr_A} = 1.768 \text{ in}^2$$

The load capacity of the lid material based on yield strength is:

$$\text{Load_Capacity}_{\text{lid}} := (0.577 \cdot S_{\text{ylid}}) \cdot \text{Ext_thrd_shr_A}$$

$$\text{Load_Capacity}_{\text{lid}} = 1.128 \times 10^4 \text{ lbf}$$

Therefore, the lifting capacity of the configuration, based on lid shear, is.

$$\text{Max_Lift_Load}_{\text{lid}_{\text{shear}}} := N \cdot \text{Load_Capacity}_{\text{lid}}$$

$$\text{Max_Lift_Load}_{\text{lid}_{\text{shear}}} = 4.51 \times 10^4 \text{ lbf}$$

The safety factor is defined as

$$\text{SF} := \frac{\text{Max_Lift_Load}_{\text{lid}_{\text{shear}}}}{W_{\text{lift}}}$$

$$\text{SF} = 14.261 > 1$$

The safety factor, based on the working load limit specified in the McMaster-Carr Catalog

$$\text{SF}_b := \frac{\text{Working_Load}}{0.25 \cdot W_{\text{lift}}}$$

$$\text{SF}_b = 11.383$$

3.AC.12 Conclusion

The preceding analysis demonstrates that the length of thread engagement at the lifting loca are conservatively set. When lifting of the component is not being performed, plugs of a non-galling material with properties equal to or better than the base material shall be in-plac provide a filler material.

3.AC.13 Length of Engagement for Circumferential Bolts in HI-TRAC Pool Lid

Input Data for Check of thread engagement

Total supported load: $W_{\text{lift}} := 119500 \cdot 1.15 \cdot \text{lbf}$ From Appendix 3.AB

with a 15% dynamic load factor

Bolt diameter $db := 1.0 \cdot \text{in}$ Holtec drawing no. 1880

Number of Bolts $NB := 36$ Holtec drawing no. 1880

$N := 8 \cdot \frac{1}{\text{in}}$ is the number of threads per inch Holtec drawing no. 1880

$L_{\text{eng}} := 0.5 \cdot \text{in}$ is the length of engagement Holtec drawing no. 1880

$A_d := \pi \cdot \frac{db^2}{4}$ $A_d = 0.785 \text{ in}^2$ is the area of the unthreaded portion of the bolt

$A_{\text{stress}} := 0.606 \cdot \text{in}^2$ is the stress area of the bolt
Per Table 3a of Machinery's Handbook, 23rd Edition, p. 1484

$d_{\text{pitch}} := 0.9188 \cdot \text{in}$ is the pitch diameter of the bolt

$dm_{\text{ext}} := 0.8512 \cdot \text{in}$ is the minor diameter of the bolt

$dm_{\text{int}} := 0.8647 \cdot \text{in}$ is the minor diameter of the hole

For conservatism, the material properties and allowable stresses for the pool lid bolts and the lid used in the qualification are taken at 350 deg F for the lid, and 300 deg. F for the bolts.

The yield and ultimate strengths of the lid, and the bolts are:

$S_{\text{ulid}} := \frac{70000}{5} \cdot \text{psi}$ $S_{\text{ubolt}} := \frac{103016 \cdot \text{psi}}{5}$
 $S_{\text{ylid}} := \frac{33150}{3} \cdot \text{psi}$ $S_{\text{ybolt}} := \frac{85100 \cdot \text{psi}}{3}$
SA-193-B7 bolts
Table 3.3.4

3.AC.13.1 Length of Engagement/Strength Calculations

In this section, it is shown that the length of thread engagement is adequate. The method and terminology of reference 3.AC.2 is followed.

$$p := \frac{1}{N} \quad \text{is the thread pitch} \quad p = 0.125 \text{ in}$$

$$H := 4 \cdot 0.21651 \cdot p \quad H = 0.108 \text{ in}$$

$$\text{Depth}_{\text{ext}} := \frac{17}{24} \cdot H \quad \text{Depth}_{\text{ext}} = 0.077 \text{ in}$$

$$\text{Depth}_{\text{int}} := \frac{5}{8} \cdot H \quad \text{Depth}_{\text{int}} = 0.068 \text{ in}$$

$$\text{dmaj}_{\text{ext}} := \text{dm}_{\text{ext}} + 2 \cdot \text{Depth}_{\text{ext}} \quad \text{dmaj}_{\text{ext}} = 1.005 \text{ in}$$

Using page 103 of reference 3.AC.2,

$$\text{Bolt_thrd_shr_A} := \pi \cdot N \cdot L_{\text{eng}} \cdot \text{dm}_{\text{int}} \cdot \left[\frac{1}{2 \cdot N} + .57735 \cdot (d_{\text{pitch}} - \text{dm}_{\text{int}}) \right]$$
$$\text{Bolt_thrd_shr_A} = 1.019 \text{ in}^2$$

$$\text{Ext_thrd_shr_A} := \pi \cdot N \cdot L_{\text{eng}} \cdot \text{dmaj}_{\text{ext}} \cdot \left[\frac{1}{2 \cdot N} + 0.57735 \cdot (\text{dmaj}_{\text{ext}} - d_{\text{pitch}}) \right]$$
$$\text{Ext_thrd_shr_A} = 1.414 \text{ in}^2$$

The load capacities of the bolt and the lid material based on yield strength are:

$$\text{Load_Capacity}_{\text{bolt}} := S_{\text{ybolt}} \cdot A_{\text{stress}} \quad \text{Load_Capacity}_{\text{bolt}} = 1.719 \times 10^4 \text{ lbf}$$

$$\text{Load_Capacity}_{\text{boltthrd}} := (0.577 \cdot S_{\text{ybolt}}) \cdot \text{Bolt_thrd_shr_A}$$
$$\text{Load_Capacity}_{\text{boltthrd}} = 1.667 \times 10^4 \text{ lbf}$$

$$\text{Load_Capacity}_{\text{lid}} := (0.577 \cdot S_{y\text{lid}}) \cdot \text{Ext_thrd_shr_A}$$

$$\text{Load_Capacity}_{\text{lid}} = 9.016 \times 10^3 \text{ lbf}$$

Therefore, the capacity of the configuration is based on base metal thread shear.

$$\text{Max_Lift_Load} := \text{NB} \cdot \text{Load_Capacity}_{\text{lid}} \quad \text{Max_Lift_Load} = 3.246 \times 10^5 \text{ lbf}$$

The safety factor is

$$\text{SF} := \frac{\text{Max_Lift_Load}}{W_{\text{lift}}} \quad \text{SF} = 2.362 > 1$$

The load capacities of the bolt and the lid material based on ultimate strength are:

$$\text{Load_Capacity}_{\text{bolt}} := S_{\text{ubolt}} \cdot A_{\text{stress}}$$

$$\text{Load_Capacity}_{\text{bolt}} = 1.249 \times 10^4 \text{ lbf}$$

$$\text{Load_Capacity}_{\text{boltthrd}} := (0.577 \cdot S_{\text{ubolt}}) \cdot \text{Bolt_thrd_shr_A}$$

$$\text{Load_Capacity}_{\text{boltthrd}} = 1.211 \times 10^4 \text{ lbf}$$

$$\text{Load_Capacity}_{\text{lid}} := (0.577 \cdot S_{\text{ulid}}) \cdot \text{Ext_thrd_shr_A}$$

$$\text{Load_Capacity}_{\text{lid}} = 1.142 \times 10^4 \text{ lbf}$$

Therefore, the load capacity is based on base metal shear.

$$\text{Max_Lift_Load} := \text{NB} \cdot \text{Load_Capacity}_{\text{lid}} \quad \text{Max_Lift_Load} = 4.112 \times 10^5 \text{ lbf}$$

and the safety factor is

$$\text{SF} := \frac{\text{Max_Lift_Load}}{W_{\text{lift}}} \quad \text{SF} = 2.992 > 1$$

Therefore, it is shown that the HI-TRAC pool lid bolts have adequate engagement length into lid to permit the transfer of the required load.

APPENDIX 3.AD 125 TON HI-TRAC TRANSFER LID STRESS ANALYSES

3.AD.1 Introduction

This appendix considers the structural analysis of the HI-TRAC transfer lid under the following limiting conditions:

- Lifting of fully loaded MPC - Normal Condition
- Horizontal Drop of HI-TRAC - Accident Condition

In the first case, it is shown that the sliding doors adequately support a loaded MPC plus the door weight, both being amplified by a dynamic load factor associated with a low speed lifting operation, and that the loads are transferred to the transfer cask body without overstress.

In the second case, analysis is performed to show that the transfer lid and the transfer cask body do not separate during a HI-TRAC horizontal drop which imposes a deceleration load on the connection. In this case, because of the geometry of the transfer lid housing, the force of separation is from the HI-TRAC since the housing impacts the ground before the HI-TRAC body; i.e., the connection needs to withstand an amplified load from the HI-TRAC loaded weight, amplified by the deceleration. Analysis is also performed to show that the bolts that act as "door stops" will keep the doors from opening due to deceleration from a side drop.

3.AD.2 References

[3.AD.2.1] Young, Warren C., *Roark's Formulas for Stress and Strain*, 6th Edition, McGraw-Hill, 1989.

[3.AD.2.2] Holtec Drawing 1928 (two sheets)

[3.AD.2.3] J. Shigley and C. Mischke, *Mechanical Engineering Design*, McGraw Hill, 1989.

[3.AD.2.4] McMaster-Carr Supply Company, Catalog No. 101, 1995.

[3.AD.2.5] Machinery's Handbook, 23rd Edition, Industrial Press

3.AD.3 Composition

This appendix was created using the Mathcad (version 8.0) software package. Mathcad uses the symbol ':=' as an assignment operator, and the equals symbol '=' retrieves values for constants or variables.

3.AD.4 General Assumptions

1. Formulas taken from Reference [3.AD.2.1] are based on assumptions that are delineated in that reference.
2. During lifting operation, the MPC is supported on a narrow rectangular section of the door. The width of the section in each of two doors is set at the span of the three wheels. Beam theory is used to calculate stresses.
3. The loading from the MPC on the door is simulated by a uniform pressure acting on the total surface area of the postulated beam section of the door.

3.AD.5 Methodology and Assumptions

Strength of Materials analysis are performed to establish structural integrity. Stresses in the transfer lid door are computed based on simplified beam analysis, where the width of the top plate beam is taken as the span of the door support wheels (see drawing 1928).

For all lifting analyses, the acceptance criteria is the more severe of ASME Section III, Subsection NF (allowable stresses per tables in Chapter 3), or USNRC Regulatory Guide 3.61 (33.3% of yield strength at temperature).

3.AD.6 Input Data (per BM-1928 and drawing 1928; weights are from Table 3.2.2, with detailed door component weights from the calculation package HI-981928)

Unsupported door top plate length	$L := 72.75 \cdot \text{in}$
Half Door top plate width	$w := 25 \cdot \text{in}$
Door top plate thickness	$t_{tp} := 2.25 \cdot \text{in}$
Thickness of middle plate	$t_{mp} := .5 \cdot \text{in}$
Thickness of bottom plate	$t_{bp} := 0.75 \cdot \text{in}$
HI-TRAC bounding dry weight	$W := 243000 \cdot \text{lbf}$
MPC bounding weight	$W_{mpc} := 90000 \cdot \text{lbf}$
Transfer Lid Bounding Weight (with door)	$W_{tl} := 24500 \cdot \text{lbf}$
Weight of door top plate (2 items)	$W_{tp} := 3762 \cdot \text{lbf}$
Door Lead shield weight (2 items)	$W_{lead} := 3839 \cdot \text{lbf}$

Weight of door bottom plate (2 items) $W_{bp} := 994 \cdot \text{lbf}$

Weight of Holtite A (2 items) $W_{ha} := 691 \cdot \text{lbf}$

Weight of door middle plate (2 items) $W_{mp} := 663 \cdot \text{lbf}$

Total door weight (2 components) excluding wheels and trucks

$W_{td} := W_{tp} + W_{lead} + W_{bp} + W_{ha} + W_{mp}$ $W_{td} = 9.949 \times 10^3 \text{ lbf}$

Weight of wheels, trucks and miscellaneous pieces $W_{misc} := 2088 \cdot \text{lbf}$

Total Load transferred by 1 set of 3 wheels including wheels, trucks, and miscellaneous items

$W_{door} := \frac{.5 \cdot (W_{td} + W_{misc})}{2}$ $W_{door} = 3.009 \times 10^3 \text{ lbf}$

Dynamic Load Factor for low speed lift $DLF := 0.15$

Young's Modulus SA-516-Gr70 @ 350 deg. F $E := 28 \cdot 10^6 \cdot \text{psi}$

Allowable membrane stress
for Level A condition @ 350 deg. F (Table 3.3.2)
(Use allowable of SA-516-Gr 70 to be conservative) $S_a := 17500 \cdot \text{psi}$

Yield strength of SA-350-LF3 @ 350 deg. F
to be conservative (Table 3.3.3) $S_y := 32700 \cdot \text{psi}$

Maximum Deceleration g level per design basis $G_{max} := 45$

3.AD.7 Analysis of Door plates Under Lift of MPC - Level A Event

The transfer lid door has a top and bottom plate connected by side plates that act as stiffeners in the loaded section. The top plate is 2.25" thick and the total span between wheel centers is 73". The bottom plate is 0.75" thick and spans 73". The side plates that connect the plates are 1" thick.

The lid door acts as a composite beam between wheel sets. To ensure conservatism, the effective width of the composite beam is taken as the distance between the outermost stiffeners. Beam theory is valid up to 1/8 of the span [Ref 3.AD.2.1]. Beyond this value, a beam begins to act as a stronger two-way plate. Therefore, a one-way beam approximation for the dimensions of this lid underestimates the capacity of the lid. The load acting on the beam is taken as the bounding weight from a fully loaded MPC plus the bounding weight of the transfer lid door assembly. The load is applied as a uniform pressure and the beam is assumed simply supported.

The geometric parameters of the system are (drawing 1928, sheet 2):

$b := w$		
$h := 8\text{-in}$	overall beam height	
$htp := t_{tp}$	thickness of top plate	$htp = 2.25\text{ in}$
$hg := 5.75\text{-in}$	height of side plate	
$hbp := t_{bp}$	thickness of bottom plate	$hbp = 0.75\text{ in}$
$tg := 1\text{-in}$	thickness of each side plate	

The centroid (measured from the top surface) and area moment of inertia of the composite beam are:

$$y_c := \frac{3 \cdot hg \cdot tg \cdot \left(htp + \frac{hg}{2} \right) + htp \cdot b \cdot \frac{htp}{2} + hbp \cdot (b - 3 \cdot tg) \cdot \left(h - \frac{hbp}{2} \right)}{htp \cdot b + 3 \cdot hg \cdot tg + hbp \cdot (b - 3 \cdot tg)}$$

$$y_c = 3.083\text{ in}$$

$$\begin{aligned} \text{Inertia} := & \frac{b \cdot htp^3}{12} + htp \cdot b \cdot \left(y_c - \frac{htp}{2} \right)^2 + \frac{tg \cdot hg^3}{4} + 3 \cdot hg \cdot tg \cdot \left(y_c - htp - \frac{hg}{2} \right)^2 \dots \\ & + \frac{(b - 3 \cdot tg) \cdot hbp^3}{12} + hbp \cdot (b - 3 \cdot tg) \cdot \left(y_c - htp - hg - \frac{hbp}{2} \right)^2 \end{aligned}$$

$$\text{Inertia} = 821.688\text{ in}^4$$

The maximum stress is due to the moment:

$$\text{Moment} := \frac{(W_{\text{mpc}} + W_{\text{td}})}{2} \cdot \frac{L}{8}$$

$$\text{Moment} = 4.545 \times 10^5 \text{ lbf}\cdot\text{in}$$

The bending stress is

$$\sigma := \frac{\text{Moment} \cdot (h - y_c) \cdot (1 + \text{DLF})}{\text{Inertia}}$$

$$\sigma = 3.127 \times 10^3 \text{ psi}$$

The stress must be less than the 33.3% of the yield strength of the material. This acceptance criteria comes from Reg. Guide 3.61. The safety factor is,

$$S_y := S_y$$

$$SF_{3.61} := \frac{S_y}{3 \cdot \sigma}$$

$$SF_{3.61} = 3.486$$

The safety factor as defined by ASME Section III, Subsection NF for Class 3 components is

$$SF_{\text{nf}} := \frac{1.5 \cdot S_a}{\sigma}$$

$$SF_{\text{nf}} = 8.394$$

Now consider the plate section between stiffeners and check to see if plate stress is acceptable. The span of the plate between stiffeners is

$$\text{span} := 12.5 \text{ in}$$

Calculate the pressure on each half of lid door due to MPC.

$$p := \frac{.5 \cdot W_{\text{mpc}} \cdot (1 + \text{DLF})}{L \cdot w}$$

$$p = 28.454 \text{ psi}$$

Calculate the pressure due to self weight

$$p_d := .5 \cdot (W_{\text{tp}}) \cdot \frac{1 + \text{DLF}}{L \cdot w}$$

$$p_d = 1.189 \text{ psi}$$

Bending moment due to pressure

$$\text{Moment} := \frac{(p + p_d) \cdot L \cdot \text{span}^2}{8}$$

$$\text{Moment} = 4.212 \times 10^4 \text{ lbf}\cdot\text{in}$$

Maximum bending stress

$$\sigma_{\text{bending}} := \frac{6 \cdot \text{Moment}}{L \cdot t_{\text{tp}}^2} \quad \sigma_{\text{bending}} = 686.179 \text{ psi}$$

(Small!!!)

Now perform a Weld Check

$$\text{Load} := (p + p_d) \cdot L \cdot w \quad \text{Load} = 5.391 \times 10^4 \text{ lbf}$$

The shear stress at the weld connection is (conservatively neglect stiffener welds)

$$\tau := \frac{\text{Load}}{2 \cdot w \cdot t_{\text{tp}}} \quad \tau = 479.227 \text{ psi} \quad \text{Low!}$$

It is concluded that the significant stresses arise only by the action of the member as a composite beam composed of plates and stiffeners. Local bending stresses in the plate are small and can be neglected

3.AD.8 Wheel Loads on Housing

$$W_{\text{door}} = 3.009 \times 10^3 \text{ lbf} \quad \text{From weight calculation - 50\% of 1 half-door}$$

$$\text{Load per wheel} \quad \text{Load}_{\text{wheel}} := \frac{(W_{\text{door}} + .25 \cdot W_{\text{mpc}}) \cdot (1 + \text{DLF})}{3}$$

$$\text{Load}_{\text{wheel}} = 9.779 \times 10^3 \text{ lbf}$$

Note that working capacities of wheels are 10000 lb per McMaster Carr Catalog [3.AD.2.4].

The wheel rides on an angle track (item 7 in dwg. 1928). The thickness of the angle is

$$t_a := 0.125 \cdot \text{in}$$

The wheel span (three wheels) is (see sheet 2, side view of Dwg. 1928)

$$s := 18.5 \cdot \text{in}$$

Therefore the direct stress in the leg of the angle is

$$\sigma_a := \frac{1}{2 \cdot \cos(45 \cdot \text{deg}) \cdot s \cdot t_a} \cdot 3 \cdot \text{Load}_{\text{wheel}}$$

$$\sigma_a = 8.97 \times 10^3 \text{ psi}$$

Overstress in this track does not impede ready retrievability of the fuel. Nevertheless, for conservatism, the safety factor in accordance with Regulatory Guide 3.61 is evaluated for the material specified for the angle.

$$\text{SF}_{\text{angle}} := \frac{36000 \cdot \text{psi}}{3 \cdot \sigma_a} \quad \text{SF}_{\text{angle}} = 1.338$$

3.AD.9 Housing Stress Analysis

The most limiting section that sets the minimum safety factor for the door housing under a lifting condition is the box structure adjacent to the track that serves as the direct load path to the bolts. In this section, a conservative estimate of the stress levels in this region is obtained and the safety factor established. The door load is transferred to the bottom plate by the wheels running on an angle track. The load is then transferred to two vertical stiffeners that form the side of the box. The top plate forming the top of the box, serves as the structure that moves the load to the bolts.

The lid bottom plate of the housing (item 2 of Dwg. 1928) that directly supports the wheel loading can be conservatively considered as a wide plate supporting the load from one of the sliding doors. The applied load is transferred to the two vertical plates (items 3 and 4 of Dwg. 1928). Figure 3.AD.2 shows the configuration for analysis. The following dimensions are obtained from the drawing

Length of analyzed section	$L_H := 25 \cdot \text{in}$	
Thickness of item 2	$t_{\text{bottom}} := 2 \cdot \text{in}$	From BM-1928
Thickness of item 3	$t_1 := 1.5 \cdot \text{in}$	
Thickness of item 4	$t_2 := 1 \cdot \text{in}$	
Width of item 21	$t_{21} := 3.5 \cdot \text{in}$	

With respect to Figure 3.AD.2, referring to the drawing, the length x is defined as $a+b$

$$x := (.5 \cdot 93) \cdot \text{in} - 36.375 \cdot \text{in}$$

$$x = 10.125 \text{ in}$$

$$\text{dimension "b"} \quad b := x - t_1 - t_2 - .5 \cdot t_1$$

$$b = 4.375 \text{ in}$$

$$\text{dimension "a"} \quad a := x - b$$

$$a = 5.75 \text{ in}$$

Compute the moment of inertia of item 2 at the root assuming a wide beam

$$I := L_H \cdot \frac{t_{\text{bottom}}^3}{12} \quad I = 16.667 \text{ in}^4$$

The maximum bending moment in the bottom plate is given as,

$$\text{Moment} := 3 \cdot \text{Load}_{\text{wheel}} \cdot b$$

$$\text{Moment} = 1.283 \times 10^5 \text{ lbf} \cdot \text{in}$$

The maximum bending stress is

$$\sigma_{\text{bending}} := \frac{\text{Moment} \cdot t_{\text{bottom}}}{2 \cdot I}$$

$$\sigma_{\text{bending}} = 7.701 \times 10^3 \text{ psi}$$

The safety factor, based on primary bending stress (ASME Code evaluation), is

$$1.5 \cdot \frac{S_a}{\sigma_{\text{bending}}} = 3.409$$

It is concluded that this region is not limiting.

The safety factor based on Reg. Guide 3.61 (compare to 33% of yield strength) is

$$\frac{S_y}{3 \cdot \sigma_{\text{bending}}} = 1.415$$

The reactions at the two support points for the section are

$$F_1 := 3 \cdot \text{Load}_{\text{wheel}} \cdot \left(1 + \frac{b}{a}\right)$$

$$F_1 = 5.166 \times 10^4 \text{ lbf}$$

$$F_2 := 3 \cdot \text{Load}_{\text{wheel}} \cdot \frac{b}{a}$$

$$F_2 = 2.232 \times 10^4 \text{ lbf}$$

Therefore, consistent with the support assumptions, the direct stress in the two stiffeners is

$$\sigma_1 := \frac{F_1}{L_H \cdot t_1} \quad \sigma_1 = 1.377 \times 10^3 \text{ psi}$$

$$\sigma_2 := \frac{F_2}{L_H \cdot t_2} \quad \sigma_2 = 892.822 \text{ psi}$$

Safety factors, using the more conservative Reg. Guide 3.61 criteria, are

$$SF_1 := \frac{S_y}{3 \cdot \sigma_1} \quad SF_1 = 7.913$$

$$SF_2 := \frac{S_y}{3 \cdot \sigma_2} \quad SF_2 = 12.208$$

3.AD.10 Bolt Stress

Figure 3.AD.3 shows the bolt array assumed to resist the lifted load when the doors are closed and when the fully loaded MPC is being supported by the doors.

The bolt tensile stress area is, for the 1" diameter bolts

$$A_b := 0.605 \cdot \text{in}^2 \quad d_{\text{bolt}} := 1 \cdot \text{in}$$

The bolt circle radius is

$$R_b := 45 \cdot \text{in}$$

The bolt angular spacing is $\theta := 10 \cdot \text{deg}$

The centroid of the nine bolts point P* in Figure 3.AD.3, assumed to carry 100% of the wheel load, is computed as follows:

$$A_{\text{total}} := 9 \cdot A_b \quad A_{\text{total}} = 5.445 \text{ in}^2$$

Compute the following sum:

$$\text{Sum} := 2 \cdot A_b \cdot R_b \cdot (1 - \cos(4 \cdot \theta)) + 2 \cdot A_b \cdot R_b \cdot (1 - \cos(3 \cdot \theta)) \dots \\ + 2 \cdot A_b \cdot R_b \cdot (1 - \cos(2 \cdot \theta)) + 2 \cdot A_b \cdot R_b \cdot (1 - \cos(\theta))$$

$$\text{Sum} = 24.145 \text{ in}^3$$

Then the centroid of the bolts is $X_{\text{bar}} := \frac{\text{Sum}}{A_{\text{total}}} \quad X_{\text{bar}} = 4.434 \text{ in}$

Compute the bolt moment of inertia about the centroid by first locating each bolt relative to the centroid. First compute some distances "z":

$$z_1 := R_b \cdot (1 - \cos(4 \cdot \theta)) - X_{\text{bar}} \quad z_1 = 6.094 \text{ in}$$

$$z_2 := R_b \cdot (1 - \cos(3 \cdot \theta)) - X_{\text{bar}} \quad z_2 = 1.595 \text{ in}$$

$$z_3 := R_b \cdot (1 - \cos(2 \cdot \theta)) - X_{\text{bar}} \quad z_3 = -1.72 \text{ in}$$

$$z_4 := R_b \cdot (1 - \cos(\theta)) - X_{\text{bar}} \quad z_4 = -3.751 \text{ in}$$

Then the bolt group moment of inertia about the centroid is,

$$I_{\text{bolts}} := 2 \cdot A_b \cdot z_1^2 + 2 \cdot A_b \cdot z_2^2 + 2 \cdot A_b \cdot z_3^2 + 2 \cdot A_b \cdot z_4^2 + A_b \cdot X_{\text{bar}}^2$$

$$I_{\text{bolts}} = 80.507 \text{ in}^4$$

The bolts must support the total wheel load acting on one rail, plus the additional load necessary to resist the moment induced about the bolt group centroid.

The moment arm is the distance from the bolt centroid to the angle guide rail

$$\text{moment_arm} := R_b - X_{\text{bar}} - 36.375 \text{ in} \quad \text{moment_arm} = 4.191 \text{ in}$$

Therefore, the bolt array must resist the following moment

$$\text{Moment}_{\text{bolts}} := 6 \cdot \text{Load}_{\text{wheel}} \cdot \text{moment_arm} \quad \text{Moment}_{\text{bolts}} = 2.459 \times 10^5 \text{ in} \cdot \text{lbf}$$

The bolt stress due to the direct load is:

$$\text{stress}_{\text{direct}} := 6 \cdot \frac{\text{Load}_{\text{wheel}}}{A_{\text{total}}} \quad \text{stress}_{\text{direct}} = 1.078 \times 10^4 \text{ psi}$$

Compute $y_1 := R_b \cdot (1 - \cos(4 \cdot \theta)) - X_{\text{bar}} \quad y_1 = 6.094 \text{ in} > X_{\text{bar}}$

Therefore, the highest bolt stress due to the bending moment is,

$$\text{stress}_{\text{moment}} := \frac{\text{Moment}_{\text{bolts}} \cdot y_1}{l_{\text{bolts}}} \quad \text{stress}_{\text{moment}} = 1.861 \times 10^4 \text{ psi}$$

Therefore, the total bolt stress to support lifting, on the heaviest loaded bolt, is

$$\sigma_{\text{bolt}} := \text{stress}_{\text{direct}} + \text{stress}_{\text{moment}} \quad \sigma_{\text{bolt}} = 2.939 \times 10^4 \text{ psi}$$

The above calculation has considered only the stress induced by the MPC and the door; that is, the stress induced in the bolts by the load transmitted through the wheels. The entire set of bolts acts to support the door housing and this induces an additional component of stress in the bolts. This is computed below:

The total bounding weight of the transfer lid is

$$W_{\text{tl}} = 2.45 \times 10^4 \text{ lbf}$$

The total door load already accounted for in the bolt analysis is

$$W_{\text{td}} := 4 \cdot W_{\text{door}} \quad W_{\text{td}} = 1.204 \times 10^4 \text{ lbf}$$

Therefore the additional average stress component in the 36 bolts is

$$\sigma_{\text{avg}} := \frac{(W_{\text{tl}} - W_{\text{td}})}{36 \cdot A_b} \quad \sigma_{\text{avg}} = 572.221 \text{ psi}$$

Therefore the absolute maximum bolt stress is

$$\sigma_{\text{bolt_max}} := \sigma_{\text{bolt}} + \sigma_{\text{avg}} \quad \sigma_{\text{bolt_max}} = 2.996 \times 10^4 \text{ psi}$$

The allowable bolt load is obtained from the ASME Code, Subsection NF, NF-3324.6 as 50% of the ultimate strength of the bolts. The bolts are assumed to be at a temperature below 200 degrees F because of their location.

$$S_{\text{ubolt}} := 115000 \cdot \text{psi} \quad @200 \text{ deg. F} \quad \text{Table 3.3.4}$$

$$S_{\text{ybolt}} := 95000 \cdot \text{psi}$$

Therefore, the bolt safety factor is

$$SF_{\text{bolts}} := \frac{.5 \cdot S_{\text{ubolt}}}{\sigma_{\text{bolt_max}}} \quad SF_{\text{bolts}} = 1.919$$

The transfer lid bolt preload required is

$$T := .12 \cdot \sigma_{\text{bolt_max}} \cdot A_b \cdot d_{\text{bolt}} \quad [3.AD.3] \quad T = 181.246 \text{ ft} \cdot \text{lbf}$$

Note that this exceeds the value calculated for the pool lid.

The safety factor using the Reg. Guide 3.61 criteria is

$$SF_{3.61} := \frac{S_{\text{ybolt}}}{3 \cdot \sigma_{\text{bolt_max}}} \quad SF_{3.61} = 1.057$$

Calculation of Thread Capacity

The following calculations are taken from Machinery's Handbook, 23rd Edition, pp 1278-1279 plus associated screw thread Table 4, p 1514.

Input Geometry Data - 1" UNC, 8 threads/inch, 2A class

$$L_e := 1.0 \cdot \text{in} \quad \text{Thread engagement length} \quad N := \frac{8}{\text{in}} \quad \text{Threads per inch}$$

$$D_m := 1 \cdot \text{in} \quad \text{Basic Major Diameter of threads}$$

$$D := .9755 \cdot \text{in} \quad \text{Minimum Major Diameter of External Threads}$$

$$E_{\text{min}} := .91 \cdot \text{in} \quad \text{Minimum Pitch Diameter of External Threads}$$

$E_{max} := .9276\text{in}$ Maximum Pitch Diameter of Internal Threads

$K_n := .89\cdot\text{in}$ Maximum Minor Diameter of Internal Threads

Input Yield Strength-Internal Threads (lid or forging); External Threads (bolts)

Values are obtained from ASME Code, Section II)

$S_{ylid} := 38000\cdot\text{psi}$ $S_{ulid} := 70000\cdot\text{psi}$ $S_{ubolt} := S_{ubolt}$

Calculation of Tensile stress area (high-strength bolt, ultimate strength exceeding 100,000 psi)

$$A_{th} := \pi \cdot \left(.5 \cdot E_{min} - \frac{0.16238}{N} \right)^2 \qquad A_{tl} := .7854 \cdot \left(D_m - \frac{.9743}{N} \right)^2$$

$$A_{th} = 0.594\text{in}^2$$

$$A_{tl} = 0.606\text{in}^2$$

$$A_t := \text{if}(S_{ubolt} > 100000\cdot\text{psi}, A_{th}, A_{tl}) \qquad A_t = 0.594\text{in}^2$$

Calculation of Shear Stress Area per the Handbook

$$A_{ext} := \pi \cdot N \cdot L_e \cdot K_n \cdot \left[\frac{0.5}{N} + 0.57735 \cdot (E_{min} - K_n) \right] \qquad A_{ext} = 1.656\text{in}^2$$

$$A_{int} := \pi \cdot N \cdot L_e \cdot D \cdot \left[\frac{0.5}{N} + 0.57735 \cdot (D - E_{max}) \right] \qquad A_{int} = 2.21\text{in}^2$$

Required Length of Engagement per Machinery's Handbook

$$L_{req} := 2 \cdot \frac{A_t}{\frac{A_{ext}}{L_e}} \qquad L_{req} = 0.717\text{in}$$

Capacity Calculation Using Actual Engagement Length

For the specified condition, the allowable tensile stress in the bolt is per ASME NF

$$\sigma_{\text{bolt}} := S_{\text{ubolt}} \cdot 0.5 \quad \sigma_{\text{bolt}} = 5.75 \times 10^4 \text{ psi}$$

The allowable shear stress in the bolt is:

$$\tau_{\text{bolt}} := \frac{.62 \cdot S_{\text{ubolt}}}{3} \quad \tau_{\text{bolt}} = 2.377 \times 10^4 \text{ psi}$$

The allowable shear stress in the lid (or flange) is

$$\tau_{\text{lid}} := 0.4 \cdot S_{\text{ylid}} \quad \tau_{\text{lid}} = 1.52 \times 10^4 \text{ psi}$$

$$F_{\text{shear_lid}} := \tau_{\text{lid}} \cdot A_{\text{int}} \quad F_{\text{shear_lid}} = 3.36 \times 10^4 \text{ lbf}$$

For the bolt, the allowable strength is the yield strength

$$F_{\text{tensile_bolt}} := \sigma_{\text{bolt}} \cdot A_{\text{t}} \quad F_{\text{tensile_bolt}} = 3.414 \times 10^4 \text{ lbf}$$

$$F_{\text{shear_bolt}} := \tau_{\text{bolt}} \cdot A_{\text{ext}} \quad F_{\text{shear_bolt}} = 3.936 \times 10^4 \text{ lbf}$$

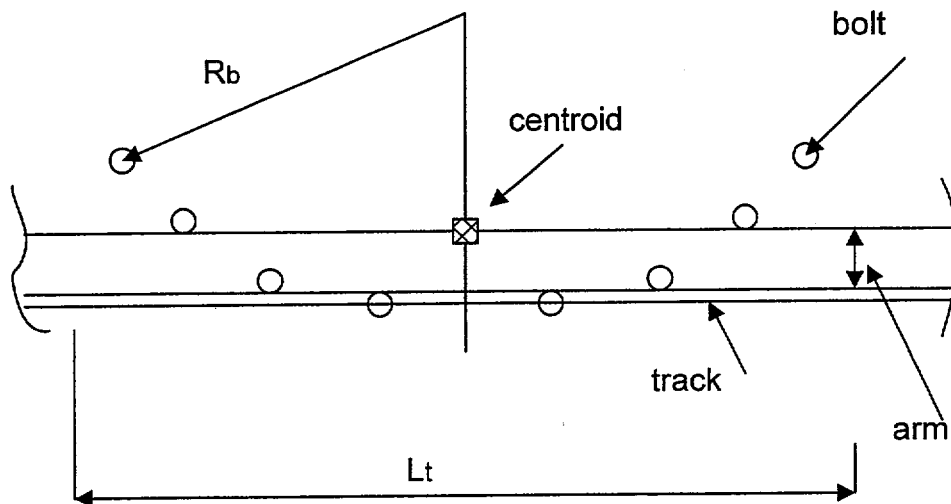
Therefore, thread shear in lid governs the design. The safety factors computed above should be multiplied by the ratio

$$\frac{F_{\text{shear_lid}}}{F_{\text{tensile_bolt}}} = 0.984$$

3.AD.11 Estimate of Primary Bending Stress in Lid Top Plate

The lid top plate maximum primary stresses develop due to the structural requirement of transferring the wheel loads to the bolt array. Based on the assumptions above as to the number of bolts participating in the support of the load, a total direct load and a bending moment is reacted by the bolt array. The active bolts have been assumed to be only those bolts in an 80 degree arc (see Figure 3.AD.3). To estimate the minimum safety factor inherent in the top plate, it is assumed that the same bending moment must also be reacted by the the lid top plate. The sketch below aids in the analysis:

The analysis is conservative as it neglects any support from either plate or bolts outside of the section identified.



The view shown is similar to the view in Figure 3.AD.3 with identification of terms for use in the following analysis;

$$\text{arm} := \text{moment_arm} \quad \text{arm} = 4.191 \text{ in}$$

$$\text{Moment} := \text{Moment}_{\text{bolts}} \quad \text{Moment} = 2.459 \times 10^5 \text{ in}\cdot\text{lbf}$$

$$L_t := R_b \cdot 2 \cdot \sin(45 \cdot \text{deg}) \quad L_t = 63.64 \text{ in}$$

The thickness of the lid top plate is

$$t_p := 1.5 \cdot \text{in} \quad \text{item 1 in BM-1928}$$

The safety factor is established by considering the bending moment in the section of top plate a distance "arm" away from the track.

$$I_p := \frac{L_t \cdot t_p^3}{12} \quad I_p = 17.899 \text{ in}^4$$

The primary bending stress is

$$\sigma_{tp} := \frac{\text{Moment} \cdot t_p}{2 \cdot I_p} \quad \sigma_{tp} = 1.03 \times 10^4 \text{ psi}$$

The limiting safety factor is obtained by consideration of the Regulatory Guide 3.61 criteria. Therefore,

$$SF_{tp} := \frac{S_y}{3 \cdot \sigma_{tp}} \quad SF_{tp} = 1.058$$

Similarly, the average shear stress developed across the section is

$$\tau_{tp} := 6 \cdot \frac{\text{Load}_{\text{wheel}}}{t_p \cdot L_t} \quad \tau_{tp} = 614.619 \text{ psi}$$

The safety factor against primary shear overstress is large.

$$SF_{\text{shear}} := .6 \cdot \frac{S_y}{3 \cdot \tau_{tp}} \quad SF_{\text{shear}} = 10.641$$

In the above safety factor calculation, the yield strength in shear is assumed as 60 of the yield strength in tension for the Reg. Guide 3.61 evaluation.

The validity of the approximate strength of materials calculation has been independently verified by a finite element analysis (see calculation package HI-981928).

3.AD.11 Separation of Transfer Lid from HI-TRAC

In the event of a side drop while HI-TRAC is in a horizontal position, the transfer lic housing will impact the ground, and the HI-TRAC body, including the MPC, will attempt to separate from the lid. Appendix 3.AN provides a detailed dynamic analysis of the handling accident and provides the interface load that must be transferred by the bolts.

From Appendix 3.AN, Section 3.AN.2.7, we find the following results for the 125-ton HI-TRAC:

$$\text{Interface_Force} := 1272000 \cdot \text{lbf}$$

We now demonstrate that this load can be transferred by a combination of bolt shear and interface friction.

3.AD.11.1 Shear Capacity of 36 SA 193 B7 bolts

$$\text{Number of bolts} \quad n_b := 36$$

$$S_{\text{ubolt}} = 1.15 \times 10^5 \text{ psi} \quad A_b := A_t$$

$$\text{Bolt_Capacity} := n_b \cdot 0.6 \cdot S_{\text{ubolt}} \cdot A_b \quad \text{Bolt_Capacity} = 1.475 \times 10^6 \text{ lbf}$$

Note that here we are performing a failure analysis

3.AD.11.2 Shear Capacity due to Friction - 125 Ton HI-TRAC

Table 8.1.5 lists the actual preload torque as $T_{\text{act}} := 270 \cdot \text{ft} \cdot \text{lbf}$

The calculated bolt torque requirement is $T = 181.246 \text{ ft} \cdot \text{lbf}$

Therefore the actual clamping force per bolt is:

$$T_{\text{clamp}} := \frac{T_{\text{act}}}{T} \cdot \sigma_{\text{bolt_max}} \cdot A_b \quad T_{\text{clamp}} = 2.649 \times 10^4 \text{ lbf}$$

Following ASME, Section III, Subsection NF, NF-3324.6(4) for a blast cleaned joint the frictional resistance for the assemblage of bolts is:

$$P_s := n_b \cdot T_{\text{clamp}} \cdot 0.31 \quad P_s = 2.957 \times 10^5 \text{ lbf}$$

Note that since we are evaluating a side drop, the actual value of the clamping force may be used since there is no other tensile load acting on the bolts.

Therefore, the total shear capacity, based on ultimate strength in shear, is

$$\text{Shear_Capacity} := \text{Bolt_Capacity} + P_s$$

$$\text{Shear_Capacity} = 1.77 \times 10^6 \text{ lbf}$$

The safety factor for lid separation is defined as

$$\text{SF} := \frac{\text{Shear_Capacity}}{\text{Interface_Force}} \quad \text{SF} = 1.392$$

It is concluded that there will be no separation of the HI-TRAC 125 from the transfer lid.

3.AD.12 Analysis of Door Lock Bolts (Item 22 of Dwg. 1928, Sheet 1)

Under the design basis side drop handling accident, the transfer lid doors (both) are restrained only by the two door lock bolts. Since the doors must remain closed to maintain shielding, these bolts need to have sufficient shear capacity to resist the door deceleration loading. The following calculation demonstrates that the door lock bolts have the desired shear capacity. The following input data is required to obtain a result:

$$G_{\max} = 45$$

$$D_{\text{bolt}} := 3.0 \cdot \text{in} \quad \text{Door lock bolt diameter per 125 ton transfer cask bill of materials.}$$

$$S_{\text{bolt}} := .42 \cdot S_{\text{ubolt}} \quad \text{Level D event per Appendix F of ASME Code}$$

$$\text{Total_Load} := 4 \cdot W_{\text{door}} \quad \text{Total_Load} = 1.204 \times 10^4 \text{ lbf}$$

Recall that W_{door} has been defined in 3.AD.8 as 50% of the weight of one(of two) doors. The door bolt area is

$$D_{\text{bolt}} = 3 \text{ in} \quad n := 4 \quad \text{Threads/inch}$$

The stress area is computed from the following formula (Machinery's Handbook, Industrial Press, NYC, 23rd Edition, p. 1279,)

$$A_{\text{bolt}} := \pi \cdot \left(\frac{D_{\text{bolt}}}{2} - \frac{0.16238}{n} \cdot \text{in} \right)^2 \quad A_{\text{bolt}} = 6.691 \text{ in}^2$$

There are two bolts which support load and there are two shear faces per bolt (see section B-B on Dwg. 1928). The shear stress in the bolt section is

$$\tau_{\text{bolt}} := \frac{\text{Total_Load} \cdot G_{\max}}{2 \cdot 2 \cdot A_{\text{bolt}}} \quad \tau_{\text{bolt}} = 2.024 \times 10^4 \text{ psi}$$

Therefore, the safety factor on bolt shear stress is

$$\text{SF}_{\text{bolt_shear}} := \frac{S_{\text{bolt}}}{\tau_{\text{bolt}}} \quad \text{SF}_{\text{bolt_shear}} = 2.387$$

and no loss of shielding will occur since the doors will be retained in place.

APPENDIX 3.AF: MPC TRANSFER FROM HI-TRAC TO HI-STORM 100 UNDER COLD CONDITIONS OF STORAGE

3.AF.1 Scope

In this calculation, estimates of operating gaps, both radially and axially, are computed for the fuel basket-to-MPC shell, and for the MPC shell-to-overpack. This calculation is in support of the results presented in Section 3.4.5. A hot MPC is lowered from a HI-TRAC transfer cask into a storage overpack assumed to be at steady state temperatures appropriate to cold conditions of storage.

3.AF.2 Methodology

Bounding temperatures are used to construct temperature distributions that will permit calculation of differential thermal expansions both radially and axially for the basket-to-MPC gaps, and for the MPC-to-overpack gaps. Reference temperatures are set at 70°F for all components. A comprehensive nomenclature listing is provided in Section 3.AF.6.

3.AF.3 References

[3.AF.1] Boley and Weiner, Theory of Thermal Stresses, John Wiley, 1960, Sec. 9.10, pp. 288-291.

[3.AF.2] Burgreen, Elements of Thermal Stress Analysis, Arcturus Publishers, Cherry Hill NJ, 1988.

3.AF.4 Calculations

3.AF.4.1 Input Data

Based on thermal calculations in Chapter 4 and results from Appendix 3.I, the following temperatures are appropriate at the hottest location of the HI-TRAC (see Figure 3.I.1 and Table 4.5.2).

The temperature change at the overpack inner shell, $\Delta T_{1h} := 0 - 70$

The temperature change at the overpack outer shell, $\Delta T_{2h} := 0 - 70$

The temperature change at the mean radius of the MPC shell, $\Delta T_{3h} := 455 - 70$

The temperature change at the outside of the MPC basket, $\Delta T_{4h} := (600 - 70) \cdot 1.1$

The temperature change at the center of the basket (helium gas), $\Delta T_{5h} := 852 - 70$

Note that the outer basket temperature is conservatively amplified by 10% to insure a bounding parabolic distribution. This conservatism serves to maximize the growth of the basket. The geometry of the components are as follows (referring to Figure 3.AF.1)

The outer radius of the overpack, $b := 66.25 \cdot \text{in}$ The inner radius of the overpack, $a := 34.75 \cdot \text{in}$

The mean radius of the MPC shell, $R_{\text{mpc}} := \frac{68.375 \cdot \text{in} - 0.5 \cdot \text{in}}{2}$ $R_{\text{mpc}} = 33.938 \text{ in}$

The initial MPC-to-storage overpack radial clearance, $RC_{\text{mo}} := .5 \cdot (69.5 - 68.5) \cdot \text{in}$
 $RC_{\text{mo}} = 0.5 \text{ in}$

This initial radial clearance value, used to perform a radial growth check, is conservatively based on the channel radius (see Dwg. 1495, Sh. 5) and the maximum diameter of the MPC. For axial growth calculations for the MPC-to-overpack lid clearance, the axial length of the overpack is defined as the distance from the top of the pedestal platform to the bottom of the lid bottom plate, and the axial length of the MPC is defined as the overall MPC height.

The axial length of the overpack, $L_{\text{ovp}} := 191.5 \cdot \text{in}$

The axial length of the MPC, $L_{\text{mpc}} := 190.5 \cdot \text{in}$

The initial MPC-to-overpack nominal axial clearance, $AC_{\text{mo}} := L_{\text{ovp}} - L_{\text{mpc}}$

$$AC_{\text{mo}} = 1 \text{ in}$$

For growth calculations for the fuel basket-to-MPC shell clearances, the axial length of the basket is defined as the total length of the basket and the outer radius of the basket is defined as the mean radius of the MPC shell minus one-half of the shell thickness minus the initial basket-to-shell radial clearance.

The axial length of the basket, $L_{\text{bas}} := 176.5 \cdot \text{in}$

The initial basket-to-MPC lid nominal axial clearance, $AC_{\text{bm}} := 1.8125 \cdot \text{in}$

The initial basket-to-MPC shell nominal radial clearance, $RC_{\text{bm}} := 0.1875 \cdot \text{in}$

The outer radius of the basket, $R_b := R_{\text{mpc}} - \frac{0.5}{2} \cdot \text{in} - RC_{\text{bm}}$ $R_b = 33.5 \text{ in}$

The coefficients of thermal expansion used in the subsequent calculations are based on the mean temperatures of the MPC shell and the basket (conservatively estimated high).

The coefficient of thermal expansion for the MPC shell, $\alpha_{\text{mpc}} := 9.338 \cdot 10^{-6}$

The coefficient of thermal expansion for the basket, $\alpha_{\text{bas}} := 9.90 \cdot 10^{-6} \text{ } 600 \text{ deg. F}$

3.AF.4.2 Thermal Growth of the Overpack

Results for thermal expansion deformation and stress in the overpack are obtained here. The system is replaced by a equivalent uniform hollow cylinder with approximated average properties.

Based on the given inside and outside surface temperatures, the temperature solution in the cylinder is given in the form:

$$C_a + C_b \cdot \ln\left(\frac{r}{a}\right)$$

where

$$C_a := \Delta T_{1h} \qquad C_a = -70$$

$$C_b := \frac{\Delta T_{2h} - \Delta T_{1h}}{\ln\left(\frac{b}{a}\right)} \qquad C_b = 0$$

Next, form the integral relationship:

$$\text{Int} := \int_a^b \left[C_a + C_b \cdot \ln\left(\frac{r}{a}\right) \right] \cdot r \, dr$$

The Mathcad program, which was used to create this appendix, is capable of evaluating the integral "Int" either numerically or symbolically. To demonstrate that the results are equivalent, the integral is evaluated both ways in order to qualify the accuracy of any additional integrations that are needed.

The result obtained through numerical integration, $\text{Int} = -1.114 \times 10^5 \text{ in}^2$

To perform a symbolic evaluation of the solution the integral "Ints" is defined. This integral is then evaluated using the Maple symbolic math engine built into the Mathcad program as:

$$\text{Int}_s := \int_a^b \left[C_a + C_b \cdot \ln\left(\frac{r}{a}\right) \right] \cdot r \, dr$$

$$\text{Int}_s := \frac{1}{2} \cdot C_b \cdot \ln\left(\frac{b}{a}\right) \cdot b^2 + \frac{1}{2} \cdot C_a \cdot b^2 - \frac{1}{4} \cdot C_b \cdot b^2 + \frac{1}{4} \cdot C_b \cdot a^2 - \frac{1}{2} \cdot C_a \cdot a^2$$

$$\text{Int}_s = -1.114 \times 10^5 \text{ in}^2$$

We note that the values of Int and Ints are identical. The average temperature change in the overpack cylinder (T_{bar}) is therefore determined as:

$$T_{\text{bar}} := \frac{2}{(b^2 - a^2)} \cdot \text{Int} \qquad T_{\text{bar}} = -70$$

In this case, the result of the calculation is obvious and simply affords an independent check!!

We estimate the average coefficient of thermal expansion for the overpack by weighting the volume of the various layers. A total of four layers are identified for this calculation. They are:

- 1) the inner shell
- 2) the shield shell
- 3) the radial shield
- 4) the outer shell

Thermal properties are based on estimated temperatures in the component and coefficient of thermal expansion values taken from the tables in Chapter 3. The following averaging calculation involves the thicknesses (t) of the various components, and the estimated coefficients of thermal expansion at the components' mean radial positions. The results of the weighted average process yields an effective coefficient of linear thermal expansion for use in computing radial growth of a solid cylinder (the overpack).

The thicknesses of each component are defined as:

$$t_1 := 1.25 \cdot \text{in}$$

$$t_2 := 0.75 \cdot \text{in}$$

$$t_3 := 26.75 \cdot \text{in}$$

$$t_4 := 0.75 \cdot \text{in}$$

and the corresponding mean radii can therefore be defined as:

$$r_1 := a + .5 \cdot t_1 + 2.0 \cdot \text{in} \qquad (\text{add the channel depth})$$

$$r_2 := r_1 + .5 \cdot t_1 + .5 \cdot t_2$$

$$r_3 := r_2 + .5 \cdot t_2 + .5 \cdot t_3$$

$$r_4 := r_3 + .5 \cdot t_3 + .5 \cdot t_4$$

To check the accuracy of these calculations, the outer radius of the overpack is calculated from r_4 and t_4 , and the result is compared with the previously defined value (b).

$$b_1 := r_4 + 0.5 \cdot t_4$$

$$b_1 = 66.25 \text{ in}$$

$$b = 66.25 \text{ in}$$

We note that the calculated value b_1 is identical to the previously defined value b. The coefficients of thermal expansion for each component, estimated based on the temperature gradient, are defined as:

$$\alpha_1 := 5.53 \cdot 10^{-6}$$

$$\alpha_2 := 5.53 \cdot 10^{-6}$$

$$\alpha_3 := 5.5 \cdot 10^{-6}$$

$$\alpha_4 := 5.53 \cdot 10^{-6}$$

Thus, the average coefficient of thermal expansion of the overpack is determined as:

$$\alpha_{\text{avg}} := \frac{r_1 \cdot t_1 \cdot \alpha_1 + r_2 \cdot t_2 \cdot \alpha_2 + r_3 \cdot t_3 \cdot \alpha_3 + r_4 \cdot t_4 \cdot \alpha_4}{\frac{a+b}{2} \cdot (t_1 + t_2 + t_3 + t_4)}$$

$$\alpha_{\text{avg}} = 5.611 \times 10^{-6}$$

Reference 3.AF.1 gives an expression for the radial deformation due to thermal growth. At the inner radius of the overpack ($r = a$), the radial growth is determined as:

$$\Delta R_{\text{ah}} := \alpha_{\text{avg}} \cdot a \cdot T_{\text{bar}}$$

$$\Delta R_{\text{ah}} = -0.014 \text{ in}$$

Similarly, an overestimate of the axial growth of the overpack can be determined by applying the average temperature (T_{bar}) over the entire length of the overpack as:

$$\Delta L_{\text{ovph}} := L_{\text{ovp}} \cdot \alpha_{\text{avg}} \cdot T_{\text{bar}}$$

$$\Delta L_{\text{ovph}} = -0.075 \text{ in}$$

As expected, the drop in temperature causes a decrease in the inner radius and the axial length of the storage overpack.

3.AF.4.3 Thermal Growth of the MPC Shell

The radial and axial growth of the MPC shell (ΔR_{mpch} and ΔL_{mpch} , respectively) are determined as:

$$\Delta R_{mpch} := \alpha_{mpc} \cdot R_{mpc} \cdot \Delta T_{3h} \quad \Delta R_{mpch} = 0.122 \text{ in}$$

$$\Delta L_{mpch} := \alpha_{mpc} \cdot L_{mpc} \cdot \Delta T_{3h} \quad \Delta L_{mpch} = 0.685 \text{ in}$$

3.AF.4.4 Clearances Between the MPC Shell and Overpack

The final radial and axial MPC shell-to-overpack clearances (RG_{moh} and AG_{moh} , respectively) are determined as:

$$RG_{moh} := RC_{mo} + \Delta R_{ah} - \Delta R_{mpch} \quad RG_{moh} = 0.364 \text{ in}$$

$$AG_{moh} := AC_{mo} + \Delta L_{ovph} - \Delta L_{mpch} \quad AG_{moh} = 0.24 \text{ in}$$

Note that this axial clearance (AG_{moh}) is based on the temperature distribution at the hottest axial location of the system.

3.AF.5 Summary of Results

The previous results are summarized here.

MPC Shell-to-Overpack

Radial clearance $RG_{moh} = 0.364 \text{ in}$ Axial clearance $AG_{moh} = 0.24 \text{ in}$

3.AF.6 Nomenclature

a is the inner radius of the overpack

AC_{bm} is the initial fuel basket-to-MPC axial clearance.

AC_{mo} is the initial MPC-to-overpack axial clearance.

AG_{bmh} is the final fuel basket-to-MPC shell axial gap for the hot components.

AG_{moh} is the final MPC shell-to-overpack axial gap for the hot components.

b is the outer radius of the overpack.

L_{bas} is the axial length of the fuel basket.

L_{mpc} is the axial length of the MPC.

L_{ovp} is the axial length of the overpack.

r_1 (r_2, r_3, r_4) is mean radius of the overpack inner shell (shield shell, concrete, outer shell).

R_b is the outer radius of the fuel basket.

R_{mpc} is the mean radius of the MPC shell.

RC_{bm} is the initial fuel basket-to-MPC radial clearance.

RC_{mo} is the initial MPC shell-to-overpack radial clearance.

RG_{bmh} is the final fuel basket-to-MPC shell radial gap for the hot components.

RG_{moh} is the final MPC shell-to-overpack radial gap for the hot components.

t_1 (t_2, t_3, t_4) is the thickness of the overpack inner shell (shield shell, concrete, outer shell).

T_{bar} is the average temperature of the overpack cylinder.

α_1 ($\alpha_2, \alpha_3, \alpha_4$) is the coefficient of thermal expansion of the overpack inner shell (shield shell, concrete, outer shell).

α_{avg} is the average coefficient of thermal expansion of the overpack.

α_{bas} is the coefficient of thermal expansion of the overpack.

α_{mpc} is the coefficient of thermal expansion of the MPC.

ΔL_{bh} is the axial growth of the fuel basket for the hot components.

ΔL_{mpch} is the axial growth of the MPC for the hot components.
 ΔL_{ovph} is the axial growth of the overpack for the hot components.
 ΔR_{ah} is the radial growth of the overpack inner radius for the hot components.
 ΔR_{bh} is the radial growth of the fuel basket for the hot components.
 ΔR_{mpch} is the radial growth of the MPC shell for the hot components.
 ΔT_{1h} is the temperature change at the overpack inner shell for hot components.
 ΔT_{2h} is the temperature change at the overpack outer shell for hot components.
 ΔT_{3h} is the temperature change at the MPC shell mean radius for hot components.
 ΔT_{4h} is the temperature change at the MPC basket periphery for hot components.

ΔT_{5h} is the temperature change at the MPC basket centerline for hot components.
 ΔT_{bas} is the fuel basket centerline-to-periphery temperature gradient.
 σ_{ca} is the circumferential stress at the overpack inner surface.
 σ_{cb} is the circumferential stress at the overpack outer surface.
 σ_r is the maximum radial stress of the overpack.
 σ_{zi} is the axial stress at the fuel basket centerline.
 σ_{zo} is the axial stress at the fuel basket periphery.

Appendix 3.AO

Not Used

Appendix 3.AP

Not Used

APPENDIX 3.AQ: HI-STORM 100 COMPONENT THERMAL EXPANSIONS; MPC-24E

3.AQ.1 Scope

In this calculation, estimates of operating gaps, both radially and axially, are computed for the fuel basket-to-MPC shell, and for the MPC shell-to-overpack. This calculation is in support of the results presented in Section 3.4.4.2.

3.AQ.2 Methodology

Bounding temperatures are used to construct temperature distributions that will permit calculation of differential thermal expansions both radially and axially for the basket-to-MPC gaps, and for the MPC-to-overpack gaps. Reference temperatures are set at 70°F for all components. Temperature distributions are computed at the location of the HI-STORM 100 System where the temperatures are highest. A comprehensive nomenclature listing is provided in Section 3.AQ.6.

3.AQ.3 References

[3.AQ.1] Boley and Weiner, Theory of Thermal Stresses, John Wiley, 1960, Sec. 9.10, pp. 288-291.

[3.AQ.2] Burgreen, Elements of Thermal Stress Analysis, Arcturus Publishers, Cherry Hill NJ, 1988.

3.AQ.4 Calculations for Hot Components (Middle of System)

3.AQ.4.1 Input Data

Based on thermal calculations in Chapter 4, the following temperatures are appropriate at the hottest axial location of the cask (Table 4.4.27 and 4.4.36).

The temperature change at the overpack inner shell, $\Delta T_{1h} := 199 - 70$

The temperature change at the overpack outer shell, $\Delta T_{2h} := 145 - 70$

The temperature change at the mean radius of the MPC shell, $\Delta T_{3h} := 347 - 70$

The temperature change at the outside of the MPC basket, $\Delta T_{4h} := (492 - 70) \cdot 1.1$

The temperature change at the center of the basket (helium gas), $\Delta T_{5h} := 650 - 70$

Note that the outer basket temperature is conservatively amplified by 10% to insure a bounding parabolic distribution. This conservatism serves to maximize the growth of the basket.

The geometry of the components are as follows:

The outer radius of the overpack, $b := 66.25 \cdot \text{in}$

The minimum inner radius of the overpack, $a := 34.75 \cdot \text{in}$

The mean radius of the MPC shell, $R_{\text{mpc}} := \frac{68.375 \cdot \text{in} - 0.5 \cdot \text{in}}{2}$ $R_{\text{mpc}} = 33.938 \text{ in}$

The initial MPC-to-overpack radial clearance, $RC_{\text{mo}} := .5 \cdot (69.5 - 68.5) \cdot \text{in}$
 $RC_{\text{mo}} = 0.5 \text{ in}$

This initial radial clearance value, used to perform a radial growth check, is conservatively based on the channel radius (see Dwg. 1495, Sh. 5) and the maximum MPC diameter. For axial growth calculations for the MPC-to-overpack lid clearance, the axial length of the overpack is defined as the distance from the top of the pedestal platform to the bottom of the lid bottom plate, and the axial length of the MPC is defined as the overall MPC height.

The axial length of the overpack, $L_{\text{ovp}} := 191.5 \cdot \text{in}$

The axial length of the MPC, $L_{\text{mpc}} := 190.5 \cdot \text{in}$

The initial MPC-to-overpack nominal axial clearance, $AC_{\text{mo}} := L_{\text{ovp}} - L_{\text{mpc}}$

$$AC_{\text{mo}} = 1 \text{ in}$$

For growth calculations for the fuel basket-to-MPC shell clearances, the axial length of the basket is defined as the total length of the basket and the outer radius of the basket is defined as the mean radius of the MPC shell minus one-half of the shell thickness minus the initial basket-to-shell radial clearance.

The axial length of the basket, $L_{\text{bas}} := 176.5 \cdot \text{in}$

The initial basket-to-MPC lid nominal axial clearance, $AC_{\text{bm}} := 1.8125 \cdot \text{in}$

The initial basket-to-MPC shell nominal radial clearance, $RC_{\text{bm}} := 0.1875 \cdot \text{in}$

The outer radius of the basket, $R_b := R_{\text{mpc}} - \frac{0.5}{2} \cdot \text{in} - RC_{\text{bm}}$ $R_b = 33.5 \text{ in}$

The coefficients of thermal expansion used in the subsequent calculations are based on the mean temperatures of the MPC shell and the basket (conservatively estimated high).

The coefficient of thermal expansion for the MPC shell, $\alpha_{\text{mpc}} := 9.015 \cdot 10^{-6}$

The coefficient of thermal expansion for the basket, $\alpha_{\text{bas}} := 9.60 \cdot 10^{-6} \text{ } 600 \text{ deg. F}$

3.AQ.4.2 Thermal Growth of the Overpack

Results for thermal expansion deformation and stress in the overpack are obtained here. The system is replaced by a equivalent uniform hollow cylinder with approximated average properties.

Based on the given inside and outside surface temperatures, the temperature solution in the cylinder is given in the form:

$$C_a + C_b \cdot \ln\left(\frac{r}{a}\right)$$

where

$$C_a := \Delta T_{1h} \quad C_a = 129$$

$$C_b := \frac{\Delta T_{2h} - \Delta T_{1h}}{\ln\left(\frac{b}{a}\right)} \quad C_b = -83.688$$

Next, form the integral relationship:

$$\text{Int} := \int_a^b \left[C_a + C_b \cdot \left(\ln\left(\frac{r}{a}\right) \right) \right] \cdot r \, dr$$

The Mathcad program, which was used to create this appendix, is capable of evaluating the integral "Int" either numerically or symbolically. To demonstrate that the results are equivalent, the integral is evaluated both ways in order to qualify the accuracy of any additional integrations that are needed.

The result obtained through numerical integration, $\text{Int} = 1.533 \times 10^5 \text{ in}^2$

To perform a symbolic evaluation of the solution the integral "Ints" is defined. This integral is then evaluated using the Maple symbolic math engine built into the Mathcad program as:

$$\text{Int}_s := \int_a^b \left[C_a + C_b \cdot \left(\ln\left(\frac{r}{a}\right) \right) \right] \cdot r \, dr$$

$$\text{Int}_s := \frac{1}{2} \cdot C_b \cdot \ln\left(\frac{b}{a}\right) \cdot b^2 + \frac{1}{2} \cdot C_a \cdot b^2 - \frac{1}{4} \cdot C_b \cdot b^2 + \frac{1}{4} \cdot C_b \cdot a^2 - \frac{1}{2} \cdot C_a \cdot a^2$$

$$\text{Int}_s = 1.533 \times 10^5 \text{ in}^2$$

We note that the values of Int and Ints are identical. The average temperature in the overpack cylinder (T_{bar}) is therefore determined as:

$$T_{\text{bar}} := \frac{2}{(b^2 - a^2)} \cdot \text{Int} \qquad T_{\text{bar}} = 96.348$$

We estimate the average coefficient of thermal expansion for the overpack by weighting the volume of the various layers. A total of four layers are identified for this calculation. They are:

- 1) the inner shell
- 2) the shield shell
- 3) the radial shield
- 4) the outer shell

Thermal properties are based on estimated temperatures in the component and coefficient of thermal expansion values taken from the tables in Chapter 3. The following averaging calculation involves the thicknesses (t) of the various components, and the estimated coefficients of thermal expansion at the components' mean radial positions. The results of the weighted average process yields an effective coefficient of linear thermal expansion for use in computing radial growth of a solid cylinder (the overpack).

The thicknesses of each component are defined as:

$$t_1 := 1.25 \cdot \text{in}$$

$$t_2 := 0.75 \cdot \text{in}$$

$$t_3 := 26.75 \cdot \text{in}$$

$$t_4 := 0.75 \cdot \text{in}$$

and the corresponding mean radii can therefore be defined as:

$$r_1 := a + .5 \cdot t_1 + 2.0 \cdot \text{in} \qquad (\text{add the channel depth})$$

$$r_2 := r_1 + .5 \cdot t_1 + .5 \cdot t_2$$

$$r_3 := r_2 + .5 \cdot t_2 + .5 \cdot t_3$$

$$r_4 := r_3 + .5 \cdot t_3 + .5 \cdot t_4$$

To check the accuracy of these calculations, the outer radius of the overpack is calculated from r_4 and t_4 , and the result is compared with the previously defined value (b).

$$b_1 := r_4 + 0.5 \cdot t_4$$

$$b_1 = 66.25 \text{ in}$$

$$b = 66.25 \text{ in}$$

We note that the calculated value b_1 is identical to the previously defined value b . The coefficients of thermal expansion for each component, estimated based on the temperature gradient, are defined as:

$$\alpha_1 := 5.782 \cdot 10^{-6}$$

$$\alpha_2 := 5.782 \cdot 10^{-6}$$

$$\alpha_3 := 5.5 \cdot 10^{-6}$$

$$\alpha_4 := 5.638 \cdot 10^{-6}$$

Thus, the average coefficient of thermal expansion of the overpack is determined as:

$$\alpha_{\text{avg}} := \frac{r_1 \cdot t_1 \cdot \alpha_1 + r_2 \cdot t_2 \cdot \alpha_2 + r_3 \cdot t_3 \cdot \alpha_3 + r_4 \cdot t_4 \cdot \alpha_4}{\frac{a+b}{2} \cdot (t_1 + t_2 + t_3 + t_4)}$$
$$\alpha_{\text{avg}} = 5.628 \times 10^{-6}$$

Reference 3.AQ.1 gives an expression for the radial deformation due to thermal growth. At the inner radius of the overpack ($r = a$), the radial growth is determined as:

$$\Delta R_{\text{ah}} := \alpha_{\text{avg}} \cdot a \cdot T_{\text{bar}}$$

$$\Delta R_{\text{ah}} = 0.019 \text{ in}$$

Similarly, an overestimate of the axial growth of the overpack can be determined by applying the average temperature (T_{bar}) over the entire length of the overpack as:

$$\Delta L_{\text{ovph}} := L_{\text{ovp}} \cdot \alpha_{\text{avg}} \cdot T_{\text{bar}}$$

$$\Delta L_{\text{ovph}} = 0.104 \text{ in}$$

Estimates of the secondary thermal stresses that develop in the overpack due to the radial temperature variation are determined using a conservatively high value of E as based on the temperature of the steel. The circumferential stress at the inner and outer surfaces (σ_{ca} and σ_{cb} , respectively) are determined as:

The Young's Modulus of the material, $E := 28300000 \cdot \text{psi}$

$$\sigma_{ca} := \alpha_{avg} \cdot \frac{E}{a^2} \left[2 \cdot \frac{a^2}{(b^2 - a^2)} \cdot \text{Int} - (C_a) \cdot a^2 \right]$$

$$\sigma_{ca} = -5200 \text{ psi}$$

$$\sigma_{cb} := \alpha_{avg} \cdot \frac{E}{b^2} \left[2 \cdot \frac{b^2}{(b^2 - a^2)} \cdot \text{Int} - \left[C_a + C_b \cdot \left(\ln \left(\frac{b}{a} \right) \right) \right] \cdot b^2 \right]$$

$$\sigma_{cb} = 3400 \text{ psi}$$

The radial stress due to the temperature gradient is zero at both the inner and outer surfaces of the overpack. The radius where a maximum radial stress is expected, and the corresponding radial stress, are determined by trial and error as:

$$N := 0.37$$

$$r := a \cdot (1 - N) + N \cdot b$$

$$r = 46.405 \text{ in}$$

$$\sigma_r := \alpha_{avg} \cdot \frac{E}{r^2} \left[\frac{r^2 - a^2}{2} \cdot T_{bar} - \int_a^r \left[C_a + C_b \cdot \left(\ln \left(\frac{y}{a} \right) \right) \right] \cdot y \, dy \right]$$

$$\sigma_r = -678.201 \text{ psi}$$

The axial stress developed due to the temperature gradient is equal to the sum of the radial and tangential stresses at any radial location. (see eq. 9.10.7) of [3.AQ.1]. Therefore, the axial stresses are available from the above calculations. The stress intensities in the overpack due to the temperature distribution are below the Level A membrane stress.

3.AQ.4.3 Thermal Growth of the MPC Shell

The radial and axial growth of the MPC shell (ΔR_{mpch} and ΔL_{mpch} , respectively) are determined as:

$$\Delta R_{mpch} := \alpha_{mpc} \cdot R_{mpc} \cdot \Delta T_{3h} \qquad \Delta R_{mpch} = 0.085 \text{ in}$$

$$\Delta L_{mpch} := \alpha_{mpc} \cdot L_{mpc} \cdot \Delta T_{3h} \qquad \Delta L_{mpch} = 0.476 \text{ in}$$

3.AQ.4.4 Clearances Between the MPC Shell and Overpack

The final radial and axial MPC shell-to-overpack clearances (RG_{moh} and AG_{moh} , respectively) are determined as:

$$RG_{moh} := RC_{mo} + \Delta R_{ab} - \Delta R_{mpch}$$

$$RG_{moh} = 0.434 \text{ in}$$

$$AG_{moh} := AC_{mo} + \Delta L_{ovph} - \Delta L_{mpch}$$

$$AG_{moh} = 0.628 \text{ in}$$

Note that this axial clearance (AG_{moh}) is based on the temperature distribution at the hottest axial location in the system.

3.AQ.4.5 Thermal Growth of the MPC-24E Basket

Using formulas given in [3.AQ.2] for a solid body of revolution, and assuming a parabolic temperature distribution in the radial direction with the center and outer temperatures given previously, the following relationships can be developed for free thermal growth.

Define $\Delta T_{bas} := \Delta T_{5h} - \Delta T_{4h}$ $\Delta T_{bas} = 115.8$

Then the mean temperature can be defined as $T_{bar} := \frac{2}{R_b^2} \cdot \int_0^{R_b} \left(\Delta T_{5h} - \Delta T_{bas} \cdot \frac{r^2}{R_b^2} \right) \cdot r \cdot dr$

Using the Maple symbolic engine again, the closed form solution of the integral is:

$$T_{bar} := \frac{2}{R_b^2} \cdot \left(\frac{-1}{4} \cdot \Delta T_{bas} \cdot R_b^2 + \frac{1}{2} \cdot \Delta T_{5h} \cdot R_b^2 \right)$$

$$T_{bar} = 522.1$$

The corresponding radial growth at the periphery (ΔR_{bh}) is therefore determined as:

$$\Delta R_{bh} := \alpha_{bas} \cdot R_b \cdot T_{bar}$$

$$\Delta R_{bh} = 0.168 \text{ in}$$

and the corresponding axial growth (ΔL_{bas}) is determined from [3.AQ.2] as:

$$\Delta L_{bh} := \Delta R_{bh} \cdot \frac{L_{bas}}{R_b}$$

$$\Delta L_{bh} = 0.885 \text{ in}$$

Note that the coefficient of thermal expansion for the hottest basket temperature has been used, and the results are therefore conservative.

3.AQ.4.6 Clearances Between the Fuel Basket and MPC Shell

The final radial and axial fuel basket-to-MPC shell and lid clearances (RG_{bmh} and AG_{bmh} , respectively) are determined as:

$$RG_{bmh} := RC_{bm} - \Delta R_{bh} + \Delta R_{mpch}$$

$$RG_{bmh} = 0.104 \text{ in}$$

$$AG_{bmh} := AC_{bm} - \Delta L_{bh} + \Delta L_{mpch}$$

$$AG_{bmh} = 1.404 \text{ in}$$

3.AQ.5 Summary of Results

The previous results are summarized here.

MPC Shell-to-Overpack

$$RG_{moh} = 0.434 \text{ in}$$

$$AG_{moh} = 0.628 \text{ in}$$

Fuel Basket-to-MPC Shell

$$RG_{bmh} = 0.104 \text{ in}$$

$$AG_{bmh} = 1.404 \text{ in}$$

3.AQ.6 Nomenclature

a is the inner radius of the overpack

AC_{bm} is the initial fuel basket-to-MPC axial clearance.

AC_{mo} is the initial MPC-to-overpack axial clearance.

AG_{bmh} is the final fuel basket-to-MPC shell axial gap for the hot components.

AG_{moh} is the final MPC shell-to-overpack axial gap for the hot components.

b is the outer radius of the overpack.

L_{bas} is the axial length of the fuel basket.

L_{mpc} is the axial length of the MPC.

L_{ovp} is the axial length of the overpack.

r_1 (r_2, r_3, r_4) is mean radius of the overpack inner shell (shield shell, concrete, outer shell).

R_b is the outer radius of the fuel basket.

R_{mpc} is the mean radius of the MPC shell.

RC_{bm} is the initial fuel basket-to-MPC radial clearance.

RC_{mo} is the initial MPC shell-to-overpack radial clearance.

RG_{bmh} is the final fuel basket-to-MPC shell radial gap for the hot components.

RG_{moh} is the final MPC shell-to-overpack radial gap for the hot components.

t_1 (t_2, t_3, t_4) is the thickness of the overpack inner shell (shield shell, concrete, outer shell).

T_{bar} is the average temperature of the overpack cylinder.

α_1 ($\alpha_2, \alpha_3, \alpha_4$) is the coefficient of thermal expansion of the overpack inner shell (shield shell, concrete, outer shell).

α_{avg} is the average coefficient of thermal expansion of the overpack.

α_{bas} is the coefficient of thermal expansion of the overpack.

α_{mpc} is the coefficient of thermal expansion of the MPC.

ΔL_{bh} is the axial growth of the fuel basket for the hot components.

ΔL_{mpch} is the axial growth of the MPC for the hot components.
 ΔL_{ovph} is the axial growth of the overpack for the hot components.
 ΔR_{ah} is the radial growth of the overpack inner radius for the hot components.
 ΔR_{bh} is the radial growth of the fuel basket for the hot components.
 ΔR_{mpch} is the radial growth of the MPC shell for the hot components.
 ΔT_{1h} is the temperature change at the overpack inner shell for hot components.
 ΔT_{2h} is the temperature change at the overpack outer shell for hot components.
 ΔT_{3h} is the temperature change at the MPC shell mean radius for hot components.
 ΔT_{4h} is the temperature change at the MPC basket periphery for hot components.
 ΔT_{5h} is the temperature change at the MPC basket centerline for hot components.
 ΔT_{bas} is the fuel basket centerline-to-periphery temperature gradient.
 σ_{ca} is the circumferential stress at the overpack inner surface.
 σ_{cb} is the circumferential stress at the overpack outer surface.
 σ_r is the maximum radial stress of the overpack.
 σ_{zi} is the axial stress at the fuel basket centerline.
 σ_{zo} is the axial stress at the fuel basket periphery.

APPENDIX 3.AR - ANALYSIS OF TRANSNUCLEAR DAMAGED FUEL CANISTER AND THORIA ROD CANISTER

3.AR.1 Introduction

Some of the items at the Dresden Station that have been considered for storage in the HI-STAR 100 System are damaged fuel stored in Transnuclear damaged fuel canisters and Thoria rods that are also stored in a special canister designed by Transnuclear. Both of these canisters have been designed and have been used by ComEd to transport the damaged fuel and the Thoria rods. Despite the previous usage of these canisters, it is prudent and appropriate to provide an independent structural analysis of the major load path of these canisters prior to accepting them for inclusion as permitted items in the HI-STAR and HI-STORM 100 MPC's. This appendix contains the necessary structural analysis of the Transnuclear damaged fuel canister and Thoria rod canister. The objective of the analysis is to demonstrate that the canisters are structurally adequate to support the loads that develop during normal lifting operations and during postulated accident conditions.

The upper closure assembly is designed to meet the requirements of NUREG-0612 [2]. The remaining components of the canisters are governed by ASME Code Section III, Subsection NG [3]. These are the same criteria used in Appendix 3.B of the HI-STAR 100 to analyze the Holtec damaged fuel container for Dresden damaged fuel.

3.AR.2 Composition

This appendix was created using the Mathcad (version 8.02) software package. Mathcad uses the symbol ':=' as an assignment operator, and the equals symbol '=' retrieves values for constants or variables.

3.AR.3 References

1. Crane Manufacture's of America Association, Specifications for Electric Overhead Traveling Cranes #70.
2. NUREG-0612, Control of Heavy Loads at Nuclear Power Plants
3. ASME Boiler and Pressure Vessel Code, Section III, July 1995

3.AR.4 Assumptions

1. Buckling is not a concern during an accident since during a drop the canister will be confined by the fuel basket.
2. The strength of the weld is assumed to decrease the same as the base metal as the temperature increases.

3.AR.5 Method

Two are considered: 1) normal lifting and handling of canister, and 2) accident drop event.

3.AR.6 Acceptance Criteria

1) Normal Handling -

- a) Canister governed by ASME NG allowables:
- b) Welds governed by NG and NF allowables;
quality factors taken from NG
stress limit = $0.3 S_u$
- c) Lifting governed by NUREG-0612 allowables.

2) Drop Accident -

- a) canister governed by ASME NG allowables:
shear = $0.42 S_u$ (conservative)
- b) Welds governed by NG and NF allowables;
quality factors taken from NG
stress limit = $0.42 S_u$

3.AR.7 Input Stress Data

The canisters is handled while still in the spent fuel pool. Therefore, its design temperature for lifting considerations is the temperature of the fuel pool water (150°F). The design temperature for accident conditions is 725°F. All dimensions are taken from the Transnuclear design drawings listed at the end of this appendix. The basic input parameters used to perform the calculations are:

Design stress intensity of SA240-304 (150°F)	$S_{m1} := 20000\text{-psi}$
Design stress intensity of SA240-304 (775°F)	$S_{m2} := 15800\text{-psi}$
Yield stress of SA240-304 (150°F)	$S_{y1} := 27500\text{-psi}$
Yield stress of SA240-304 (775°F)	$S_{y2} := 17500\text{-psi}$
Ultimate strength of SA240-304 (150°F)	$S_{u1} := 73000\text{-psi}$
Ultimate strength of SA240-304 (775°F)	$S_{u2} := 63300\text{-psi}$

Ultimate strength of weld material (150°F)	$S_{u_w} := 70000 \cdot \text{psi}$
Ultimate strength of weld material (775°F)	$S_{u_{wacc}} := S_{u_w} - (S_{u1} - S_{u2})$
Weight of a BWR fuel assembly (D-1)	$W_{\text{fuel}} := 400 \cdot \text{lbf}$
Weight of 18 Thoria Rods (Calculated by Holtec)	$W_{\text{thoria}} := 90 \cdot \text{lbf}$
Bounding Weight of the damaged fuel canister (Estimated by Holtec)	$W_{\text{container}} := 150 \cdot \text{lbf}$
Bounding Weight of the Thoria Rod Canister (Estimated)	$W_{\text{rodcan}} := 300 \cdot \text{lbf}$
Quality factor for full penetration weld (visual inspection)	$n := 0.5$
Dynamic load factor for lifting	$\text{DLF} := 1.15$

The remaining input data is provided as needed in the calculation section

3.AR.8 Calculations for Transnuclear Damaged Fuel Canister

3.AR.8.1 Lifting Operation (Normal Condition)

The critical load case under normal conditions is the lifting operation. The key areas of concern for ASME NG analysis are the canister sleeve, the sleeve to lid frame weld, and the lid frame. All calculations performed for the lifting operation assume a dynamic load factor of 1.15 [1].

3.AR.8.1.1 Canister Sleeve

During a lift, the canister sleeve is loaded axially, and the stress state is pure tensile membrane. For the subsequent stress calculation, it is assumed that the full weight of the damaged fuel canister and the fuel assembly are supported by the sleeve. The magnitude of the load is

$$F := \text{DLF} \cdot (W_{\text{container}} + W_{\text{fuel}}) \quad F = 632 \text{ lbf}$$

From TN drawing 9317.1-120-4, the canister sleeve geometry is

$$i_{\text{sleeve}} := 4.81 \cdot \text{in} \quad t_{\text{sleeve}} := 0.11 \cdot \text{in}$$

The cross sectional area of the sleeve is

$$A_{\text{sleeve}} := (i_{\text{sleeve}} + 2 \cdot t_{\text{sleeve}})^2 - i_{\text{sleeve}}^2 \quad A_{\text{sleeve}} = 2.16 \text{ in}^2$$

Therefore, the tensile stress in the sleeve is

$$\sigma := \frac{F}{A_{\text{sleeve}}} \quad \sigma = 292 \text{ psi}$$

The allowable stress intensity for the primary membrane category is S_m per Subsection NG of the ASME Code. The corresponding safety margin is

$$SM := \frac{S_{m1}}{\sigma} - 1 \quad SM = 67.5$$

3.AR.8.1.2 Sleeve Welds

The top of the canister must support the amplified weight. This load is carried directly by the fillet weld that connects the lid frame to the canister sleeve. The magnitude of the load is conservatively taken as the entire amplified weight of canister plus fuel.

$$F = 632 \text{ lbf}$$

The weld thickness is $t_{\text{base}} := 0.09 \text{ in}$

The area of the weld, with proper consideration of quality factors, is

$$A_{\text{weld}} := n \cdot 4 \cdot (id_{\text{sleeve}} + 2 \cdot t_{\text{sleeve}}) \cdot 0.7071 \cdot t_{\text{base}} \quad A_{\text{weld}} = 0.64 \text{ in}^2$$

Therefore, the shear stress in the weld is

$$\tau := \frac{F}{A_{\text{weld}}} \quad \tau = 988 \text{ psi}$$

From the ASME Code the allowable weld shear stress, under normal conditions (Level A), is 30% of the ultimate strength of the base metal. The corresponding safety margin is

$$SM := \frac{0.3 \cdot S_{u1}}{\tau} - 1 \quad SM = 21.2$$

3.AR.8.1.3 Lid Frame Assembly

The Lid Frame assembly is classified as a NUREG-0612 lifting device. As such the allowable stress for design is the lesser of one-sixth of the yield stress and one-tenth of the ultimate strength.

$$\sigma_1 := \frac{S_{y1}}{6} \quad \sigma_2 := \frac{S_{u1}}{10}$$

$$\sigma_1 = 4583 \text{ psi} \quad \sigma_2 = 7300 \text{ psi}$$

For SA240-304 material the yield stress governs. $\sigma_{\text{allowable}} := \sigma_1$

The total lifted load is $F := \text{DLF} \cdot (W_{\text{container}} + W_{\text{fuel}})$ $F = 632 \text{ lbf}$

The frame thickness is obtained from Transnuclear drawing 9317.1-120-11

$$t_{\text{frame}} := 0.395 \cdot \text{in}$$

The inside span is the same as the canister sleeve $\text{id}_{\text{sleeve}} = 4.81 \text{ in}$

The area available for direct load is

$$A_{\text{frame}} := (\text{id}_{\text{sleeve}} + 2 \cdot t_{\text{frame}})^2 - \text{id}_{\text{sleeve}}^2 \quad A_{\text{frame}} = 8.224 \text{ in}^2$$

The direct stress in the frame is

$$\sigma := \frac{F}{A_{\text{frame}}} \quad \sigma = 77 \text{ psi}$$

The safety margin is

$$\text{SM} := \frac{\sigma_{\text{allowable}}}{\sigma} - 1 \quad \text{SM} = 58.59$$

The bearing stress at the four lift locations is computed from the same drawing

$$A_{\text{bearing}} := 4 \cdot t_{\text{frame}} \cdot (2 \cdot 0.38 \cdot \text{in}) \quad A_{\text{bearing}} = 1.201 \text{ in}^2$$

$$\sigma_{\text{bearing}} := \frac{F}{A_{\text{bearing}}} \quad \sigma_{\text{bearing}} = 526.732 \text{ psi} \quad \text{SM} := \frac{\sigma_{\text{allowable}}}{\sigma_{\text{bearing}}} - 1 \quad \text{SM} = 7.7$$

3.AR.8.2 60g End Drop of HI-STAR 100 (Bounding Accident Condition since HI-STORM limit is 45g's)

The critical member of the damaged fuel canister during the drop scenario is the bottom assembly (see Transnuclear drawing 9317.1-120-5). It is subjected to direct compression due to the amplified weight of the fuel assembly and the canister. The bottom assembly is a 3.5" Schedule 40S pipe. The load due to the 60g end drop is

$$F := 60 \cdot (W_{\text{fuel}} + W_{\text{container}}) \quad F = 33000 \text{ lbf}$$

The properties of the pipe are obtained from the Ryerson Stock Catalog as

$$\text{od} := 4 \cdot \text{in} \quad \text{id} := 3.548 \cdot \text{in} \quad t_{\text{pipe}} := \frac{(\text{od} - \text{id})}{2} \quad t_{\text{pipe}} = 0.226 \text{ in}$$

The pipe area is

$$A_{\text{pipe}} := \frac{\pi}{4} \cdot (\text{od}^2 - \text{id}^2) \quad A_{\text{pipe}} = 2.68 \text{ in}^2$$

The stress in the member is

$$\sigma := \frac{F}{A_{\text{pipe}}} \quad \sigma = 12316 \text{ psi}$$

The allowable primary membrane stress from Subsection NG of the ASME Code, for accident conditions (Level D), is

$$\sigma_{\text{allowable}} := 2.4 \cdot S_{m2} \quad \sigma_{\text{allowable}} = 37920 \text{ psi}$$

The safety margin is

$$SM := \frac{\sigma_{\text{allowable}}}{\sigma} - 1 \quad SM = 2.1$$

To check the stability of the pipe, we conservatively compute the Euler Buckling load for a simply supported beam.

The Young's Modulus is

$$E := 27600000 \cdot \text{psi}$$

Compute the moment of inertia as

$$I := \frac{\pi}{64} \cdot (\text{od}^4 - \text{id}^4) \quad I = 4.788 \text{ in}^4$$

$L := 22\text{-in}$

$$P_{\text{crit}} := \pi^2 \cdot \frac{E \cdot I}{L^2} \quad P_{\text{crit}} = 2.695 \times 10^6 \text{ lbf}$$

The safety margin is

$$SM := \frac{P_{\text{crit}}}{F} - 1 \quad SM = 80.654$$

3.AR.8.3 Conclusion for TN Damaged Fuel Canister

The damaged fuel canister and the upper closure assembly are structurally adequate to withstand the specified normal and accident condition loads. All calculated safety margins are greater than zero.

3.AR.9 Calculations for Transnuclear Thoria Rod Canister

3.AR.9.1 Lifting Operation (Normal Condition)

The critical load case under normal conditions is the lifting operation. The key areas of concern for ASME NG analysis are the canister sleeve, the sleeve to lid frame weld, and the lid frame. All calculations performed for the lifting operation assume a dynamic load factor of 1.15.

3.AR.9.1.1 Canister Sleeve

During a lift, the canister sleeve is loaded axially, and the stress state is pure tensile membrane. For the subsequent stress calculation, it is assumed that the full weight of the Thoria rod canister and the Thoria rods are supported by the sleeve. The magnitude of the load is

$$F := \text{DLF} \cdot (W_{\text{rodcan}} + W_{\text{thoria}}) \quad F = 449 \text{ lbf}$$

From TN drawing 9317.1-182-1, the canister sleeve geometry is

$$id_{\text{sleeve}} := 4.81 \cdot \text{in} \quad t_{\text{sleeve}} := 0.11 \cdot \text{in}$$

The cross sectional area of the sleeve is

$$A_{\text{sleeve}} := (id_{\text{sleeve}} + 2 \cdot t_{\text{sleeve}})^2 - id_{\text{sleeve}}^2 \quad A_{\text{sleeve}} = 2.16 \text{ in}^2$$

Therefore, the tensile stress in the sleeve is

$$\sigma := \frac{F}{A_{\text{sleeve}}} \quad \sigma = 207 \text{ psi}$$

The allowable stress intensity for the primary membrane category is S_m per Subsection NG of the ASME Code. The corresponding safety margin is

$$SM := \frac{S_{m1}}{\sigma} - 1 \quad SM = 95.5$$

3.AR.9.1.2 Sleeve Welds

The top of the canister must support the amplified weight. This load is carried directly by the fillet weld that connects the lid frame to the canister sleeve. The magnitude of the load is conservatively taken as the entire amplified weight of canister plus Thoria rod.

$$F = 449 \text{ lbf}$$

The weld thickness is $t_{\text{base}} := 0.09 \cdot \text{in}$ (assumed equal to the same weld for the damaged fuel canister)

The area of the weld, with proper consideration of quality factors, is

$$A_{\text{weld}} := n \cdot 4 \cdot (id_{\text{sleeve}} + 2 \cdot t_{\text{sleeve}}) \cdot 0.7071 \cdot t_{\text{base}} \quad A_{\text{weld}} = 0.64 \text{ in}^2$$

Therefore, the shear stress in the weld is

$$\tau := \frac{F}{A_{\text{weld}}} \quad \tau = 701 \text{ psi}$$

From the ASME Code the allowable weld shear stress, under normal conditions (Level A), is 30% of the ultimate strength of the base metal. The corresponding safety margin is

$$SM := \frac{0.3 \cdot S_{ul}}{\tau} - 1 \quad SM = 30.3$$

3.AR.9.1.3 Lid Frame Assembly

The Lid Frame assembly is classified as a NUREG-0612 lifting device. As such the allowable stress for design is the lesser of one-sixth of the yield stress and one-tenth of the ultimate strength.

$$\sigma_1 := \frac{S_{y1}}{6} \qquad \sigma_2 := \frac{S_{u1}}{10}$$
$$\sigma_1 = 4583 \text{ psi} \qquad \sigma_2 = 7300 \text{ psi}$$

For SA240-304 material the yield stress governs. $\sigma_{\text{allowable}} := \sigma_1$

The total lifted load is $F := \text{DLF} \cdot (W_{\text{rodcan}} + W_{\text{thoria}})$ $F = 449 \text{ lbf}$

The frame thickness is obtained from Transnuclear drawing 9317.1-182-8. This drawing was not available, but the TN drawing 9317.1-182-4 that included a view of the lid assembly suggests that it is identical in its structural aspects to the lid frame in the damaged fuel canister.

$$t_{\text{frame}} := 0.395 \cdot \text{in}$$

The inside span is the same as the canister sleeve $\text{id}_{\text{sleeve}} = 4.81 \text{ in}$

The area available for direct load is

$$A_{\text{frame}} := (\text{id}_{\text{sleeve}} + 2 \cdot t_{\text{frame}})^2 - \text{id}_{\text{sleeve}}^2 \qquad A_{\text{frame}} = 8.224 \text{ in}^2$$

The direct stress in the frame is

$$\sigma := \frac{F}{A_{\text{frame}}} \qquad \sigma = 55 \text{ psi}$$

The safety margin is

$$\text{SM} := \frac{\sigma_{\text{allowable}}}{\sigma} - 1 \qquad \text{SM} = 83.04$$

The bearing stress at the four lift locations is computed from the same drawing

$$A_{\text{bearing}} := 4 \cdot t_{\text{frame}} \cdot (2 \cdot 0.38 \cdot \text{in}) \qquad A_{\text{bearing}} = 1.201 \text{ in}^2$$

$$\sigma_{\text{bearing}} := \frac{F}{A_{\text{bearing}}} \qquad \sigma_{\text{bearing}} = 373.501 \text{ psi} \qquad \text{SM} := \frac{\sigma_{\text{allowable}}}{\sigma_{\text{bearing}}} - 1 \qquad \text{SM} = 11.27$$

3.AR.9.2 60g HI-STAR End Drop (Bounds Accident Condition in HI-STORM)

The critical member of the damaged fuel canister during the drop scenario is the bottom assembly. Transnuclear drawing 9317.1-120-5). It is subjected to direct compression due to the amplified weight of the Thoria rods and the canister.

$$F := 60 \cdot (W_{\text{thoria}} + W_{\text{rodcan}}) \quad F = 23400 \text{ lbf}$$

The properties of the pipe are obtained from the Ryerson Stock Catalog as

$$\text{od} := 4 \cdot \text{in} \quad \text{id} := 3.548 \cdot \text{in} \quad t_{\text{pipe}} := \frac{(\text{od} - \text{id})}{2} \quad t_{\text{pipe}} = 0.226 \text{ in}$$

The pipe area is

$$A_{\text{pipe}} := \frac{\pi}{4} \cdot (\text{od}^2 - \text{id}^2) \quad A_{\text{pipe}} = 2.68 \text{ in}^2$$

The stress in the member is

$$\sigma := \frac{F}{A_{\text{pipe}}} \quad \sigma = 8733 \text{ psi}$$

The allowable primary membrane stress from Subsection NG of the ASME Code, for accident conditions (Level D), is

$$\sigma_{\text{allowable}} := 2.4 \cdot S_{m2} \quad \sigma_{\text{allowable}} = 37920 \text{ psi}$$

The safety margin is

$$\text{SM} := \frac{\sigma_{\text{allowable}}}{\sigma} - 1 \quad \text{SM} = 3.3$$

To check the stability of the pipe, we compute the Euler Buckling load for a simply supported beam.

The Young's Modulus is

$$E := 27600000 \cdot \text{psi}$$

Compute the moment of inertia as

$$I := \frac{\pi}{64} \cdot (\text{od}^4 - \text{id}^4) \quad I = 4.788 \text{ in}^4$$

$L := 22 \cdot \text{in}$

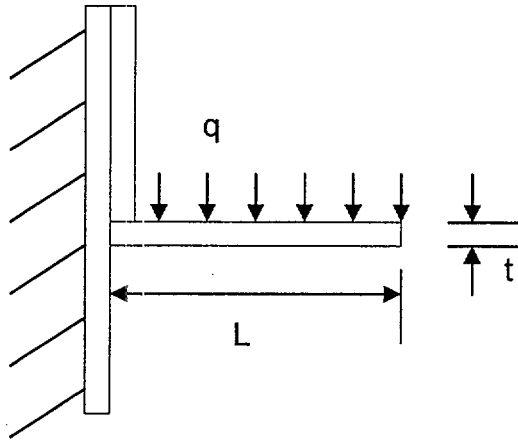
$$P_{\text{crit}} := \pi^2 \cdot \frac{E \cdot I}{L^2} \quad P_{\text{crit}} = 2.695 \times 10^6 \text{ lbf}$$

The safety margin is

$$\text{SM} := \frac{P_{\text{crit}}}{F} - 1 \quad \text{SM} = 114.153$$

3.AR.9.4 60g HI-STAR Side Drop (Bounds Accident Condition for HI-STORM)

The Thoria Rod Separator Assembly is shown in TN drawings 9317.1-182-1 and 9317.1-182-3. under the design basis side drop or tipover accident, we examine the consequences to one of the rod support strips acting as a cantilever strip acted upon by self-weight and the weight of one Thoria rod.



Weight of 1 rod per unit length

$$\text{length} := 113.16 \cdot \text{in}$$

$$w_{\text{rod}} := 90 \cdot \frac{\text{lbf}}{18} \cdot \frac{1}{\text{length}}$$

$$w_{\text{rod}} = 0.044 \frac{\text{lbf}}{\text{in}}$$

Weight of support per unit length (per drawing 9317.1-182-3)

$$L := 1.06 \cdot \text{in}$$

$$t := 0.11 \cdot \text{in}$$

$$w_{\text{sup}} := .29 \cdot \frac{\text{lbf}}{\text{in}^3} \cdot L \cdot t$$

$$w_{\text{sup}} = 0.034 \frac{\text{lbf}}{\text{in}}$$

Amplified load (assumed as a uniform distribution)

$$q := 60 \cdot (w_{\text{rod}} + w_{\text{sup}})$$

$$q = 4.68 \frac{\text{lbf}}{\text{in}}$$

$$\text{Moment} := \frac{q \cdot L^2}{2}$$

$$\text{Moment} = 2.629 \text{ in} \cdot \text{lbf}$$

Bending stress at the root of the cantilever beam is

$$\sigma := 6 \cdot \frac{\text{Moment}}{1 \cdot \text{in} \cdot t^2}$$

$$\sigma = 1.304 \times 10^3 \text{ psi}$$

Shear stress at the root of the cantilever

$$\tau := q \cdot \frac{L}{t \cdot 1 \cdot \text{in}}$$

$$\tau = 45.098 \text{ psi}$$

Large margins of safety are indicated by these stress results.

3.AR.9.5 Conclusion for TN Thoria Rod Canister

The Thoria rod canister is structurally adequate to withstand the specified normal and accident condition loads. All calculated safety margins are greater than zero.

3.AR.10 General Conclusion

The analysis of the TN damaged fuel canister and the TN Thoria rod canister have demonstrated that all structural safety margins are large. We have confirmed that the TN canisters have positive safety margins for the HI-STAR 100 governing design basis loads. The HI-STAR design basis handling accident load bounds the corresponding load for HI-STORM. Therefore, the loaded TN canisters from ComEd Dresden Unit#1 can safely be carried in both the HI-STAR and HI-STORM 100 Systems.

3.AR.11 List of Transnuclear Drawing Numbers

9317.1-120 - 2,3,4,5,6,7,8,9,10,11,13,14,15,17,18,19,20,21,22,23

9317.1-182- 1,2,3,4,5,6

APPENDIX 3.AS - ANALYSIS OF GENERIC PWR AND BWR DAMAGED FUEL CONTAINERS

3.AS.1 Introduction

This appendix contains an analysis of the damaged fuel containers that are used for the HI-STAR 100 MPC-24E and MPC-68, respectively. The objective of the analysis is to demonstrate that the two types of storage containers are structurally adequate to support the loads that develop during normal lifting operations and during an end drop.

The lifting bolt of each containers is designed to meet the requirements set forth for Special Lifting Devices in Nuclear Plants [2]. The remaining components of the damaged fuel container are compared to ASME Code Section III, Subsection NG allowable stress levels.

3.AS.2 Composition

This appendix was created using the Mathcad (version 2000) software package. Mathcad uses the symbol ':=' as an assignment operator, and the equals symbol '=' retrieves values for constants or variables.

3.AS.3 References

1. Crane Manufacture's of America Association, Specifications for Electric Overhead Traveling Cranes #70.
2. ANSI N14-6, Special Lifting Devices for Loads Greater than 10000 lbs. in Nuclear Plants.
3. ASME Boiler and Pressure Vessel Code, Section III Subsection NG, July 1995
4. Roark's Formulas for Stress & Strain, 6th Edition, 1989.
5. Kent's Mechanical Engineers' Handbook, Design and Production Volume, 12th Edition, 1965
6. ASME, "Boiler & Pressure Vessel Code," Section II, Part D-Material Properties, July 1, 1995

3.AS.4 Assumptions

1. Buckling is not a concern during an accident since during a drop the canister will be supported by the walls of the fuel basket.
2. The strength of the weld is assumed to decrease the same as the base metal as the temperature is increased.

3.AS.5 Method

Two cases are considered: 1) normal handling of container, and 2) accident drop event.

3.AS.6 Acceptance Criteria

1) Normal Handling -

- a) Container governed by ASME NG[3] allowables:
shear stress allowable is 60% of membrane stress intensity
- b) Welds are governed by NG Code allowables; stress limit = 60% of tensile stress intensity (per Section III, Subsection NG-3227.2).
- c) Lifting bolt is governed by ANSI N14-6 criteria

2) Drop Accident -

- a) Container governed by ASME Section III, Appendix F allowables:
(allowable shear stress = 0.42 Su)

3.AS.7 Input Data for MPC-24E (PWR) Damaged Fuel Container

The damaged fuel container is only handled while still in the spent fuel pool. Therefore, its design temperature for lifting considerations is the temperature of the fuel pool water (150°F). The design temperature for accident conditions is 725°F. All dimensions are taken from Dwg. 2776. The basic input parameters used to perform the calculations are:

Design stress intensity of SA240-304 (150°F)	$S_{m1} := 20000 \cdot \text{psi}$	Table 1.A.1
Design stress intensity of SA240-304 (725°F)	$S_{m2} := 15800 \cdot \text{psi}$	
Yield stress of SA240-304 (150°F)	$S_{y1} := 27500 \cdot \text{psi}$	Table 1.A.3
Yield stress of SA240-304 (725°F)	$S_{y2} := 17500 \cdot \text{psi}$	
Ultimate strength of SA240-304 (150°F)	$S_{u1} := 73000 \cdot \text{psi}$	Table 1.A.2
Ultimate strength of SA240-304 (725°F)	$S_{u2} := 63300 \cdot \text{psi}$	
Minimum Yield stress of SA564-630 (200°F)	$S_{by} := 97100 \cdot \text{psi}$	Table 2.3.5
Minimum Ultimate strength of SA564-630 (200°F)	$S_{bu} := 135000 \cdot \text{psi}$	

Weight of a PWR fuel assembly (allowable maximum value)	$W_{\text{fuel}} := 1507 \cdot \text{lbf}$
Weight of the damaged fuel container	$W_{\text{container}} := 173 \cdot \text{lbf}$
Wall thickness of the container sleeve	$t_{\text{sleeve}} := 0.075 \cdot \text{in}$
Dimension of the square baseplate	$d_{\text{bplate}} := 8.75 \cdot \text{in}$
Thickness of the baseplate	$t_{\text{bplate}} := 0.75 \cdot \text{in}$
Diameter of baseplate through hole	$d_{\text{bph}} := 2 \cdot \text{in}$
Number of baseplate through holes	$N_{\text{bph}} := 5$
Diameter of the baseplate spot weld	$d_{w_{\text{base}}} := 0.125 \cdot \text{in}$
Inner dimension of the container sleeve	$id_{\text{sleeve}} := 8.75 \cdot \text{in}$
Wall thickness of container collar	$t_{\text{collar}} := 0.21 \cdot \text{in}$
Distance from end of sleeve to top of engagement slot	$d_{\text{slot}} := 0.1875 \cdot \text{in}$
Thickness of the load tab	$t_{\text{tab}} := 0.125 \cdot \text{in}$
Width of the load tab	$w_{\text{tab}} := 2.0 \cdot \text{in}$
Thickness of the closure plate	$t_{\text{cp}} := 0.5 \cdot \text{in}$
Radius of the lifting bolt	$r_{\text{bolt}} := 0.1875 \cdot \text{in}$
Weight density of the stainless steel	$\gamma_{\text{ss}} := 0.283 \cdot \frac{\text{lbf}}{\text{in}^3}$
Thickness of the nut	$t_{\text{nut}} := 0.346 \cdot \text{in} \quad [5]$
Length of the bolt	$L_{\text{bolt}} := 2.0 \cdot \text{in}$
Height of the bolt head	$t_{\text{bolt}} := 0.268 \cdot \text{in} \quad [5]$
Thickness of the washer	$t_{\text{washer}} := 0.125 \cdot \text{in}$
Dynamic load factor for lifting [1]	$\text{DLF} := 1.15$

3.AS.7 Calculations for MPC-24E Damaged Fuel Container

3.AS.7.1 Lifting Operation (Normal Condition)

The critical load case under normal conditions is the lifting operation. The key areas of concern are the container sleeve, the weld between the sleeve and the base of the container, the container upper closure, and the lifting bolt. All calculations performed for the lifting operation assume a dynamic load factor of 1.15.

3.AS.7.1.1 Container Sleeve (Item 1)

During a lift, the container sleeve is loaded axially, and the stress state is pure tensile membrane. For the subsequent stress calculation, it is assumed that the full weight of the damaged fuel container and the fuel assembly are supported by the sleeve. The magnitude of the load is

$$F := DLF \cdot (W_{\text{container}} + W_{\text{fuel}}) \quad F = 1932 \text{ lbf}$$

The cross sectional area of the sleeve is

$$A_{\text{sleeve}} := (id_{\text{sleeve}} + 2 \cdot t_{\text{sleeve}})^2 - id_{\text{sleeve}}^2 \quad A_{\text{sleeve}} = 2.65 \text{ in}^2$$

Therefore, the tensile stress in the sleeve is

$$\sigma := \frac{F}{A_{\text{sleeve}}} \quad \sigma = 730 \text{ psi}$$

The allowable stress intensity for the primary membrane category is S_m per Subsection NG of the ASME Code. The corresponding safety factor is

$$SF := \frac{S_m}{\sigma} \quad SF = 27.4$$

3.AS.7.1.2 Base Weld (Between Item 1 and Item 7)

The base of the container must support the amplified weight of the fuel assembly. This load is carried directly by 16 spot welds (4 on each side) which connect the base to the container sleeve. The weight of the baseplate is

$$W_{\text{bplate}} := \left(d_{\text{bplate}}^2 - N_{\text{bph}} \cdot \frac{\pi}{4} \cdot d_{\text{bph}}^2 \right) \cdot t_{\text{bplate}} \cdot \gamma_{\text{ss}} \quad W_{\text{bplate}} = 13 \text{ lbf}$$

The total load carried by the spot welds is

$$F := \text{DLF} \cdot (W_{\text{fuel}} + W_{\text{bplate}}) \quad F = 1748 \text{ lbf}$$

The area of the weld is

$$A_{\text{weld}} := 4 \cdot 4 \cdot \frac{3.14 \cdot d_{\text{wbase}}^2}{4} \quad A_{\text{weld}} = 0.2 \text{ in}^2$$

Therefore, the amplified shear stress in the weld is

$$\sigma := \frac{F}{A_{\text{weld}}} \quad \sigma = 8907 \text{ psi}$$

From the ASME Code the allowable weld shear stress, under normal conditions (Level A), is 60% of the membrane strength of the base metal. The corresponding safety factor is

$$\text{SF} := \frac{0.6 \cdot S_{\text{m1}}}{\sigma} \quad \text{SF} = 1.3$$

3.AS.7.1.3 Container Collar (Items 1 and 2)

The load tabs of the upper lock device engage the container collar during a lift. The load transferred to the engagement slot, by a single tab, is

$$F := \frac{\text{DLF} \cdot (W_{\text{container}} + W_{\text{fuel}})}{4} \quad F = 483 \text{ lbf}$$

The shear area of the container collar is

$$A_{\text{collar}} := 2 \cdot d_{\text{slot}} \cdot (t_{\text{sleeve}} + t_{\text{collar}}) \quad A_{\text{collar}} = 0.107 \text{ in}^2$$

The shear stress in the collar is

$$\sigma := \frac{F}{A_{\text{collar}}} \quad \sigma = 4519 \text{ psi}$$

The allowable shear stress from Subsection NG, under normal conditions, is

$$\sigma_{\text{allowable}} := 0.6 \cdot S_{\text{m1}} \quad \sigma_{\text{allowable}} = 12000 \text{ psi}$$

Therefore, the safety factor is

$$SF := \frac{\sigma_{\text{allowable}}}{\sigma} \quad SF = 2.7$$

3.AS.7.1.4 Load Tabs (Item 3)

The load tabs of the lock device engage the container collar during a lift. The shear area of each tab is

$$A_{\text{tab}} := t_{\text{tab}} \cdot W_{\text{tab}} \quad A_{\text{tab}} = 0.25 \text{ in}^2$$

The shear stress in the tab is

$$\tau_{\text{tab}} := \frac{F}{A_{\text{tab}}} \quad \tau_{\text{tab}} = 1.932 \times 10^3 \text{ psi}$$

Therefore, the safety factor is

$$SF := \frac{0.6 \cdot S_{m1}}{\tau_{\text{tab}}} \quad SF = 6.211$$

3.AS.7.1.4 Upper Closure (Item 4)

The damaged fuel container is lifted by a bolt at the center of the upper closure plate. Assuming that the square upper closure plate is simply supported at the boundary and loaded by a uniform concentric circle of radius of the bolt, we can use the formula given in Table 26 of Ref. [4] to calculate the maximum bending stress of the plate. For a square plate, the coefficient of the stress formula is:

$$\beta := 0.435$$

The maximum bending stress in the plate is

$$\sigma_{\text{max}_c} := \frac{3 \cdot (W_{\text{container}} + W_{\text{fuel}}) \cdot \text{DLF}}{2 \cdot \pi \cdot t_{\text{cp}}^2} \cdot \left[(1 + 0.3) \cdot \ln \left(\frac{2 \cdot \text{id}_{\text{sleeve}}}{\pi \cdot r_{\text{bolt}}} \right) + \beta \right]$$

$$\sigma_{\text{max}_c} = 1.787 \times 10^4 \text{ psi}$$

The allowable primary stress for the plate, per Subsection NG of ASME code, is

$$\sigma_{\text{allowable}_cp} := 1.5S_{m1} \quad \sigma_{\text{allowable}_cp} = 3 \times 10^4 \text{ psi}$$

Safety factor $SF := \frac{\sigma_{\text{allowable_cp}}}{\sigma_{\text{max_c}}} \quad SF = 1.678$

3.AS.7.1.5 Lifting Bolt (Item 5)

The stress area of the 1/2-12UNC bolt is

$$A_{\text{bolt}} := 0.0773 \cdot \text{in}^2 \quad [5]$$

The tensile stress in the bolt $\sigma_{\text{bolt}} := \frac{(W_{\text{container}} + W_{\text{fuel}}) \cdot \text{DLF}}{A_{\text{bolt}}} \quad \sigma_{\text{bolt}} = 2.499 \times 10^4 \text{ psi}$

The lifting bolt must meet the requirements set forth for Special Devices [2]. As such the allowable tensile stress for design is the lesser of one-third of the yield stress and one-fifth of the ultimate strength.

$$\sigma_1 := \frac{S_{\text{by}}}{3} \quad \sigma_2 := \frac{S_{\text{bu}}}{5}$$

$$\sigma_1 = 32367 \text{ psi} \quad \sigma_2 = 27000 \text{ psi}$$

For SA193-B8 material the yield stress governs at the lifting temperature.

$$\sigma_{\text{allowable}} := \sigma_2$$

Safety factor $SF := \frac{\sigma_{\text{allowable}}}{\sigma_{\text{bolt}}} \quad SF = 1.08$

Now check the thread engagement of the bolt. The minimum required length of the bolt is

$$L_{\text{engage}} := t_{\text{cp}} + t_{\text{washer}} + t_{\text{tab}} + 2 \cdot t_{\text{nut}} \quad L_{\text{engage}} = 1.442 \text{ in}$$

The length of the bolt is $L_{\text{bolt}} = 2 \text{ in}$

Therefore, the thread engagement requirement is satisfied.

3.AS.7.2 60g End Drop (Accident Condition)

The critical member of the damaged fuel container, during a postulated upside down end drop scenario, is the 16 spot welds. The total load applied to the welds in a 60g end drop is

$$F_{\text{drop}} := 60 \cdot W_{\text{bplate}}$$

$$F_{\text{drop}} = 774.983 \text{ lbf}$$

$$\sigma := \frac{F_{\text{drop}}}{A_{\text{weld}}}$$

$$\sigma = 3949 \text{ psi}$$

$$\sigma_{\text{allowable}} := 0.42 \cdot S_{u2}$$

$$\sigma_{\text{allowable}} = 26586 \text{ psi}$$

The safety factor is

$$SF := \frac{\sigma_{\text{allowable}}}{\sigma}$$

$$SF = 6.7$$

3.AS.8 Input Data for MPC-68 BWR Damaged Fuel Container

The damaged fuel container is only handled while still in the spent fuel pool. Therefore, its design temperature for lifting considerations is the temperature of the fuel pool water (150°F). The design temperature for accident conditions is 725°F. All dimensions are taken from the Dwg. 2775. The basic input parameters used to perform the calculations are:

Design stress intensity of SA240-304 (150°F)	$S_{m1} := 20000 \cdot \text{psi}$	Table 1.A.1
Design stress intensity of SA240-304 (725°F)	$S_{m2} := 15800 \cdot \text{psi}$	
Yield stress of SA240-304 (150°F)	$S_{y1} := 27500 \cdot \text{psi}$	Table 1.A.3
Yield stress of SA240-304 (725°F)	$S_{y2} := 17500 \cdot \text{psi}$	
Ultimate strength of SA240-304 (150°F)	$S_{u1} := 73000 \cdot \text{psi}$	Table 1.A.2
Ultimate strength of SA240-304 (725°F)	$S_{u2} := 63300 \cdot \text{psi}$	
Total weight of the loaded container	$W_{\text{load}} := 700 \cdot \text{lbf}$	
Wall thickness of the container sleeve	$t_{\text{sleeve}} := 0.035 \cdot \text{in}$	
Dimension of the square baseplate	$d_{\text{bplate}} := 5.7 \cdot \text{in}$	
Thickness of the baseplate	$t_{\text{bplate}} := 0.5 \cdot \text{in}$	

Diameter of baseplate through hole	$d_{bph} := 1.25 \cdot \text{in}$
Number of baseplate through holes	$N_{bph} := 4$
Diameter of spot welds	$d_{w_{base}} := 0.125 \cdot \text{in}$
Inner dimension of the container sleeve	$id_{sleeve} := 5.701 \cdot \text{in}$
Thickness of the tube cap top plate	$t_{cap_{tp}} := 0.5 \cdot \text{in}$
Diameter of the hole on the top plate	$d_{tph} := 1.25 \cdot \text{in}$
Thickness of the tube cap side plate	$t_{cap_{sp}} := 0.035 \cdot \text{in}$
Width of the side plate	$w_{sp} := 4 \cdot \text{in}$
Length of the locking slot	$L_{slot} := 3.05 \cdot \text{in}$
Width of locking slot	$w_{slot} := 0.34 \cdot \text{in}$
Distance between locking bar center to the top plate bottom	$L_{l_{bar}} := 1.5 \cdot \text{in}$
Thickness of locking bar	$t_{bar} := 0.1 \cdot \text{in}$
Width of the locking bar	$w_{l_{bar}} := 0.25 \cdot \text{in}$
Diameter of the lifting bolt	$d_{bolt} := 1.0 \cdot \text{in}$
Length of the lifting bolt	$L_{bolt} := 1.0 \cdot \text{in}$
Stress area of the bolt	$A_{bolt} := 0.6051 \cdot \text{in}^2$
Weld size at the bolt and top plate connection	$ww_{bolt} := \frac{1}{16} \cdot \text{in}$
Weight density of the stainless steel	$\gamma_{ss} := 0.283 \cdot \frac{\text{lbf}}{\text{in}^3}$
Dynamic load factor for lifting [1]	$DLF := 1.15$

3.AS.9 Calculations for MPC-68 Damaged Fuel Container

3.AS.9.1 Lifting Operation (Normal Condition)

The critical load case under normal conditions is the lifting operation. The key areas of concern are the container sleeve, the spot welds, the tube cap plates, and the lifting bolt. All calculations performed for the lifting operation assume a dynamic load factor of 1.15.

3.AS.9.1.1 Container Sleeve (Item 1)

During a lift, the container sleeve is loaded axially, and the stress state is pure tensile membrane. For the subsequent stress calculation, it is assumed that the full weight of the damaged fuel container and the fuel assembly are supported by the sleeve. The magnitude of the load is

$$F := \text{DLF} \cdot W_{\text{load}} \qquad F = 805 \text{ lbf}$$

The minimum cross sectional area, located at the locking slot elevation, of the sleeve is

$$A_{\text{sleeve}} := (i_{\text{sleeve}} + 2 \cdot t_{\text{sleeve}})^2 - i_{\text{sleeve}}^2 - 4 \cdot L_{\text{slot}} \cdot t_{\text{sleeve}} \qquad A_{\text{sleeve}} = 0.38 \text{ in}^2$$

Therefore, the tensile stress in the sleeve is

$$\sigma := \frac{F}{A_{\text{sleeve}}} \qquad \sigma = 2 \times 10^3 \text{ psi}$$

The allowable stress intensity for the primary membrane category is S_m per Subsection NG of the ASME Code. The corresponding safety factor is

$$\text{SF} := \frac{S_m}{\sigma} \qquad \text{SF} = 9.3$$

The tube may tearout at those four slots. From the ASME Code the allowable shear stress, under normal conditions (Level A), is 60% of the membrane strength of the metal. The minimum distance between the slot center line to top edge of the tube is determined as

$$d_{\text{slot}} := \frac{F}{0.6 \cdot S_m \cdot 8 \cdot t_{\text{sleeve}}} + \frac{W_{\text{slot}}}{2} \qquad d_{\text{slot}} = 0.41 \text{ in}$$

The tube won't tearout since the center line of the slot is located below the top edge at a distance of

$$L_{\text{1_bar}} = 1.5 \text{ in}$$

3.AS.9.1.2 Spot Weld

Some of the container parts are connected by spot welds at three locations: (1) between base plate of the container and the sleeve (2) between the locking bars and the tube cap side plates, and (3) between the tube cap side plates and the top plate. At each location, there are at least 12 spot welds to carry the load. To evaluate the structural integrity of these spot welds, the load applied to the welds is conservatively assumed to be the weight of the fully loaded container in each case.

The total load carried by the spot welds is

$$F := DLF \cdot W_{\text{load}} \qquad F = 805 \text{ lbf}$$

The minimum total area of the weld connection is

$$A_{\text{weld}} := 12 \cdot \frac{3.14 \cdot d_{\text{wbase}}^2}{4} \qquad A_{\text{weld}} = 0.15 \text{ in}^2$$

Therefore, the amplified shear stress in the weld is

$$\sigma := \frac{F}{A_{\text{weld}}} \qquad \sigma = 5469 \text{ psi}$$

From the ASME Code the allowable weld shear stress, under normal conditions (Level A), is 60% of the membrane strength of the base metal. The corresponding safety factor is

$$SF := \frac{0.6 \cdot S_{\text{ml}}}{\sigma} \qquad SF = 2.2$$

3.AS.9.1.3 Tube cap top plate (Item 2A)

The damaged fuel container is lifted through a lifting bolt welded to the center of the tube cap top plate. Assuming that the square top plate is simply supported at the boundary and loaded by a uniform concentric circle of radius of the bolt, we can use the formula given in Table 26 of Ref. [4] to calculate the maximum bending stress in the plate. For a square plate, the coefficient in the stress formula is:

$$\beta := 0.435 \qquad r_{\text{bolt}} := \frac{d_{\text{bolt}}}{2}$$

The maximum bending stress in the plate is

$$\sigma_{\text{max}_c} := \frac{3 \cdot W_{\text{load}} \cdot DLF}{2 \cdot \pi \cdot t_{\text{cap_tp}}^2} \cdot \left[(1 + 0.3) \cdot \ln \left(\frac{2 \cdot id_{\text{sleeve}}}{\pi \cdot r_{\text{bolt}}} \right) + \beta \right]$$

$$\sigma_{\max_c} = 4.631 \times 10^3 \text{ psi}$$

$$\text{Safety factor} \quad SF := \frac{\sigma_{\text{allowable_cp}}}{\sigma_{\max_c}} \quad SF = 6.479$$

3.AS.9.1.4 Tube cap side plate (Item 2B)

Four locking bars are welded to each of the four side plates. These side plates are bent to allow the locking bars to fit into the slots of the tube for lifting the container. Subsequent to bending, the side plates are forced to be vertical by the locking "ring" which pushes the locking bars into the slots in the container walls. While the side plates are deformed into the plastic range during the initial insertion over the canister tube process, the lowering of the locking ring reverses the state of stress in the side plates. It is required that the side plate should not reach the ultimate stress value during this single cycle of loading .

$$\text{Deflection of the side plate} \quad d_{sp} := t_{bar} \quad d_{sp} = 0.1 \text{ in}$$

The bending stress of the side plate is calculated by assuming that the side plate behaves as a cantilever beam.

$$E_{sp} := 2.7 \cdot 10^7 \cdot \text{psi} \quad L_{\text{bend_sp}} := L_{1_bar} + \frac{W_{1_bar}}{2}$$

$$\sigma_{sp} := \frac{1.5 E_{sp} \cdot d_{sp} \cdot t_{cap_sp}}{L_{\text{bend_sp}}^2} \quad \sigma_{sp} = 5.368 \times 10^4 \text{ psi}$$

The bending stress is less than the ultimate stress of the material (73 ksi) and therefore acceptable.

3.AS.9.1.5 Lifting Bolt (Item 5)

$$\text{The stress area of the bolt is} \quad A_{\text{bolt}} = 0.605 \text{ in}^2$$

$$\text{The tensile stress in the bolt} \quad \sigma_{t_bolt} := \frac{W_{\text{load}} \cdot \text{DLF}}{A_{\text{bolt}}} \quad \sigma_{t_bolt} = 1.33 \times 10^3 \text{ psi}$$

The lifting bolt must meet the requirements set forth for Special Devices [2]. As such the allowable tensile stress for design is the lesser of one-third of the yield stress and one-fifth of the ultimate strength.

$$\sigma_1 := \frac{S_{y1}}{3} \quad \sigma_1 = 9167 \text{ psi} \quad \sigma_2 := \frac{S_{u1}}{5} \quad \sigma_2 = 14600 \text{ psi}$$

For SA240-304 material the yield stress governs at the lifting temperature.

$$\sigma_{\text{allowable}} := \sigma_1$$

Safety factor $SF := \frac{\sigma_{\text{allowable}}}{\sigma_{t_bolt}} \quad SF = 6.89$

The bolt is welded to the tube cap top plate by the 1/16 fillet weld surrounding the periphery of the bolt. The shear stress in the weld is

$$\tau_{b_weld} := \frac{DLF \cdot W_{\text{load}}}{\pi \cdot d_{\text{bolt}} \cdot (0.707 \cdot ww_{\text{bolt}})} \quad \tau_{b_weld} = 5.799 \times 10^3 \text{ psi}$$

From the ASME code the allowable weld shear stress, under normal condition (level A), is 60% of the membrane strength of the base metal. The corresponding safety factor is

$$SF := \frac{0.6 \cdot S_{m1}}{\tau_{b_weld}} \quad SF = 2.069$$

3.AS.9.2 60g End Drop (Accident Condition)

The critical member of the damaged fuel container, under a postulated top down end drop scenario (that would occur only when the MPC is in transit), is the 16 spot welds. The total load applied to the welds in a 60g end drop (while installed in a HI-STAR 100 overpack) is

$$W_{\text{bplate}} := \left(d_{\text{bplate}}^2 - N_{\text{bph}} \cdot \frac{\pi}{4} \cdot d_{\text{bph}}^2 \right) \cdot t_{\text{bplate}} \cdot \gamma_{ss} \quad W_{\text{bplate}} = 4 \text{ lbf}$$

$$F_{\text{drop}} := 60 \cdot W_{\text{bplate}} \quad F_{\text{drop}} = 234.165 \text{ lbf}$$

$$\sigma := \frac{F_{\text{drop}}}{A_{\text{weld}}} \quad \sigma = 1591 \text{ psi} \quad \sigma_{\text{allowable}} := 0.42 \cdot S_{u2} \quad \sigma_{\text{allowable}} = 26586 \text{ psi}$$

The safety factor is

$$SF := \frac{\sigma_{\text{allowable}}}{\sigma} \quad SF = 16.7$$

3.AS.10 Conclusion

Both of the two types of damaged fuel containers are structurally adequate to withstand the specified normal and accident condition loads. All calculated safety factors are greater than one, which demonstrates that all acceptance criteria have been met or exceeded.